SPECTROPHOTOMETRY OF INTERSTELLAR ABSORPTION BANDS

William John Zealey

Presented for the Degree of Doctor of Philosophy

UNIVERSITY OF EDINBURGH

February 1974

SUMMARY

Photographic, Electronographic and Photoelectric methods of photometry and spectrophotometry of the 'Diffuse Interstellar Absorption Lines' are discussed.

A scanning, photoelectric spectrophotometer was developed and the initial observations of the line at 4430A presented.

Electronographic observations of the line at 4430A were made and the spectra reduced to give a profile of the line. The occurrence of an emission wing to the blue is discussed.

Photographic and electronographic spectrophotometry of reddened OB stars in the region $10^{o} \ll l^{II} \ll 20^{o}$ was carried out and the correlations of the diffuse lines with reddening and other Galactic parameters are discussed. Possible correlations between the strength of the 4430A and 6284A bands and the angle of polarisation were found.

Previous results on the strength of the 4430A line were collated and investigated for similar correlations. The variation of the ratio of the strength of the band to reddening with Galactic longitude was found to relate well to the Galactic structure as outlined by the distribution of open clusters.

SPECTROPHOTOMETRY OF INTERSTELLAR ABSORPTION BANDS

CONTENTS

1. INTRODUCTION

1.1 Past Observations

The realisation of the interstellar nature of the Calcium H and K (Hartmann, 1904) and the Sodium D (Heger, 1919) lines led to the possibility that other species of atoms and molecules might also cause stationary absorption lines in the spectra of distant stars. The discovery of absorptions broader than those caused by atomic absorption and of different structure to the known molecular lines led to the terminology

Diffuse Interstellar Absorption Lines

or Unidentified Interstellar Absorption Bands.

The first diffuse interstellar absorption lines were recognised as such over forty years ago, although earlier records of Cannon (1901), Heger (1919) and Wright (1921) show that observations of lines at 4430A, 5782, 5797A and 6283A had been made. In the intervening period, in spite of many investigations, the causes of these lines have yet to be firmly identified.

In the past most of the observations have been concerned with the intensity and profile of the strongest of the lines in the blue, at 4430A. Systematic observations in the red have been carried out by Merril et al (1937), who observed the Sodium D lines as well as those at 5780A, 5796A, and 6283A. Butler, Seddon, Thompson and Wilson have, between the years 1955 and 1961, extended the observations of Baker (1949). Accurate equivalent widths for the diffuse lines in both the red and blue

are given by the authors. Herbig (1966: 1967), Walker et al.(1967), York (1971) and Honneycutt (1972) have all observed highly reddened stars in both the red and blue. Recent work by Bromage (1971) and Bromage and Nandy (1973) has covered stars in the heavily reddened Cygnus OB2 region, while earlier work on the lines in the blue (1971a) revealed anomalous profiles in these lines. Wu (1972) has studied the lines at 5780A and 5797A at high resolution while Murdin (1972) observed the 6283A region at lower resolution.

For an historical background to the observations reference should be made to Beals and Blanchet (1938), for those concerning more recent work Bromage (1971) and Kelly (1972) provide good reviews.

Following a discussion of the character of the diffuse lines an assessment of the methods used in their observation will best introduce this investigation.

1.2 The Diffuse Lines Character

F.M. Johnson (1970) gives a list of twenty-five diffuse lines observed by Herbig and attributed to similar mechanisms. These absorptions are presented in Table I along with the observed half widths. Of these lines the most obvious, in the spectrum of any reddened star, are those at 4430A, 5780A, 6284A and 6614A. Only the lines at 4430A and 6284A have half widths greater than four Angstroms. The remainder all have half widths larger than those associated with the atomic lines.

Here we will restrict discussion to the more frequently measured lines, marked by an asterisk in

TABLE I

Line	Width	Line	Width
4428A	20A*	4501A	3A
4727A	4A	4762A	4A
4883A	40A	5362A	5A
5420A	10A	5448A	14A
5705A	4A	5780A	2.5A*
5797A	1.2A*	5778A	17A
6175A	30A	6196A	1A
6284A	4A*	6376A	2A
6379A	1A	6010A	5A
5844A	4A	6203A	2A*
6270A	1.5A*	5487A	5A
6614A	1A*	6661A	1A
5850A	1A		

* lines observed in this investigation

Table I.

(i) 4430A

The region in which the band lies is one in which severe blending with stellar features is experienced, particularly in B2 and B3 supergiants. The extreme width of the feature, up to 150A in Herbig (1970), Wilson (1958) and York (1971), makes measurement of the equivalent width difficult (Baker, 1955). Further confusion lies in the profile of the band. Several observers find emission wings of varying extent to the blue and red (York; Walker 1963) or to the blue alone (Bromage, 1971; Bruck et al. 1969). Earlier investigators found only shallow absorption wings giving rise to an approximately symmetric profile (Wampler, 1966; Herbig, 1970; Wilson, 1958). These conflicting profiles indicate the difficulty in defining the continum across a feature of indeterminate extent.

Stellar blending accounts for nearly half of the equivalent width of the 4430A band in B2 supergiants (Butler and Seddon, 1960). A full discussion of this blending is to be found in Bromage's work. It is low at spectral types of B8 or B9 and is decreasing in types earlier than B1. (Fig. 1.1). The main blending is caused by HeI, CII, NII, OII, MgII, AII and FeIII. The sometimes extensive wings of the Balmer line H γ may also affect the fitting of a continuum over the band. These wings may be found in all main sequence stars or in emission type supergiants (Hutchings).

Figure 1.1

Intensity of Blends near 4430 Å

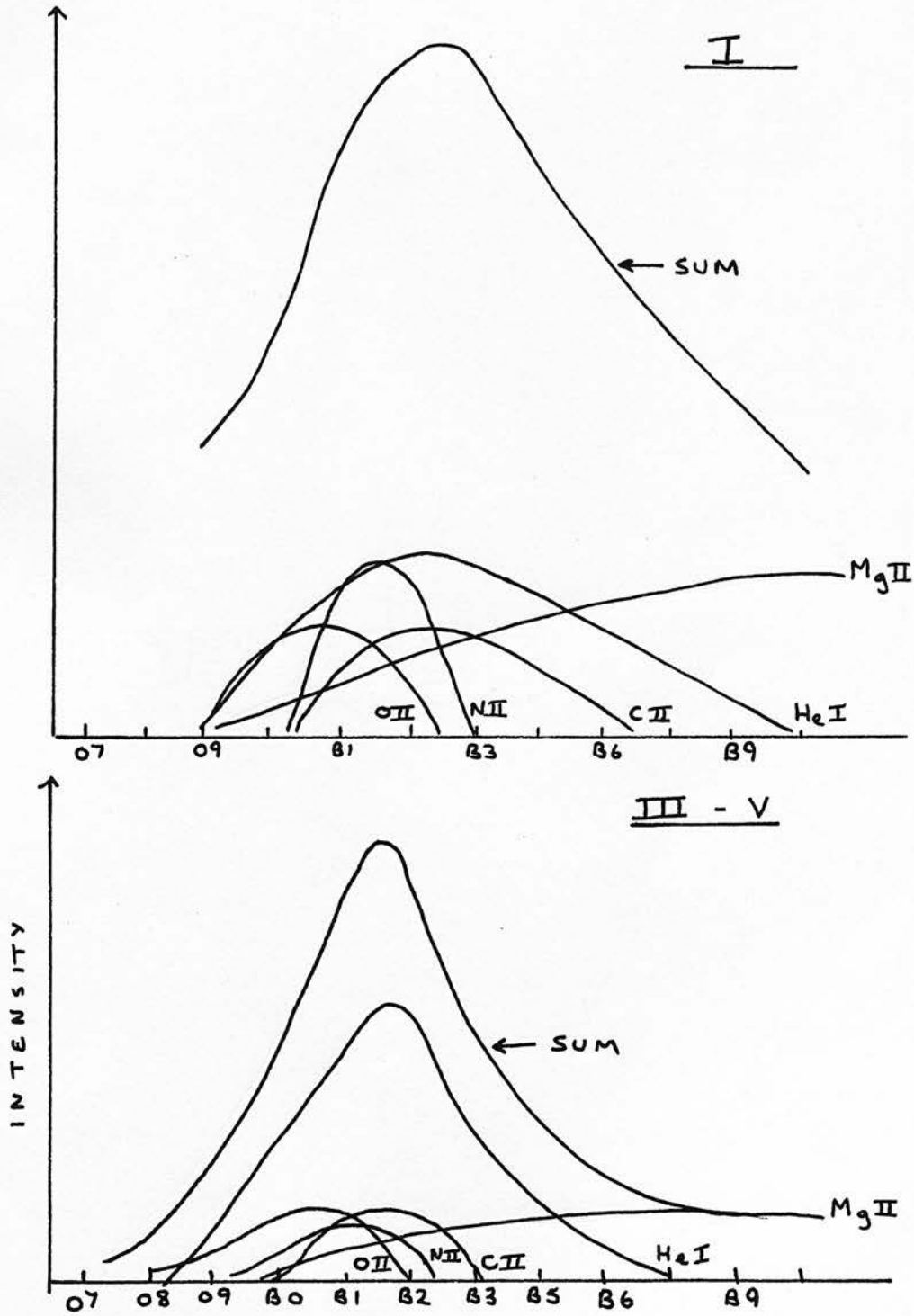

For these reasons the central intensity of the band is a better measure of its strength than the feature's equivalent width (Baker). Seddon (1967) finds that a Gaussian profile is a good fit to the band.

Deeming and Walker (1967) have compared all observations made prior to 1966, stressing the above problems.

(ii) 4760A

This feature is a band with a half width of eight Angstroms and lies in an area clear of stellar blending. The line is seen only in supergiants and has an intensity one third that of the 4430A feature (Butler and Seddon, 1958). Walker et.al. find that the line appears as a discontinuity in their reddening curves, while York finds features at 4750A and 4772A. Bromage too finds nearby features at 4726A and 4740A as well as a possible emission wing to the violet.

(iii) 4890A

This diffuse line lies between the Balmer line Hβ and the Helium line at 4922A. The half width of thirty-three Angstroms makes this line broader than that at 4430A, although measurement is made difficult by the strong blending. Seddon (1968) again finds that a Gaussian profile is a good fit and draws attention to the possible effect of the line on Crawford's H β photometry. Bromage finds that the profile is asymmetric as does Wilson (1958), while Herbig and York find a complex structure of at least two components.

Figure 1.2

The Diffuse Interstellar Lines in the Red

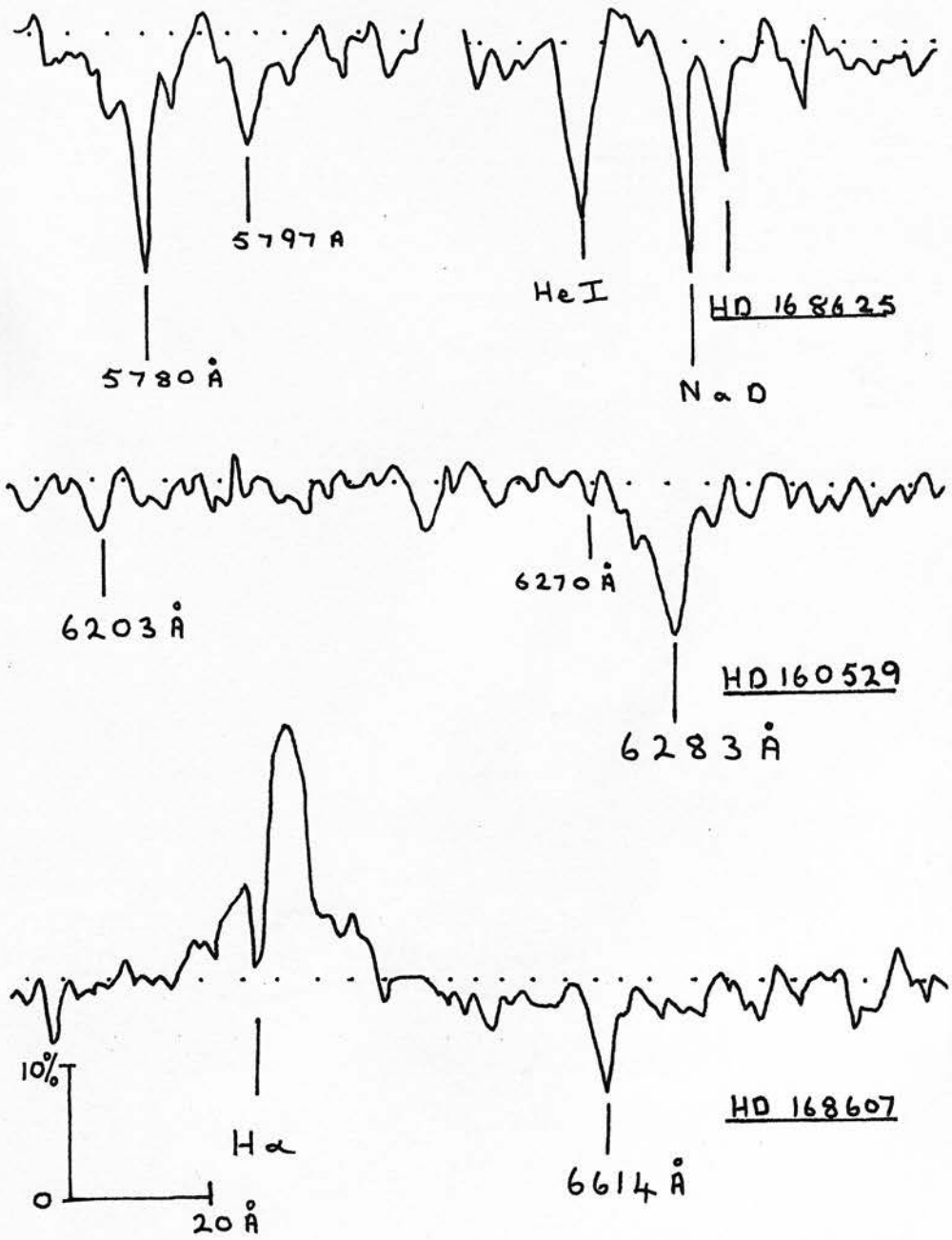

(iv) 5780A

This area is affected by atmospheric absorptions. Wu (1972), Bromage and York all find a shallow band to the blue of the main feature. The diffuse line is three Angstroms in half width and more intense than the 4430A absorption, while the shallow overlying band is seventeen Angstroms in half width.

(v) 5797A

This area is similarly affected by atmospheric absorptions as well as a possible SiliconII blend. Half the intensity of the preceeding line, 5780A, that at 5797A is one Angstrom wide. According to York this line has complex wings although Bromage finds none. Wu at high resolution finds an asymmetric profile, steeper to the blue.

(vi) 5844A

Herbig found a line four Angstroms wide to the blue of the Helium line at 5876A. A depression can be seen in some of the spectra of this investigation and also that of Bromage. In this region York finds a complex of features in some of his stars.

(vii) 6180A

A broad, weak band at 6175A, this region shows extensive wings (York). Herbig finds a half width of thirty Angstroms for this line and Walker et al. noted

a change of slope of the reddening curves in this region.

(viii) 6203A

Superimposed on the previous absorption is the diffuse line 6203A. Two Angstroms wide, the line is believed to be correlated with those at 6180A and 6284A. (Seddon, 1967).

(ix) 6270A

The atmospheric oxygen alpha band head lies close to this line. Lying in the wings of the 6284A band, the line has a half width of two Angstroms.

(x) 6284A

This strong line is much affected by the atmospheric absorption already mentioned. With a half width of four Angstroms, the line has absorption wings (York). Work by Murdin indicates that the line strength to colour excess ratio varies with galactic longitude. The line correlates well with the absorption at 4430A.

(xi) 6614A

This diffuse line is two Angstroms wide and has a central intensity comparable to that of the 4430A band.

From this summary of the diffuse features it is clear that the total absorption for which they account is large.

In early type stars they are the most obvious features in the red, after Hα, Helium I and the Sodium lines. In spite of the fact that reddened stars are fainter in the blue than the red, more observations have been made in the former region. Although this imbalance is in part caused by the sensitivities of early emulsions and photocathodes more systematic work in the red has been possible in recent years. The difficulties in measuring the diffuse lines have already been mentioned. A fuller discussion in relation to the observational methods now follows.

1.3 Observational Methods

The earliest methods in use were photographic with poor calibration and 'eye' estimates of the intensity of the absorptions. (Heger, 1921; Cannon, 1919; Wright, 1921; Morgan, 1939, 1944; Sherman, 1939). These methods however established the interstellar nature of the lines (Merril, 1930, 1934, 1936; Merril and Humason, 1938). The use of calibrated spectra (Beals and Blanchet, 1938) and tracings of the spectra began the systematic investigation of the 4430A band. Since then photographic methods have been supplemented by photoelectric measurements (Wampler, 1966; Kellmann, 1970; Stoekley and Dressler, 1964; Honneycutt, 1972; Walker et.al., 1967). Filter photometry too has been used on the diffuse lines (Walker, 1963; Wampler, 1963; Kristenson et.al., 1965; Baerentzen et.al.,1967; Ahearn, 1971;

Murdin, 1972). Extensions of the photographic methods to fainter, more reddened stars have been made possible by the use of image intensifiers (Wu) and the calibration problems partially avoided by the introduction of 'Spectracon' intensifiers (Brand, 1967; Bromage et.al.).

We shall now discuss more fully the accuracy and problems involved in the four methods:-

(i) Photographic

(ii) Photoelectric filter photometry

(iii) Photoelectric scanning

(iv) Image intensifiers

(i) Photographic Measurement

Early efforts in photography were uncalibrated and although they established the interstellar nature of the lines, accurate intensities were not available. Not until Beals and Blanchet (1938) and Merril et.al. (1938) used calibration techniques and microphotometry, was useful spectrophotometry done. Until the fifties calibration was by means of tube sensitometers or step wedges at a single wavelength close to the feature to be measured. Photographic intermittency effects were taken into account by using a rotating sector to simulate the widening of the stellar spectra. More recent calibration methods use calibration spectrographs (Baker, 1955), photoelectrically calibrated step slits and filters and rotating sectors.

Apart from good calibration, observation of the

the diffuse lines requires a dispersion of at least seventy Angstroms per millimetre, although Treanor (1964) and Roslund (1968) have attempted to use objective prism plates at dispersions near one hundred Angstroms per millimetre to measure the 4430A band. They found difficulty in separating the stellar lines from the band. Duke's observations, which give larger absorptions for '4430' than most others, were made at a dispersion of 123 A/mm. In order to remove the blending a resolution of one Angstrom is sufficient.

Given a well calibrated spectrum, there remains the problem of defining the continuum over the lines. This is not too difficult in the cases of the narrow features, and it may either be hand drawn or computer fitted to regions unaffected by stellar lines. However in the case of broader absorptions, in a region where stellar lines affect the continuum more strongly than in the red, rectification of the spectrum is difficult. In the investigations of the 4430A band by Duke, Underhill (1956), Walker et.al., Greenstein and Aller (1950), Roslund, Buscombe and Kennedy (1969) the continuum was hand drawn. In each case the 4430A band was probably truncated and continuum regions defined within its wings. This gives rise to the variations in absorption found by the observers, especially where it is the equivalent width that is measured.

A more satisfactory method involves the comparison of the reddened star with an unreddened one of the same

spectral type, or with a mean spectrum derived from several unreddened stars (Baker). The latter method has provided some of most accurate observations of the diffuse lines when applied to early type stars by Butler and Thompson (1961) and Butler and Seddon (1958: 1960). More recently York, Bromage and Hutchings et al. have applied the former method to more reddened stars. This method depends on accurate M.K. types being available, so limiting the method to well observed stars. Further accuracy may be obtained by coadding several spectra together so reducing grain noise. Similar noise reduction has been accomplished by computer filtering (Rusconi and Sedmak,1971; Hutchinson, 1971; Bonsak, 1971).

There still remains the problem of separating the diffuse lines from the stellar blends or telluric bands. This is frequently done by assuming the symmetric profile of either the blend or the diffuse line and reflecting the unblended half. (Merril et.al. Bromage).

Finally photographic emulsions show a drop in sensitivity in the green, restricting observations somewhat. The rapid variations in sensitivity in this area has hindered investigation of the bands found by Herbig and York.

(ii) Photoelectric Filter Photometry

Such observations often use three filters with band widths of around twenty Angstroms, two defining the continuum and the third centred on the diffuse line under study. (Walker; Rudkjobing et.al.). An alternative method involves the use of two filters, one of wider bandpass than the other, centred on the features (Murdin; Walker; A'Hearn, 1972).

Observations made in this way show marked variations with spectral type (Walker; Gammelgard, 1968) and these must be calibrated out by observing unreddened stars of the same type. Atmospheric blending is also a problem and this is more difficult to remove (Murdin).

In order to relate the observations to the central depth of the feature a comparison series of spectrographic observations needs to be available, to establish conversion relations.

This method is fast although observations are badly affected by blending.

(iii) Scanning

This is potentially the most accurate method of measuring the diffuse line strengths. Use of photon-counting techniques is more efficient than D.C. methods (Morton, 1968; Tull, 1968). Most systems that have been used in the past have used the scanning of the grating of a spectrophotometer to analyse spectra (Wampler; Kellman; Honneycutt; Stoekley and Dressler; Walker et.al.)

This type of scanning although slow allows the whole of the visible spectrum to be scanned. However it also requires that the sky transparency remains constant during a scan or the use of a monitor channel to take such variations into account (Stoekley and Dressler). The problem of defining a continuum again arises and similar comparison methods to those used in the photographic investigations have been undertaken.

An alternative way of reducing the effects of sky variations is found in rapid scanning. Such methods have been exploited more in the field of solar analysis and research where high resolution and restricted scan length are of use.

The main errors in scanning the diffuse lies in the low resolution of about three Angstroms so far used. This causes the blending by stellar lines to be nearly inseparable from the diffuse lines. High resolution observations of the more narrow lines would therefore seem to be more productive than the observations of broad, blended bands.

(iv) Image Intensifiers.

Use of some form of image intensifier allows the study of the less intense lines at higher dispersions than has previously been possible. Recent observations by Wu have used an echelle spectrograph and intensifier combination to examine the 5780A, 5796A lines.

Use of nuclear emulsions as the recording medium has recently made higher resolution, lower grain noise possible as well as removing the need for photometric calibration (Kahan and Cohen, 1969, 1972; Griboval 1972, Brand, 1967). The introduction of these with the 'Spectracon' intensifiers has enabled accurate work to be carried out on faint, highly reddened stars in this programme.

It may be seen that of the several methods available photographic methods are still to the fore. Photoelectric scanning techniques and 'Spectracons' are now developed sufficiently to extend observations to fainter stars. For this investigation into the profile of the 4430A band and its relation to the other diffuse lines, photographic methods in the red were used, while lines in the blue were observed using 'Spectracons' on the I.N.T., the 74-inch Radcliffe telescope and on the 36-inch telescope at The Royal Observatory Edinburgh. The photographic work was confined to stars in the Sagittarius region and correlations between the lines observed and galactic parameters were investigated. Comparisons between equivalent widths of stellar lines measured using the 'Spectracon' and photographic methods were made to establish that the intensifier is capable of accurate spectrophotometry. To further substantiate this a photon counting, fast scanning system was designed and built in co-operation

with Mr. S. Salter of The Department of Machine Intelligence and Perception of Edinburgh University.

1.4 Star Selection

In order to utilise the prevailing conditions and equipment to the full, the procedure of star selection is important.

The criteria for selection of stars for the 36-inch 74-inch and 98-inch observations are similar in some respects. In all cases exposures of less than one hour were advisable in order to reduce the effects of the drift observed in 'Spectracons' (McGee et.al., 1972). The problems of using stripping emulsion and the need to coadd several spectra obtained with the 36-inch required that a large number of spectra be taken in poor conditions. For this reason observations were restricted to stars brighter than Mv = 7. To be certain of measurable 4430A absorption stars with colour excesses greater than Eb-v = 0.4^{m} were chosen. For reasons fully discussed by Bromage all the stars observed were super giants.

Use of the 74-inch and 98-inch telescopes required in addition a capability to operate in conditions of full Moon. For these telescopes stars with magnitudes less than Mv = 10 were chosen.

Early type stars are mainly found in clusters and associations. Observational lists were drawn from

the associations of Ruprecht (1964) and Morgan (1953). Star lists and charts of open clusters were taken from Hoag and Iriate (1961). Details of the stars were from Hiltner (1956) and the U.S. Naval Photometric Catalogue. The finding charts used were B.D. and C.P.D. charts as well as the Smithsonian charts and plates from Hoag and Iriate.

A discussion of the instrumentation in use will be followed by a full analysis of observations and their relation to previous results.

2. THE SPECTRACON OBSERVATIONS

2.1 A Description

The conception of an intensifier in which the transfer optics were avoided (Zacharov and Dowden, 1960) led in 1962 to the prototype 'Spectracon' (McGee et.al., 1962). In these intensifiers electrons are accelerated and focussed by electric and magnetic fields before passing out of the tube by way of a thin mica window. The electron image is recorded on nuclear emulsion which is pressed against the window.

These early tubes have now evolved into fairly rugged, simple, commercially produced tubes in use in specially designed spectrographs at the R.G.O. and Pretoria. Descriptions of the 'Spectracon' and its development are to be found in the 'Symposia of Photoelectronic Imaging Devices' (McGee et.al.). All of the tubes used at R.O.E. over the years (Bromage, Brand) have been built at Imperial College and most of the published results have been obtained with tubes built after 1967.

The intensifier consists of a photocathode (S11 or S20), twenty-six annuli and a back aluminised mica window all contained in a soda lime tube. Only the photocathode and first annulus have direct connections with the external chain of bleeder resistors. The remaining annuli are maintained at a constant voltage

by electrical leakage through the tube's walls. The photocathode is thus maintained at forty kilovolts with respect to the grounded window. The whole assembly is potted in silastomer and coated in colloidal graphite as precaution against corona discharge. Two window sizes are in use, the 'narrow' 2.5cm. x .5c.m. and the 'wide' 2.5cm. x 1cm. Window thickness of five microns are usual although four micron windows have been used, providing transmissions of 75% of the 40Kv. electrons.

Focussing is by an axial magnetic field supplied by a shielded solenoid, providing a field of 160G over the whole of the electron's 28 cm. path. The MkIIIb solenoid is liquid cooled over the front 60%, so reducing thermal emission. The rear 40% is heated by the coil and maintains the mica window of the 'Spectracon' above the dew point.

Contact between the mica and the emulsion is achieved by a spring loaded applicator by which means up to eight exposures may be made at one loading. Initially stripping emulsions were used in spite of serious handling difficulties; These have recently been superseded by melinex backed emulsions (15 micron emulsion on 1/1000" Melinex).

A diagram of the 'Spectracon' is to be found in Figure 2.1.

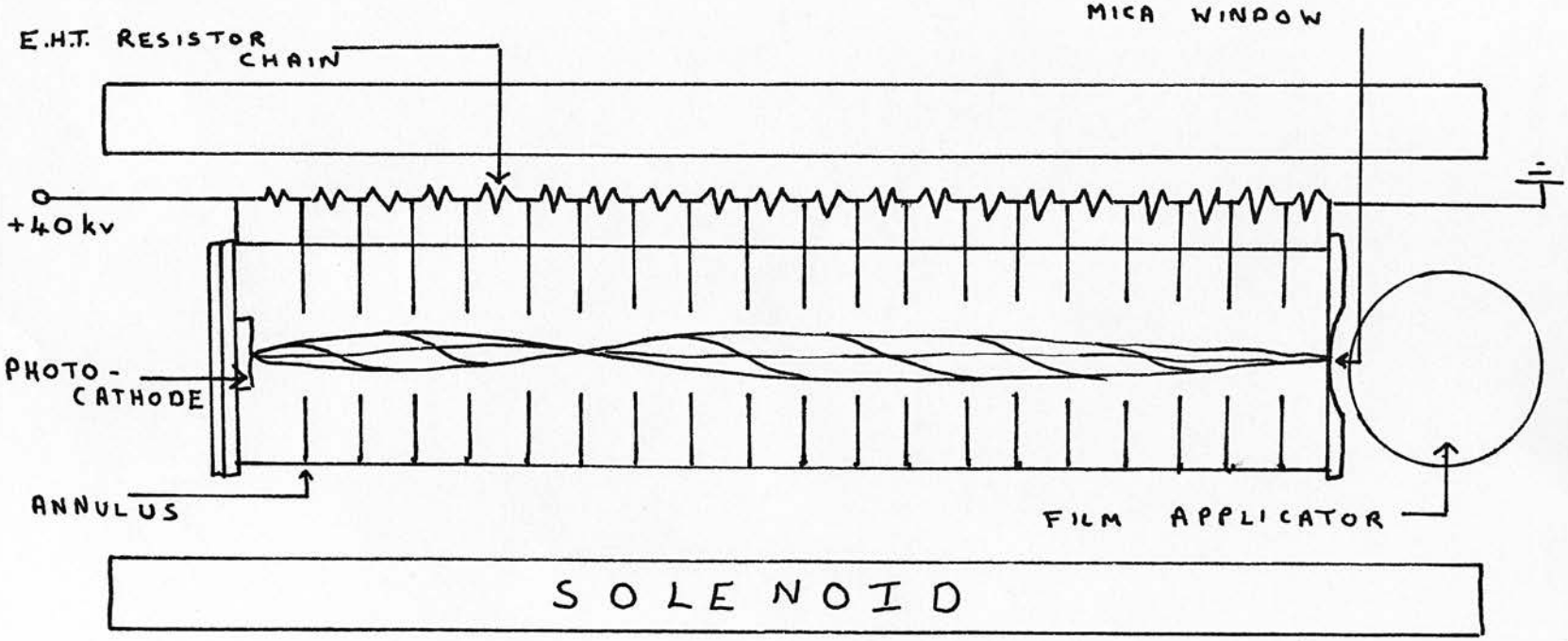

Figure 2.1

Diagram of the Spectracon

2.2 Use at the 36" Spectrograph

The 'Spectracon' was mounted as described by Brand and Bromage on the rear of the camera back of the 36-inch spectrograph. The F/3 exit beam meant that the full resolution of the intensifier could not be used if the maximum throughput of the spectrograph was to be made use of. Assuming an optimistic seeing disc of two seconds of arc, a resolution of fifty line pairs a millimetre was possible.

The E.H.T. supply was a Brandenburg 906 capable of delivering up to 60Kv. at 400mA. with 1% stability. The negative supply was led by a modified coaxial cable, stripped of its earth braiding and sealed inside a $\frac{3}{4}$" P.V.C. tube, to a junction box. This box accepted the cable from the 'Spectracon', connecting it to the E.H.T. supply in an oil filled bath. Only one major E.H.T. breakdown occurred in the system in two years and that was caused by cracked insulation at the Brandenburg socket.

The focussing current was supplied by a Hewlett Packard, Harrison 6290A D.C. power supply and monitored by an Avometer in series. Cooling of the coil was by an open circuit system utilising pumped glycol as the coolant. The system could be cooled but it was found to be adequate operating at room temperature in the winter months.

2.3 Initial Alignment

Rough focussing in the laboratory was carried out

using a projected resolution pattern. For an approximate optical focus and 40Kv. E.H.T., current focussing was carried out from 1.8 to 2.2 Amps at ·05Amp intervals. For the best supply current a series of optical focus exposures were carried out at the telescope, then the current focussing repeated for that best optical focus. For the initial laboratory exposures a white light source was used, while at the telescope a Helium discharge lamp was in use. Once focussed the spectrum was orientated so that it lay away from any conspicuous photocathode defects, revealed on the uniformity exposure plates. For this a white light source and blue filter were rigidly mounted in a tube 30cms. long and equipped with a 45° prism. Mounted on the 'Spectracon' baseplate the system could provide uniform illumination of the photocathode.

2.4 Stellar Exposures

Although the 'Spectracon' is equipped with deflection coils, no use was made of them for widening the spectra. All exposures made at the F/3 focus of the Cassegrain Spectrograph were widened by use of the oscillating glass block within the spectrograph. The leads of the deflection coils were connected to earth. Use was also made of the telescope's exposure meter and autoguiding facilities.

TABLE II "A"

SPECTRACON OBSERVATIONS ON THE 36"

SPECTROGRAPH AND IMAGE TUBE SETTINGS FOR FORTY ANGSTROMS PER MILLIMETRE OBSERVATIONS

Tube numbers B 162, B 195 S11

B 226, B 227 S20 both tubes broke down

Grating 3 Rotation 57.2 Flat mirror 2.35 Curved 2.8

Tilt 2.5 degrees Order 1 Focus 12.0 to 12.5

EHT 40KV Coil Current 1.9 to 2.1 amps.

JOYCE LOEBL MICRODENSITOMETER SETTINGS

Slit 12.5 microns

Slit height 0.3 mm.

Pen damping 2

Scale 830

Step 12.5 microns

Wedge A (0.022D/cm.)

Differentiation 5

Set zero 010

At the beginning of each evening focus tests were carried out, allowing an hour to elapse after "switch on" to let the system stabilise. Similarly exposure tests were made each evening on a bright star to achieve plate densities of .5D. At least twice during each observing run a uniformity exposure was made.

The region observed was between 4000A and 5000A at 40A/mm. and with a resolution of .8A. The slit of the spectrograph was 120 microns wide in order to accept images up to two seconds in diameter and was masked to provide an almost square aperture. This reduced the effects of sky background to some extent. Full details of all settings may be found in Table II.

2.5 Emulsions

The available nuclear emulsions in use with the 'Spectracon' are Ilford XM,L4, and G5. Of these XM is fast but grainy, G5 medium speed and fine grain and L4 slow but very fine grained. All are available in stripping emulsion form, 5μ emulsion on 10μ gel, and in the backed form, 10μ emulsion on 2/1000" Melinex. In addition G5 is available in backed form on 1/1000" Melinex.
In order to reduce damage to the mica window by possible abrasion the 2/1000" backed emulsions were rejected.
In information rate, speed and resolution G5 emulsion lies between XM and L4 (Fig. 2.2). It is believed that while L4 is linear in response at densities of up to

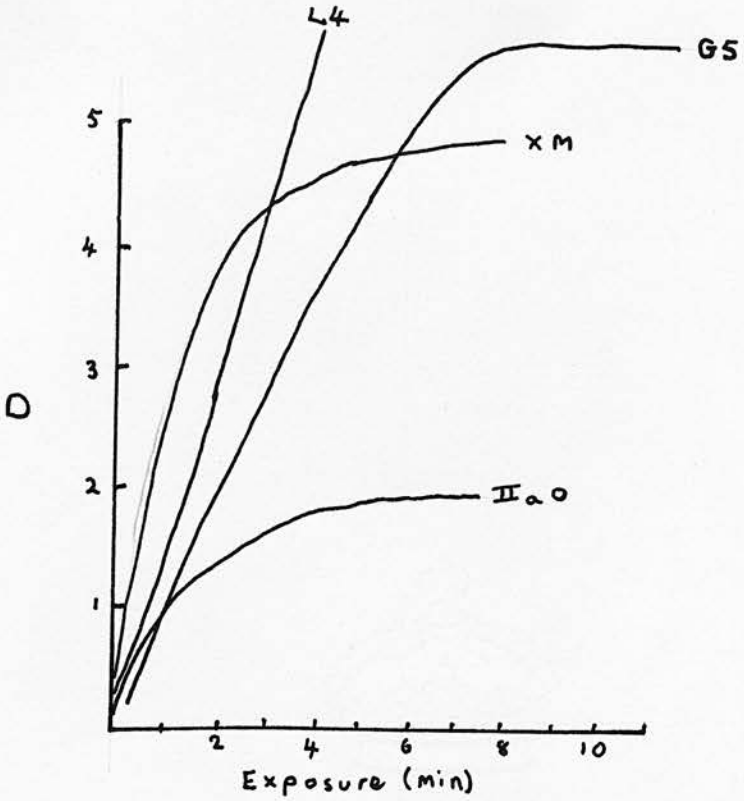

Figure 2.3
Linearity of Emulsions (KAHAN)

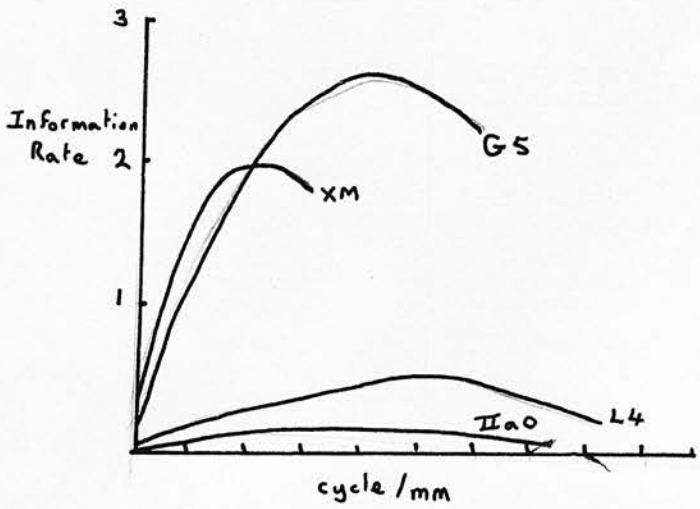

Figure 2.2
Information Storage of Emulsions (KAHAN)

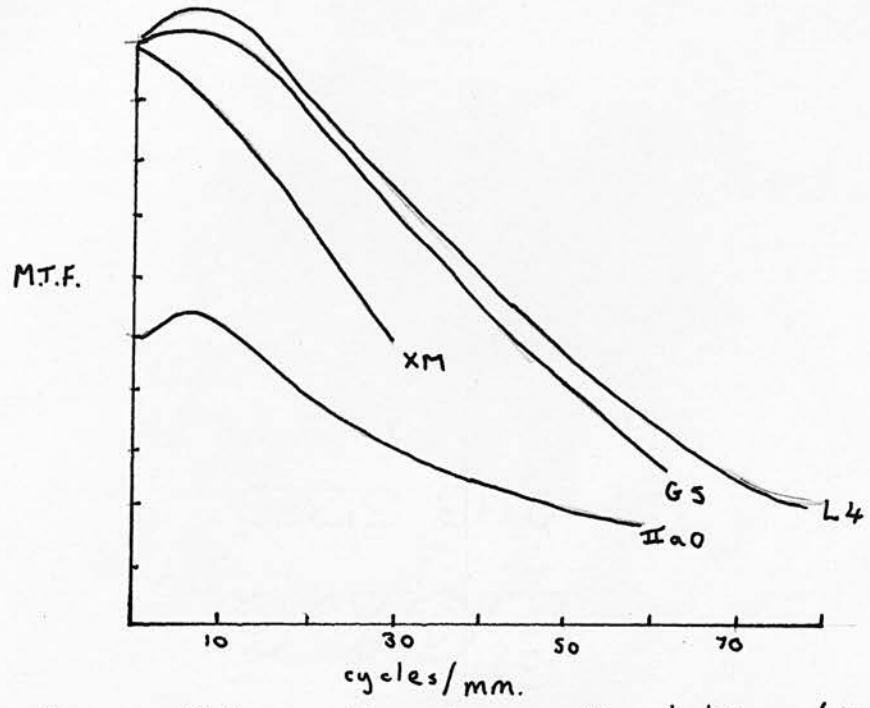

Figure 2.3 Emulsion Resolution (KAHAN)

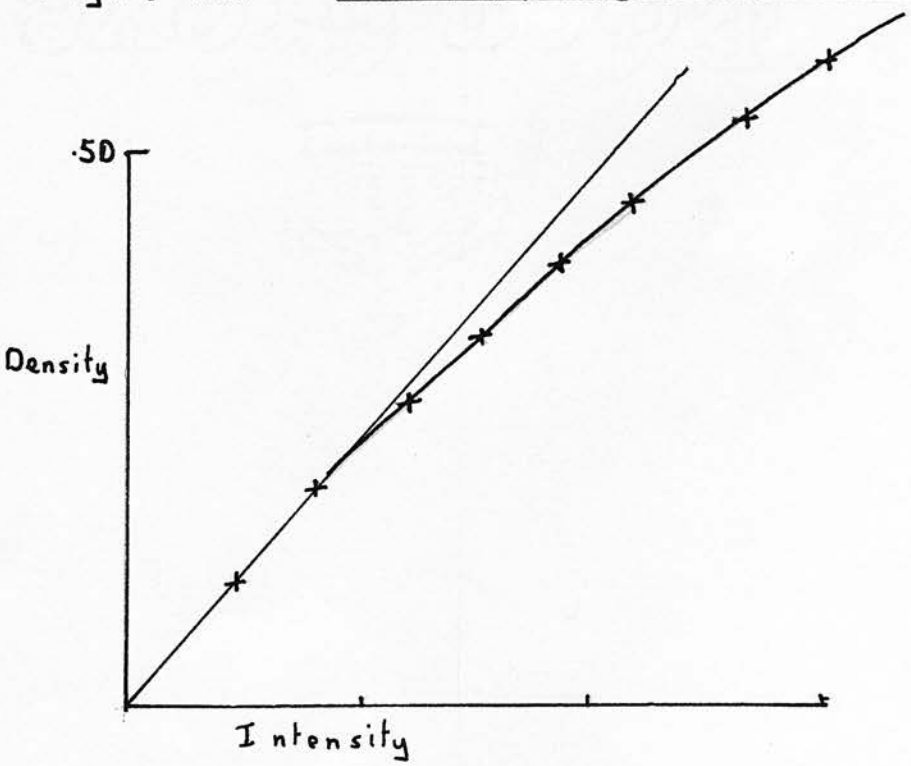

Figure 2.4 Linearity of G5 (BRAND)

5D, G5 departs from such linearity above 1D (Brand, Bacik et.al., 1972; Kahan and Cohen) (Fig. 2.3 ; 2.4).

From the details available it was decided that G5 was the most suitable emulsion if observations were confined to less than 1D in density. Circumstances beyond control dictated the initial use of stripping emulsions but later thin backed emulsions became available. We will discuss these seperately.

(i) Stripping Emulsions

These emulsions consist of emulsion coated gelatin supported on glass backing plates. In use the emulsion is cut into one inch wide strips and attached to the film applicator. After exposure the strip is mounted, emulsion, upwards, on a gelatin covered glass slide and developed normally. It was during this final stage that a large percentage of emulsions parted from their slides, causing a loss of the plate.

The preparation of fresh glass slides was also tedious and was carried out as follows. (Airey et.al. 1970). A glass backing plate and several smaller mounting plates were thoroughly cleaned in a solution of concentrated nitric acid, hydrofluoric acid and Teepol. These were then washed and dried, before the backing plate was polished with a solution of 2% Dimethyldichlorosilane in Carbon Tetrachloride, in order to make it water repellent. After washing the

acids resulting from the surface reaction from the plate, it was dried and placed on a heated rubber pad. A warm solution of gelatin in glycerin, to which a hardening agent had been added, was pipetted onto the casting block and the smaller mounting plates placed carefully on top. Care was needed to avoid the trapping of air bubbles in the gelatin-glass interface. The whole assembly was then placed in a moist atmosphere in a fridge and stored for up to two days before use.

In use the mounting plates were gently removed from the casting block and slightly warmed. The emulsion was bent into a loop, the centre of which was touched down onto the mounting plate. The ends of the emulsion were allowed to fall flat onto the gelatin surface of the plate and then the plate was left in a dessicating jar for ten minutes before development.

Development was for five minutes in D19B, constantly agitated and under the recommended safe light. After washing in a stop bath the emulsion was fixed in Kodak Rapid with added hardener for 15 minutes and further washed before drying in a forced draught cabinet. At all stages of development the emulsion had a tendency to float off it's backing plate. Various hardeners, both in the gelatin and in the fixer, had little effect. Similarly the use of distilled water and the use of a different developer. As a result the development had to be monitored throughout and to be abruptly

halted when signs of separation were evident. The remaining stages were then completed after allowing the plate to dry. A full evaluation of the reasons for separation would be complex. Similar problems have been experienced at Pretoria, although Herstmonceux workers find no such problems. It would seem that the chief cause is the ion concentration differentials found, in the various stages of development, across the gelatin liquid interface. These cause the swelling and contracting of the backing gelatin and emulsion gelatin at different rates. Recent development of thin, backed emulsions removes some of the need to use this mounting procedure.

(ii) Backed Emulsions

The 1/1000" and 2/1000" Melinex backed emulsions were developed in an identical way to the stripping emulsions. They require no such backing plates for mounting and were held by clips at both ends and so suspended in the developing solutions. (Bromage).

2.6 Plate Reduction

To reduce the grain noise of the spectra it was decided to coadd several spectra of each star. (Bromage). For this a digital representation of the spectra was obtained by scanning the plates with a Joyce Loebl microdensitometer with punched paper tape output. A graphical representation was also available from a Servoscribe so that obviously defective spectra could be discarded and small defects could be located for

later removal. Initial trials were carried out to select the best settings for the sampling slit, feedback and other controls. For these the pen table and lever arm were connected and punch output not used.

A step size of 12.5μ (.5A) and a sampling slit width of 12μ were chosen and the illuminating slit adjusted to just overfill the latter. Slit heights of between 0.3mm. and 0.5mm were used. In general wedge 'A' was used with a specified slope of 0.022D/mm. While the mounted stripping emulsions were treated as normal plates the backed emulsions were mounted under a cover slips.

The spectrum was aligned so that the table motion was in the direction of dispersion by using to the full any calibration spectra on the plates. A 'fog' scan was made with the slit positioned slightly above the spectrum, viewing an unexposed part of the plate, and with a step length of 100μ and identical settings as for the main scan. The main scans of the spectra were then made at 12.5μ steps. All scans were begun at the same datum position identified by a sharp photocathode defect near 5000A.

Removal of nonuniformity effects was carried out by taking scans of the uniformity exposures for each set of observations. To aid computer reduction each scan was terminated by punching '0' on the output tape. At the end of each set of scans a pen calibration was

carried out. Throughout the measurements no settings were altered and adequate time was allowed after switch on for the microdensitometer to stabilise.

2.7 Computer Reduction

Analysis of each spectra was such as to require

(i) subtraction of fog levels.

(ii) removal of non-uniformity effects.

(iii) removal of plate defects.

(iv) the coadding of other spectra.

(v) the fitting of a continuum.

It was found that the fog varied smoothly across the plates and that interpolation between fog levels taken at 100μ intervals was sufficiently accurate.

It was also found sufficient to remove only the low frequency variations in the non-uniformity effects. The uniformity tapes were therefore smoothed by computer fitting a fourth order polynomial and the resulting tape used in the main programme.

To facilitate coadding spectra each scan was plotted using WZ220. The output was in the form of a plot using the line-printer mode because this was the fastest way of plotting several thousand points. All programmes were written in Algol for the use on the Elliot 4100 computer, then at the Royal Observatory. The programme WZ220 first fitted a mean continuum to the raw data, scaled every other point by the interpolated continuum and then plotted on the line-printer the rectified

spectrum. From this the position of flaws, dirt and the datum mark could be found.

The main programmes WZ202 and WZ2022 were then supplied with data determining the datum position, areas of good data, the number of points in each spectrum, the number of spectra to be coadded, as well as the continuum positions. Data tapes of the fog scans and uniformity scans were also supplied along with the spectrum tapes.

For each good data point, following the datum mark, the interpolated fog value was subtracted and the result stored, along with the number of good, coincident data points added into that location. These stored sums were later used to compute a mean, so producing a smooth spectrum showing no discontinuities. However some degree of scaling was necessary to fit discontinuities together. The non-uniformities were then removed by dividing each point by its associated point on the uniformity scan tape. Continuum values were calculated for every ten data points or less and a third order polyfit used to fit the continuum. This polyfit ran up to five times, rejecting each time data lying more than three percent from the calculated continuum. The spectrum was then rectified and plotted on a graph plotter. Intensities and the sum of the percentage deviations from the continuum were also output.

Two programmes that were written to reduce the data differ only in the order of fitting the continuum and the main body of the programme. WZ202 coadds the spectra first then calculates the continuum while WZ2022 fits continuua and then coadds the rectified spectra. Little difference was observed in the resultant spectra.

The polyfitting of the continuum over such a large area between 4481A and 4300A causes difficulty when fits of order greater than three are used. While the fit is then good in the continuum region large oscillations can occur in the 4430A area.

2.8 Continuum and Line Position

The line lists for early type stars were taken from the publications of the R.O.E. covering O6 to A0 stars, in the 3800A to 6600A region. To check the completeness of these references use was made of Moore's Multiplet Tables along with lists from Williams (1936), Sinnerstad (1961), Rudnick (1936) and work of the Dominion Astrophysical Observatory. From these lists continuum regions lying at least two angstroms from the line centres were identified, and reduced to distances from the datum mark used in measuring the spectra. Two lists were prepared, one for types B1 to B3 and a second for types B5 to A0.

Any errors in defining the continuum regions were

later taken care of by successive continuum polyfits.

2.9 Errors

The main error lies in the fitting of the continuum to the spectra. Since the procedure rejects points lying 3% of the continuum value from the fitted line the probable error is less than ∓2%. Comparison with the photographic work done at Edinburgh lends some confidence to the linearity of the G5 emulsion within the density limits imposed.

The accuracy in wavelength determination is set only by the resolution of these observations although some degradation occurs in the coadding of spectra. Some error is also introduced by the original setting up of the plates and the positioning of the datum mark. Such positioning is accurate to half a step (∓0.25A).

During the course of using the 'Spectracon' work was carried out on the spatial non-uniformity of response of the cathode and mica window (N.U.R.C.A.M.) of the device. Brand and Smyth (1966) and later Bromage analysed this and found variations in response of up to 25% over the field. Low spatial frequencies can be calibrated out but the higher ones caused mainly by cathode dead-spots or pinholes (Bacik, 1972) are more difficult to deal with. Discussion with McGee indicated that the main non-uniformities arise in the photocathode although

some may result from cleavage within the mica window. (Bromage) In both S11 'Spectracons' used in this investigation the non-uniformity showed as a slow increase across the field with no major low frequency variations greater than ∓5%. High frequency components in the form of pin hole defects are common in both tubes but could be avoided.

A series of N.U.R.C.A.M. exposures were carried out for the shortlived S20 tube and showed 25% variations in response as well as possible cleavage lines. This 'Spectracon' subsequently broke down internally after slowly losing it's vacuum.

A N.U.R.C.A.M. diagram of the S11 used for this series of observations is given in Figure 2.5. The resolved elements are 200μ by 50μ .

2.10 Drift

Another problem studied was the stability of image geometry of the tubes over long periods. Both S11 tubes along with the first I.T.L. tube were tested for image drift.

These tests were in the form of double exposures of resolution patterns, of the bar type, separated by up to two hours. Periods of up to five hours were allowed for the equipment to stabilise in. To ensure that mechanical vibrational effects were minimised all exposures were controlled from a distance.

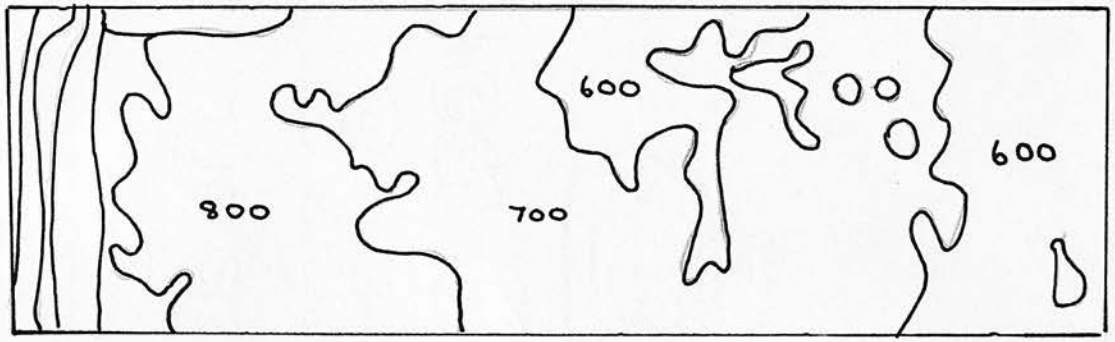

Figure 2.5

N.U.R.C.A.M. DIAGRAM FOR SII

Drift for the tubes B162 and B195 was less than 30μ in an hour at periods one hour or more after switch on. Such drift rates would not seriously affect the resolution achieved in this investigation in exposures of up to ten minutes.

I.T.L. 01 had previously shown drifting of 40μ per hour and up to 75μ per hour (Milsom) although lesser drift rates were found at Imperial College. The drift direction and magnitude varied across the field, being parallel to the window's longer axis in one half of the field and perpendicular in the other.

In all subsequent work the observational programmes were based around exposures of less than half an hour, to limit drift effects.

2.11 The Spectracon in Pretoria and at the I.N.T.

In extending the use of the intensifier to fainter stars, use was made of the 'Unit Spectrographs' of the Radcliffe 74-inch reflector and the 98-inch I.N.T. These spectrographs were designed for 'Spectracons' as the main detector with a back-up Carnegie cascade intensifier. (Palmer and Milsom, 1972). To match the resolution of the 'Spectracon' a fast F/2.2 or F/1.4 camera utilising Maksutov optics is used. Facilities for offset guiding, comparison spectra and exposure readings are incorporated along with circular apertures and slit masks. The spectrum can be widened manually or

electronically.

For both the Radcliffe and I.N.T. observations circular masks and electronic widening were used. Preliminary alignment and focussing of the intensifiers was carried out by staff at the observatories. The E.H.T. supplies, in both cases Miles HiVolt packs, were monitored with digital voltmeters.

Exposures were in all cases made on G5 emulsion, those at the I.N.T. on the stripping variety while those at Pretoria were made on the Melinex backed type. Development in Pretoria was for six minutes in 'Microphen' at 68 degrees, the dish being constantly agitated. I.N.T. plates were developed in the nitrogen bubble tank for four minutes in 'ID2' again at 68 degrees.

At both Pretoria and Sussex the resolution was limited by the seeing disc of the stars. The Pretoria observations were made at a dispersion of 55A/mm. with a resolution of between 1 and 1.5A. At the I.N.T. resolutions similar to these were obtained at 75A/mm.

The accurate determination of the profile of the 4430A band required a large number of spectra to be co-added. Because allocation of large telescope time precluded such a programme it was decided to achieve accurate central depths of the feature instead. Reduction of the 74-inch and 98-inch spectra by the method used to determine profiles was decided against

because of the extreme amount of manual intervention required in the computer reduction.

Instead each spectrum and associated fog levels from 4200A to 4600A was digitised from microdensitometer chart recordings, using a 'Ferranti Freescan' digitiser. The output was in the 'stream X' mode, values of trace height and wavelength being punched at increments of 1.5A in wavelength. To fit a continuum, the same continuum regions were used as those of Bromage(1971). These were digitised, omitting absorption lines and plate defects. The region of the 4430A feature from 4390A to 4490A was also digitised and after subtraction of fog levels a third order polynomial representing the computed continuum was used to rectify the spectrum in this area. The central depth of the feature was then measured from the line printer and graphical output.

In the region digitised it was noted that due to a fortuitous combination of instrumental and stellar effects the recorded continuum showed little curvature. Approximate results using a hand fitted straight line continuum were found to agree well with the later computed ones.

The errors due to instrumental noise are of the order of $\pm 2\%$, those associated with the digitising $\pm 1\%$. The error in computing a continuum is therefor small and the main error in determining the central depth of the feature is of the order $\pm$ 2%.

TABLE III

STELLAR DETAILS

HD No	MK	Eb-v	Ac 4430%	Comment
13267	B5Ia	----	----	-----
21389	A0Ia	0.54	8.5	Reflection
36371	B5III	0.42	7.5	-----
41398	B2Ib	0.48	6.0	-----
42087	B2.5Ib	0.42	5.0	-----
91316	B1Ib	0.12	2.0	-----
183143	B7Ia	1.26	15.0	-----
208501	B8I	0.83	low	-----
223960	A0Ia	0.69	7.5	-----
B Ori.	B8Ia	0.06	----	unreddened
4694	B3Ia	0.92	11.0	-----
209678	B2Ia	0.63	11.0	Ceph OB1
210809	O9Ib	0.36	6.0	"
212455	B5Iab	0.54	5.0	"
217035	BOV	0.76	8.0	Ceph OB3
217061	B1V	0.95	6.0	"
217086	O5	0.95	10.0	"
216711	B1V	0.88	8.0	"
216927	B9Ia	0.92	9.0	Ceph OB1
235781	B6Ib	0.57	4.0	"
216532	O8	0.54	8.0	Ceph OB3

2.12 Results

Of the 111 spectra taken on the 36-inch telescope 75 were traced, the remainder being affected by poor focussing or development faults. Of these 75, 61 were free enough from flaws to be coadded to yield low noise spectra. The majority of spectra were rejected for the following reasons.

(i) Poor Focus.

(ii) N.U.R.C.A.M. flaws.

(iii) Underexposure or development.

(iv) Scratched emulsion.

(v) Reticulation caused by excessive use of hardener.

(vi) Overlapping images.

It has been stated in several papers that for wide bands the best measure of the absorption is the central depth and not it s equivalent width. From the resulting spectra both central intensities and equivalent widths of the main features were measured. The equivalent widths were measured by planimeter and are the mean of five such measures.

A comparison between the line widths and those of Butler and Seddon shows a good correlation (Fig. 2.6). Since these observations were both made on the same spectrograph the use of a 'Spectracon' for spectrophotometry is justified.

The relation between the depth of 4430A and

Figure 2.6

A Comparison between the Spectracon and Edinburgh Line Measurements

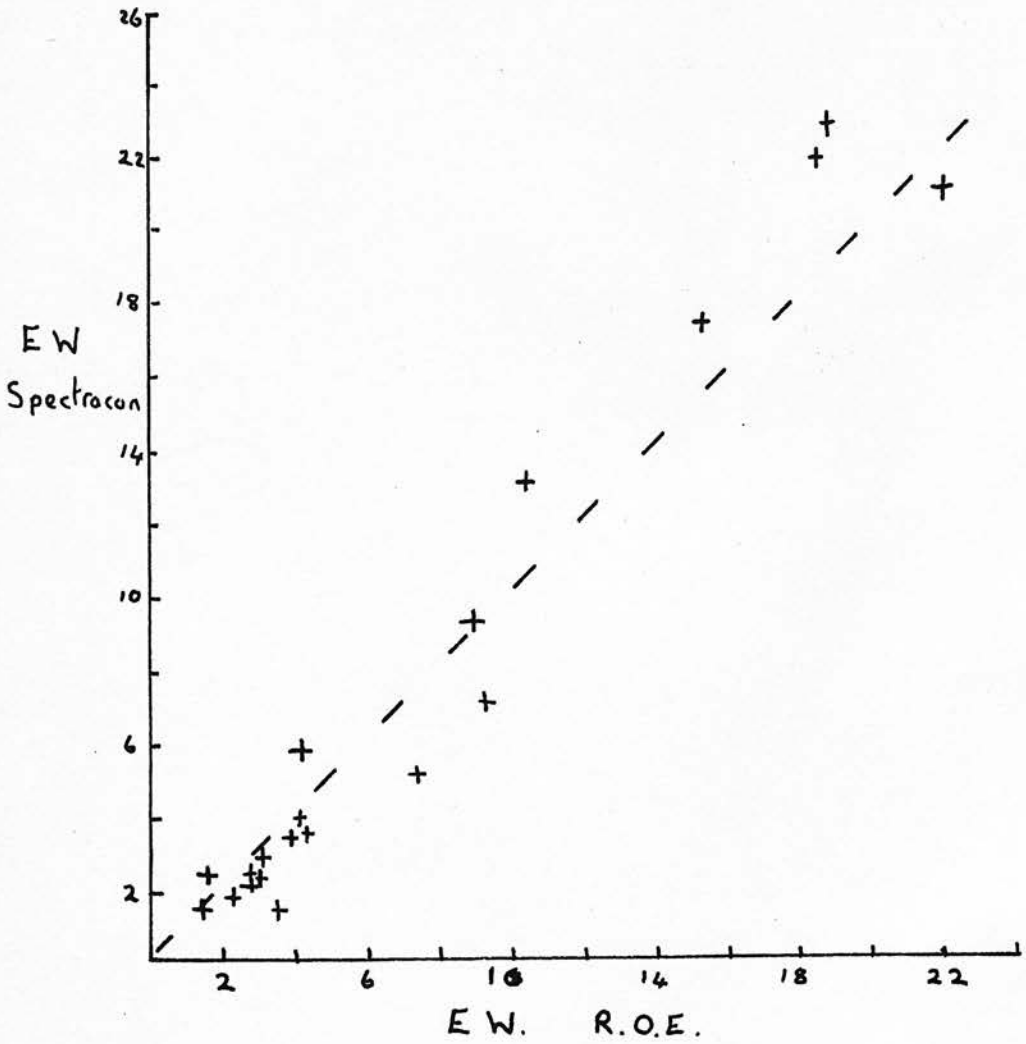

colour excess is shown in Fig 2.8 and includes all observations made in this investigation as well as those of Bromage. A full discussion of this relation is reserved for later.

The main reason for the detailed reduction of the 36-inch observations was to examine the profile of the 4430A band. Bromage and others have found emission wings to this feature. In the one star common to this investigation and that of Bromage, HD. 21389, an emission wing to the blue may be seen (Fig. 2.7). The intensity of this emission is no greater than 3% with a central absorption of 8%. Bromage found values for the emission of 4% and an absorption of 5%. This star is an emission type star and shows variable Balmer lines. Further it lies in a reflection nebula (Racine, 1965; Dorschner, 1965). These may well affect the profile of the 4430A band. It is interesting to note that several other stars which showed emission wings to the band in Bromage's work lie in reflection nebulae.

The well studied star HD 183143 can be seen to have a deep absorption of fifteen percent with shallow wings, similar to those found by Herbig and Wilson. These extend for fifty Angstroms either side of the main absorption and are truncated by the continuum areas and appear to be in emission.

Finally the slightly reddened star HD 91316.

Figure 2.7

The Profile of 4430 Å Band

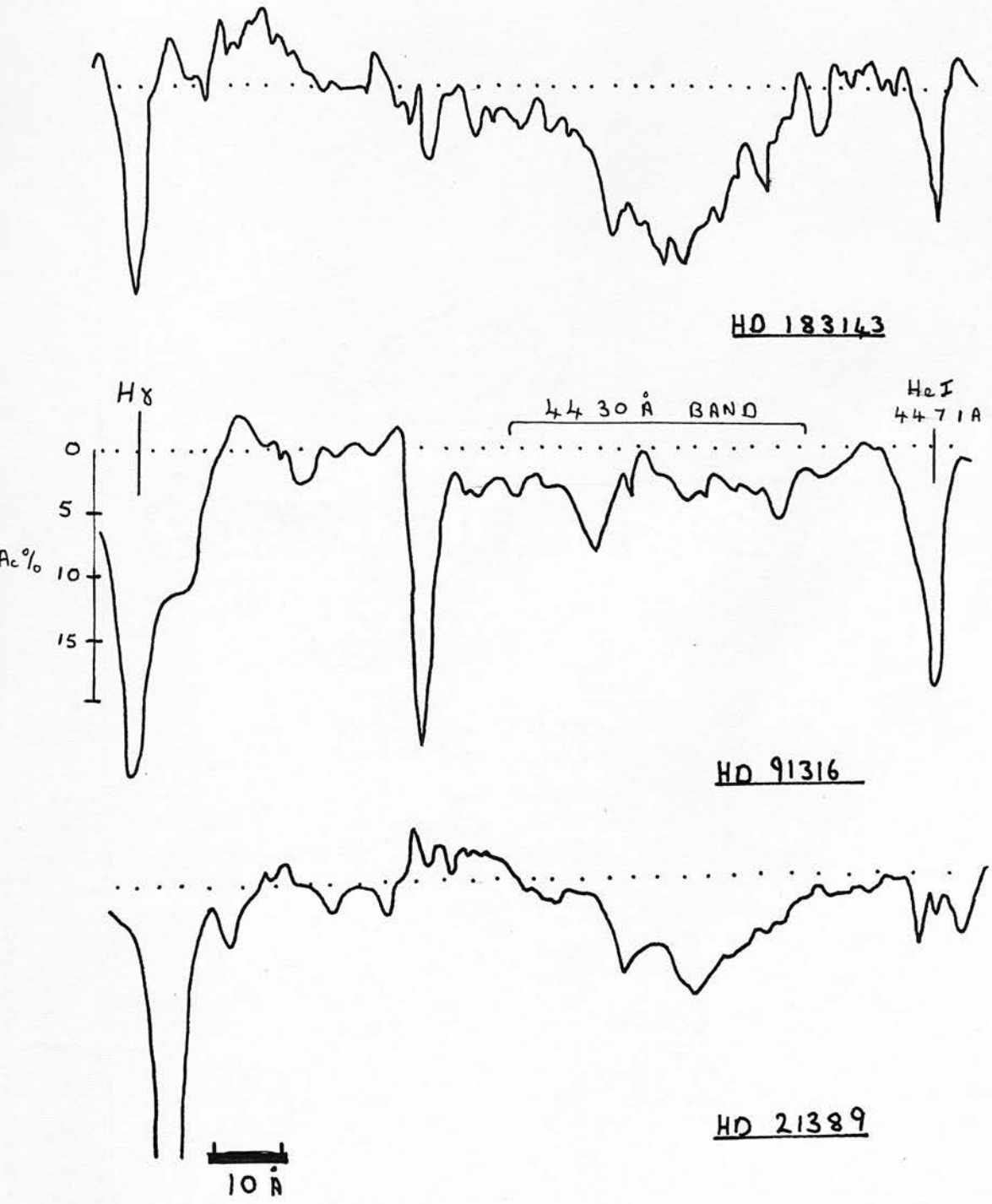

Figure 2.7

The Profile of the 4430 Å Band

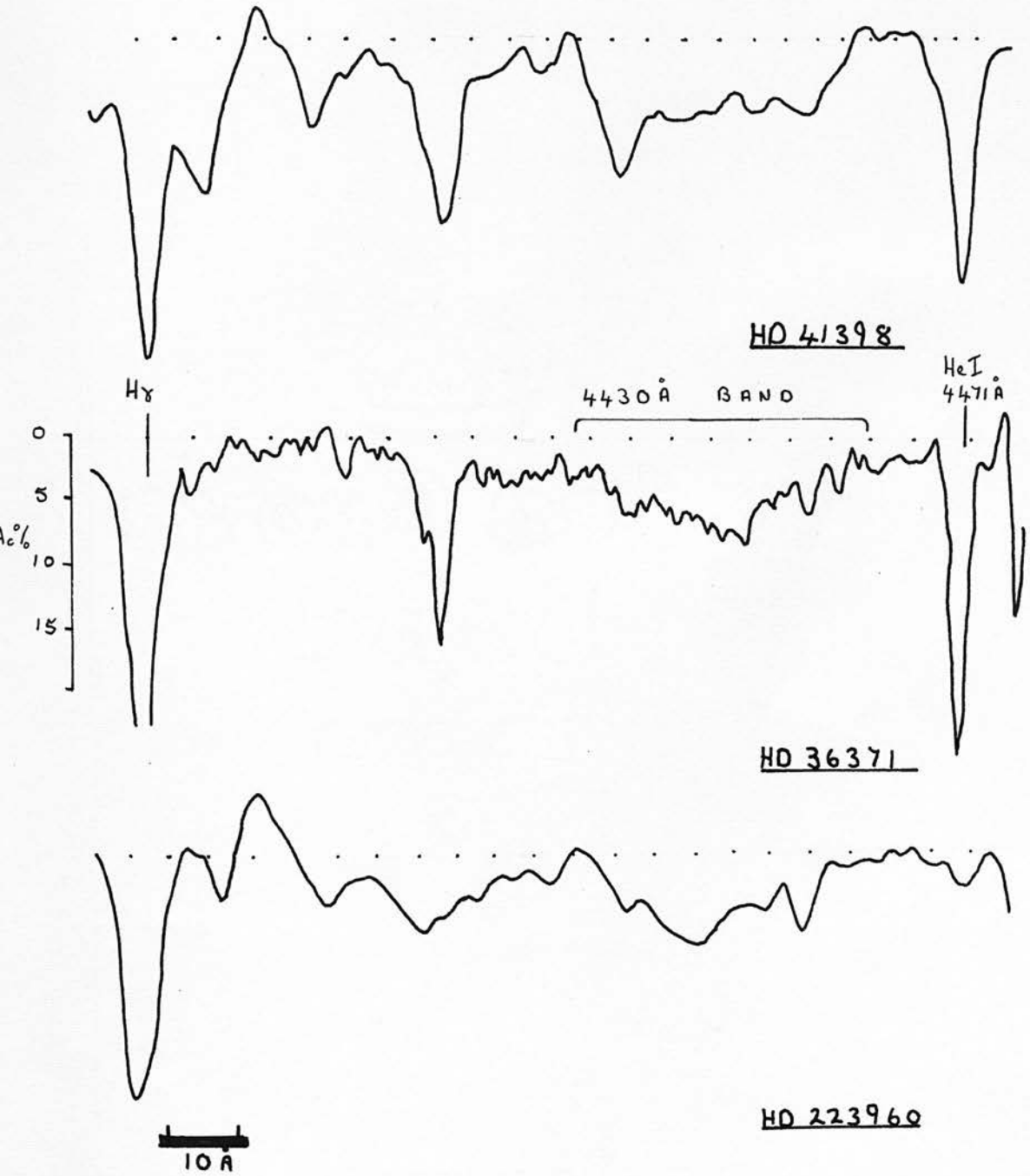

Figure 2.8

The 4430Å σ E_{B-V} Relation

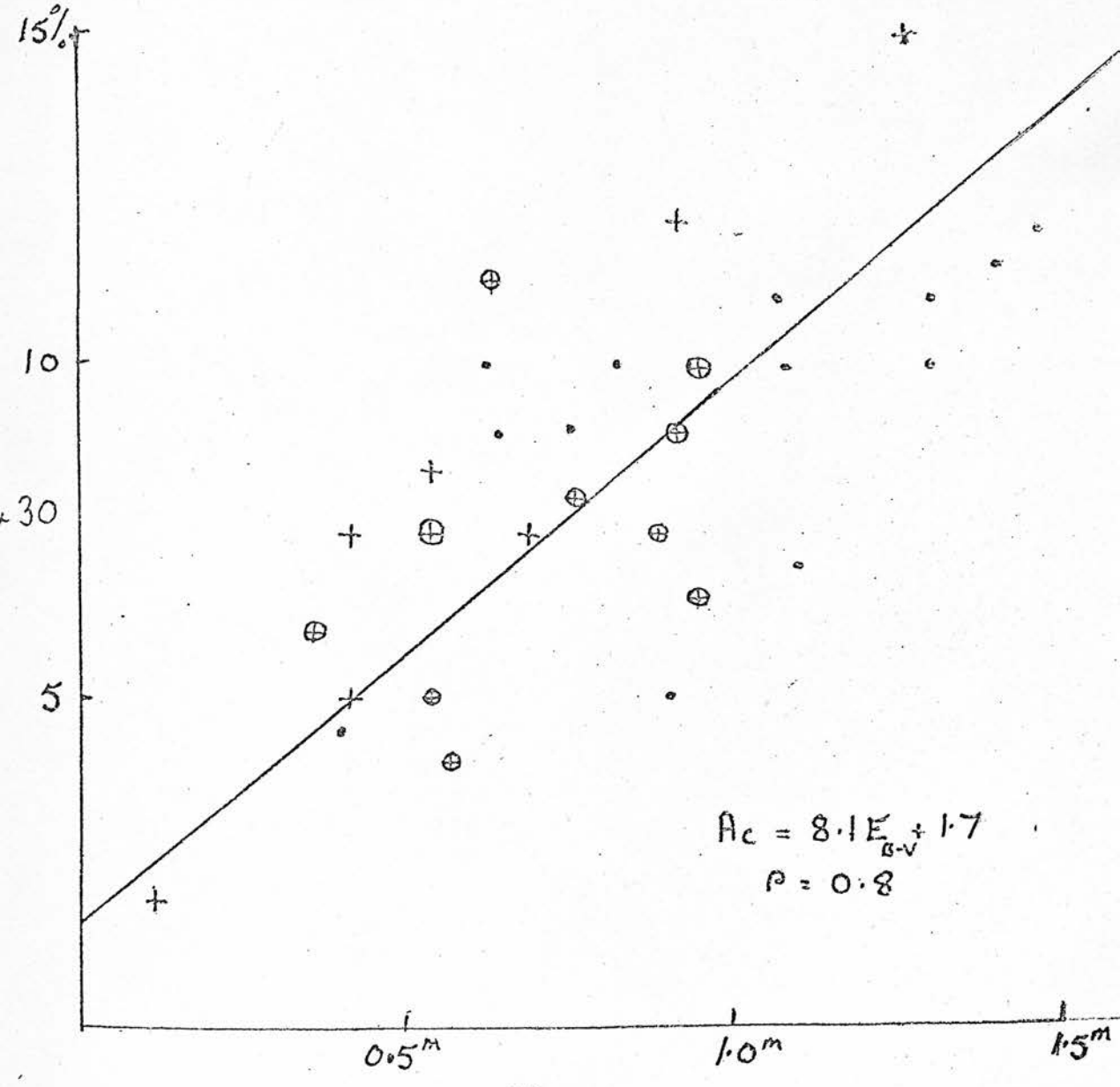

+ 36-inch observations ± 1% in A_c
⊕ 98-inch observations ± 2% in A_c
• 74-inch observations ± 2% in A_c

slight absorption is seen in confirmation of the low values observed by Wampler. Previous values were however larger and were probably confused by the strong stellar blends.

The profiles seen in the remaining stars do not show such emission wings and appear to be symmetric. The band intensities are however such that large emission features could not be expected.

Figure 2.9 The 4430 Å BAND IN HD 212455

3. COUDE OBSERVATIONS IN PRETORIA

3.1 A Description

All of the coude work here described was carried out in the southern hemisphere, the stars being chosen as previously. The telescope used was the Radcliffe 74-inch reflector at Pretoria. The coude spectrograph, dating from the 1960's is built around a Bausch and Lomb 8" x 6" grating operating in the first order in the red. A set of four cameras are available giving dispersions from 13.6 to 82A/mm. Auxiliary equipment includes an integrating exposure meter and a semi-automatic trailing system by which means widening of the spectrum is accomplished. Use is made of a dove prism to align the drift in R.A. with the slit length.

For work in which the longest possible spectral range was required, coupled with good resolution the F/1 field flattened Schmidt 'V' camera was chosen, giving a dispersion of 82A/mm. in the first order red. To ease measurement difficulties the spectra were widened to the full 0.2mm. possible with the system. A slit width of 60 μ was used, giving maximum illumination of the grating as well as a resolution of 1.5A. The emulsion used was 103aF, especially sensitive between 4500A and 6700A. This emulsion is stated to have a moderately coarse grain structure, with a resolving power between

56 and 68 line pairs per mm. It shows slight improvement in speed over Kodak II plates and though inferior in resolving power suited these observations where the resolution was seeing limited to 1.5A. Discussion with the staff at Radcliffe led to the belief that the gain in speed was worth the loss in resolution.

3.2 Calibration

Photometric calibration was achieved by the use of a calibration, grating spectrograph. Plates cut from the same plate material as the stellar plates were exposed for times, comparable with the stellar exposures, in the spectrograph and were later developed with the associated batch of stellar spectra. The calibration spectrograph utilised a Czerny Turner system, a chopped Neon light source and a stepped slit mask of twelve widths. The slit ratios had been both calculated from geometric considerations and determined empirically (Warren; Bromage, 1971). The ratios used were those which had been determined photoelectrically.

Wavelength calibration was achieved by exposing a Neon comparison spectrum before and after each stellar exposure.

3.3 Observational Procedure

At the beginning of each night a bright star was

centred in the finder, coude finder and on the slit of the spectrograph, before exposure tests were carried out. At the same time the R.A and declination errors in the setting circles were noted. Each star was located by use of C.P.D. and Smithsonian charts or of the plates of Hoag and Applequist. For each star the dove prism was adjusted so that drift in R.A. was along the slit. Drift rates were set so that during one exposure the star drifted along the slit about thirty times. Wavelength calibration exposures were made before and after each stellar exposure, care being taken to disturb the spectrograph as little as possible. Up to five exposures were possible on each plate by changing the angle of elevation of the camera to the optical axis.

Development of the plates was four up to ten minutes in Microphen, at 68°F, while being constantly agitated. They were then washed, fixed in Kodak Rapid and washed before drying.

3.4 Plate Analysis

Immediately after a night's observing a first 'look' was made of the spectra in order that any bad spectra could be retaken. The full microdensitometry of the plates was carried out according to standard procedures at Edinburgh. The whole analysis took several months and three methods were evolved to deal with it.

Initially several microdensitometer scans were made using the pen mode and approximate settings of the Joyce

Loebl. (Figure 3.1) By varying these settings the optimum were found for good resolution and low noise recordings. (Table IV). Pen tracings were then made for all the spectra at 16A/cm chart scale, for three regions near 5800A, 6300A and 6500A. Fog levels in adjacent areas were also scanned along with the wavelength calibration. With each batch of plates the calibration plates were also measured and their densities converted to Baker densities. Calibration graphs were then drawn and used to convert line strengths to intensities below a hand drawn continuum. These values were of fair accuracy for the sharp lines but were superseded by computer reduced values.

Each spectrum was digitised in the way described for the 'Spectracon' observations, along with adjacent fog levels. For each batch of plates the associated calibration plate was scanned at four wavelengths, 6600A, 6300A, 5900A and 5700A, in a direction perpendicular to that of the dispersion. At the end of each day's measurements a calibration was carried out that related the digital output to plate density.

For each level of the calibration plate a mean density was established and the interpolated fog levels subtracted. Using a table computed by Bromage for all the available Joyce Loebl wedges the step densities were converted to Baker Densities (Baker, 1955; De Vaucouleurs, 1968). This form of calibration plot gives

Figure 3.1

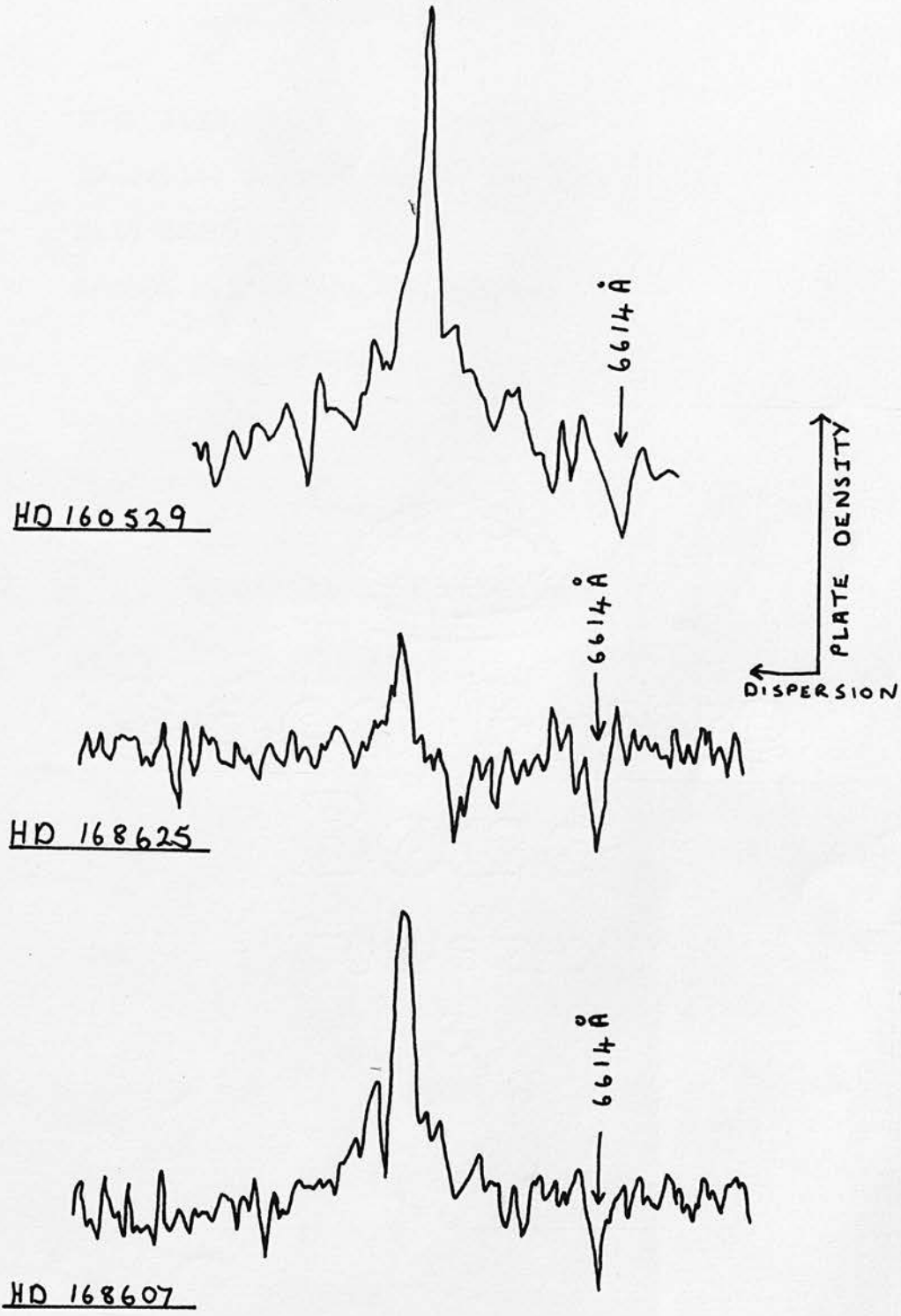

Examples of Traces of Spectra of Reddened Stars at Hα

TABLE IV

JOYCE LOEBL SETTINGS

STEP SIZE 12.5 Microns (1A)

PROJECTED SLIT WIDTH 20 Microns (1.6A)

SLIT HEIGHT 0.1 mm.

SOURCE SLIT WIDTH 30 Microns

========

TABLE V

Calibration Details (Warren)

SLIT	WIDTH	LOG I (GEOMETRIC)	LOG I (PHOTOELECTRIC)
1	29	0.000	$\bar{1}$.606
2	45	0.180	$\bar{1}$.964
3	57	0.290	0.164
4	79	0.429	0.350
5	122	0.615	0.594
6	171	0.763	0.773
7	237	0.902	0.908
8	327	1.042	1.048
9	446	1.177	1.181
10	629	1.326	1.327
11	879	1.472	1.469
12	1209	1.610	1.605

an almost linear relation between logI and the Baker Density. (Harris, 1969)

$$\Delta = \log_{10}(10^{D} - 1)$$

A least squares computer programme was then used to provide slope and intercepts for the calibration straight lines. Any points found on examination to lie far from the line were discarded and the fit done again. It was found that the gradients and intercepts varied little between the 5700A and the 5900A lines, so the calibration obtained for the 5900A region was used.

The main reduction of the spectra was handled point by point by a computer. However an early evaluation was made by defining regions of continuum at either side of the line under study. For each continuum between ten and twenty points were taken and averaged. Since for most regions of the spectra the deviation of the continuum tracing from a straight line over a small region was slight these averages could be taken to represent the interpolated continuum above the line. This continuum value and the line's value were then converted to intensity by means of the calibration curve, and the intensity of the line as a percentage of the continuum calculated. Though the values arrived at are fairly rough it was found that agreement with later values was good, except in the area of 5700A where the linearity of the continuum is very approximate.

TABLE VI

Band Integration Regions

Line	from	to	number of points	Error in EW
6614A	6622A	6606A	16	± 12 pm
6284A	6296A	6276A	20	13
Na D	5901 5892	5892 5884	20	13
5797	5791	5803	12	10
5780	5785	5775	10	9
6270	6275	6265	10	9
6200	6206	6194	12	10

= = = = = = = = = =

TABLE VII

Stellar Lines in the Red

Hydrogen Alpha	6560A	Carbon II	5889A
Helium I	6678A	""	5891A
Helium I	5876A	"	6578A
Silicon II	6371A	"	6582A
"	6347A	Sulphur II	6286A
"	5863A	"	6305A
"	5800A	"	6287A
"	5806A	Aluminiun II	5723A
Nitrogen II	5711A	Sodium I	5890A
"	6379A	"	5895A
"	5747A		

Fig 3.3

Histogram of Errors from Continuum Fit of the Coudé Spectra

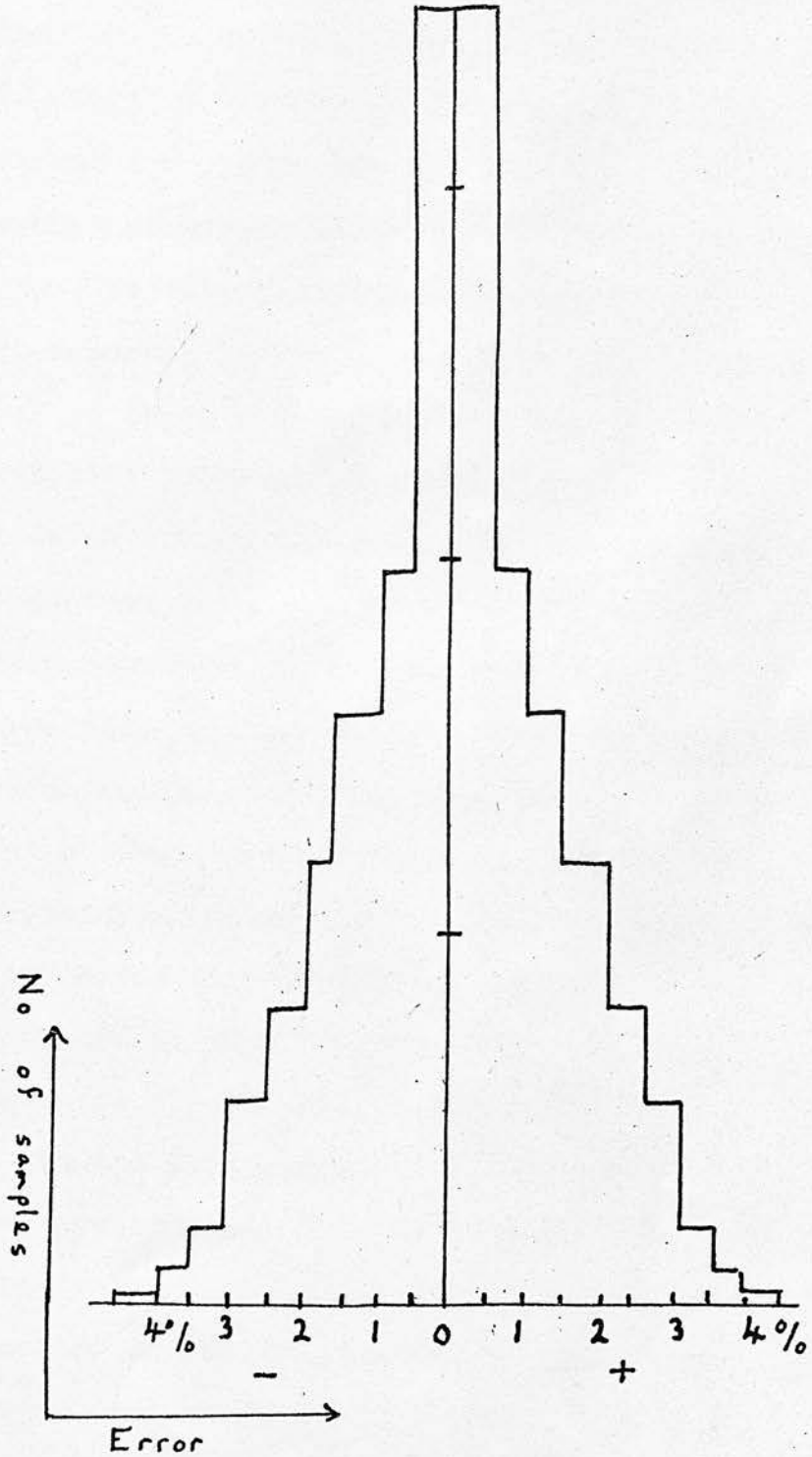

The main computer reduction was carried out point by point after an initial print out of values for the whole spectrum. From this print out the areas 5800A, 6300A and 6500A were identified from their positions relative to the Helium and Hydrogen lines. A programme WZ60 was then used to select data from these regions, subtract the fog levels and convert the values to intensities. A second programme WZ400 then fitted a continuum to each region, rejecting data lying over three percent from the fitted curve, before recomputing the continuum. A rejection level of three percent was set to reject most of the absorption lines and plate defects while having little effect on the actual continuum. Analysis of several spectra showed that the standard deviation associated with the fitted continuum was less than 1.5 %. A histogram of the deviations from the continuum is shown in figure 3.3. To ensure that only data near lines was omitted full print out was given during computation, enabling the discriminator level to be raised if required. The spectrum was then rectified and displayed in graphical and numerical form. Finally the equivalent widths were calculated for the sharper features.

In the region from 6276A to 6298A there 23 telluric lines mentioned in Rowland's Revised Solar Tables. From these tables came the line positions of possible blends affecting the diffuse bands. To gain some insight into

the telluric band the lines were grouped in one Angstrom blocks and the total absorption for each block calculated using relative strengths from Griffin's Atlas of Arcturus and the Utrecht Solar Atlas. There appeared to be two easily distinguishable blocks outside the 6284A band. From observations of unreddened stars made at low latitudes this was confirmed and two relationships found for these blocks, as well as the band overlying the 6284A feature.

$$A_c 6284A = 0.6 A_c 6277A \quad \text{for OII}$$

$$EW\ 6284 = 7x\ A_c 6277 \quad \text{for OII}$$

The corrections made using these relations agreed well with corrections based on the air-mass constants (Bromage and Nandy, 1973) and those based on the reflection of the unaffected half of the diffuse band profile. Few of the spectra reduced were made at zenith distances of greater than 45 degrees.

3.5 Stellar Lines in the Red

In reddened early type stars the chief lines apart from those of Helium (5876A and 6678A) and Hydrogen (6560A) are the interstellar lines and bands(Table VII). Of these those of Sodium (5890A and 5895A) and the diffuse line at 6284A are especially important. Other lines due to Silicon II, Sulphur II, Carbon II, Aluminium II and Nitrogen II are also seen.in this investigation.The most troublesome effects are however caused by the Telluric

Figure 3.2

The Atmospheric Alpha Band a 6284Å Band

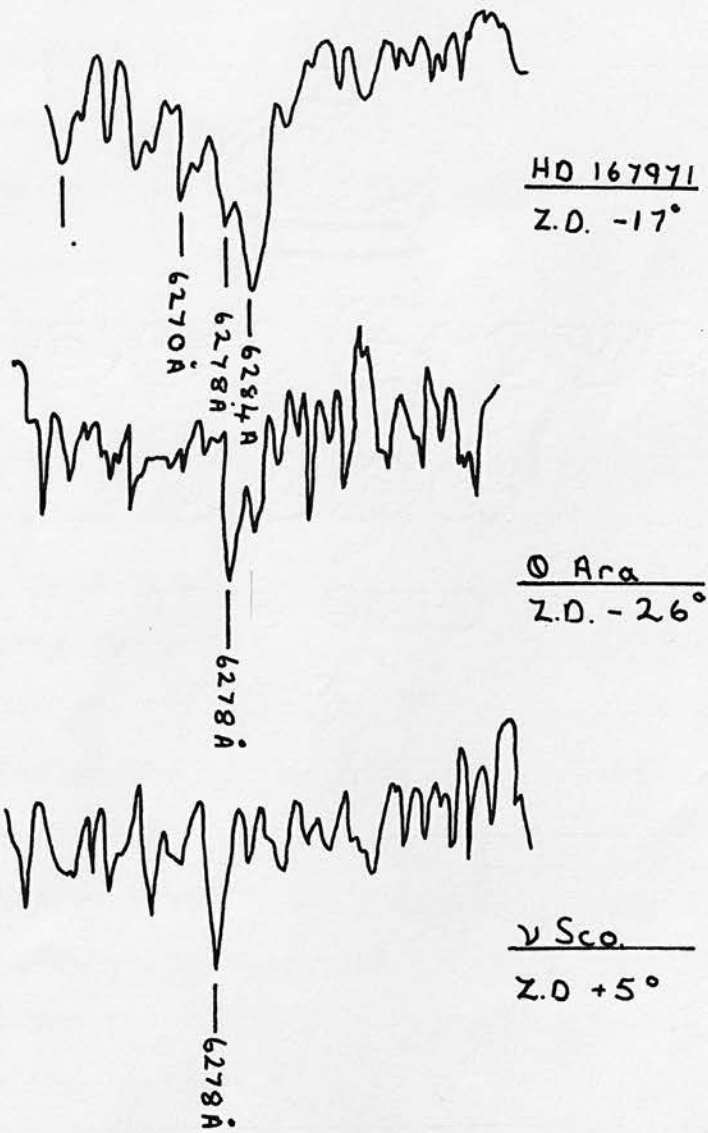

band systems at 6276A and 5780A. (Van de Hulst, 1945) Panofski, 1943; Babcock and Herzberg, 1948). The removal of the Alpha band has been discussed already. The effects of the 3-0 band at 5780Å have not however been removed.

3.6 Error Analysis

In the above methods error analysis is not simple. The errors may arise from

(i) Calibration.

(ii) Continuum fitting.

(iii) In the digitising of the spectra.

The largest errors probably arise in the calibration procedure. To minimise these all of the spectra were developed with their calibration plates, both were digitised using the same settings and on the same day, and both were reduced in the same manner. The calibration curves were drawn using wedges with overlapping ranges. Deviations from the straight line of the calibration curves were less than 3%. In this manner it was noted that a wedge quoted by the manufacturers as being of slope .11D/cm. was in fact .13D/cm., a fact that would not have been obvious if only one wedge had been used throughout.

Errors arising from the line fit to the calibrations are at worst two to three percent (Appendix). Larger errors arise from noise. From a statistical analysis of several spectra the R.M.S. deviation over twenty points is again about two percent.

Errors arising from fitting of the continuum are thus small.

Errors may also arise in the digitising of the fog level. The fog levels varied only slowly and the error in digitising is about one percent.

The errors in central depths should therefore be of the order of $\pm$ 3 %. The error in determining the line's equivalent widths is a combination of these errors and can be calculated from

$$S.D. = \sqrt{N} \times s.d.$$

where s.d. is the error for each point of the spectrum. The equation is an approximation of that given by Baker (1949) and is derived in the Appendix. The errors are stated in Table VI.

Analysis of the broad bands near 6180A and 5780A were not undertaken as they were shallow and close to the noise level and regions of sensitivity variations.

4. THE SCANNING SPECTROPHOTOMETER

4.1 Introduction

The design of a scanning spectrophotometer was begun in order to study the profile of the feature at 4430A and to investigate the wavelength dependence of polarisation within this feature. To date the system has operated on two stars and comparison between the results obtained with the 'Spectracon' and the scanner have been made.

Boksenberg said "The fundamental limitation in detecting radiation at low levels is due to the quantum nature of the radiation. The information in an image may be expressed as spatial and temporal variation in the number of photons. The problem of detecting and recording such an image lies in counting the number of photons in each image element." Thus an ideal detector should have the characteristics:-

(i) Of recording every photon with equal weight and in a noise free way.

(ii) Retaining spatial information.

(iii) Retaining temporal information.

(iv) To have infinite information storage capacity.

The last of these can be best approached by computer storage methods. The second is limited by the instruments resolution and the third affected by scintillation.

In the design of this device it was hoped that fast scanning would overcome much of the transparency variations, as well as atmospheric seeing and scintillation. Rapid scanning cannot however remove the high frequency components of the scintillation and all that was attempted here was the reduction of these and the removal of the lower frequency sky transparency and scintillation. It is possible to reduce such effects by continuous monitoring of the whole spectrum (Stoekley and Dressler). The scanner was therefore designed to be capable of operating in both the fast scan mode and the slower mode with a monitor channel. The latter mode is at present being used to test the mechanical and electronic stability of the system.

The use of photon counting methods was decided upon because these are capable of better results than D.C. techniques and are well suited to digital control (James, 1967; Tull, 1968). Discussion of the photon counting will follow in the next part.

The scanner was designed to work on the present 36-inch spectrograph in the F/3 camera beam. This raised some problems in obtaining the required 1cm. scan with a resolution of .025cm. (5A at a dispersion of 40A/mm.). An investigation into the various fast scanning methods, using reflection off, or refraction through, rotating glass blocks, found that such methods were incapable

of giving the required resolution and scan length in an F3 beam. The available methods of electronic scanning, involving vidicons and image dissector tubes were too expensive although probably the best solution to the difficulty. Rotation of the grating would preclude the use of a fast scanning mode.

Eventually a design utilising a moving, analysing slit in the camera focal plane was settled on. Behind this was placed the photomultiplier head. The difficulty then lay in fitting the optics, mechanics and electronics into the confined space available.

The scanner was built in two sections, the mechanical scanning section and the photon detection and control system. The former was designed and built entirely by Mr. S. Salter of the Department of Machine Intelligence and Perception of this University. The second was designed and built by the author.

4.2 Photon Counting

To evaluate the signal to noise ratio or the errors involved in photon counting systems we deal with the statistics of photoemission, and secondary emission of photons. Although the emission of photons obeys Bose-Einstein statistics when a black body is the source, for all bodies of practical interest the approximation of Boltzmann statistics may be used in the visible spectrum.

The R.M.S. deviation from the average number of

detected photons is then simply the square root of that number. Although this argument neglects the dark current of the detector, this can be reduced by the cooling of the detector or by the use of specially designed tubes. The information rate using pulse counting techniques can be 1.2 times faster than the equivalent D.C. system. (Morton, 1968; Baum, 1962; Tull, 1968). A higher signal to noise ratio is also the result of using photon counting (Lynds et al., 1967). These advantages arise in part from the elimination of variations in the gain of the device and the filtering that is possible to discriminate against electrons not arising in the photo-cathode (Foord et al., 1969).

A fuller discussion of the methods used in this device follow.

4.3 Atmospheric Scintillation

Since the application of A.C. methods to stellar photometry interest has arisen in atmospheric transparency variations. The most complete discussion of these effects is to be found in a review by Whimbush (1961), who defines several effects of which the following concern this investigation.

(i) Integrated light scintillation.

(ii) Colour scintillation.

(iii) Polarisation scintillation.

(iv) Image motion.

Ellison and Seddon found that for low altitudes the predominant frequencies of the scintillation were the lower frequencies, while near the zenith the effect of these decreased, leaving the high frequency component. They (Ellison and Seddon, 1952) also noted no large colour effects while using the 36-inch reflector at R.O.E. Similar colour scintillation was also noted by Hoag et al. (1951) as well as the normal scintillation in integrated light.

Image motion of the order of 10" arc and low frequencies has been studied by Hosfield (1954) and has been shown to be sensitive to local turbulence. Similarly the high frequency image 'dancing' has been attributed to the air in front of the mirror (Steavenson, 1935).

To reduce the effects of the long period atmospheric transparency variations scan times of one minute will suffice. The scintillation will then be integrated over this period and the error of the observations will no longer be purely due to photon statistics. A scan of one second will appreciably reduce even these scintillation effects although the high frequency components will remain. The longer period image wander is easily compensated for by autoguiding, and since with apertures of 36-inch there seems to be little colour scintillation this should be of no bother.

4.4 Mechanical Design

As previously mentioned the design of the scanning section called for a long scan of 2.5cm. maximum and 1cm in normal use. To achieve a straight line motion over such a distance and at high accelerations and speeds was only possible by the use of low friction hinge systems. Of these the most suitable was found to be the "Watts Linkage" (Figure 4.1). The analysing slit is mounted on two such systems and driven across the spectrum, through six wires, by a stepping motor. Behind the scanning mechanics lies the photon detection system. The whole sequence of operations is controlled by a series of scalers operating off clock pulses.

In order to discuss the system properly it is best to discuss it in its various mechanical and electronic parts.

(i) Slit Suspension (Figure 4.2)

The straight line linkages involved were "Watts Linkages". One such linkage consists of two radius arms hinged to the base plate of the scanner at one end and at the other free end to a rigid cross member. The mid point of this cross beam moves in a close approximation to a straight line. An analysis of the motion is difficult but an approximate solution shows that for a linkage with radius arms of length R and a cross beam length L the deviation from straight line motion is

$$\frac{S^5}{2 L R^3}$$

Figure 4.1

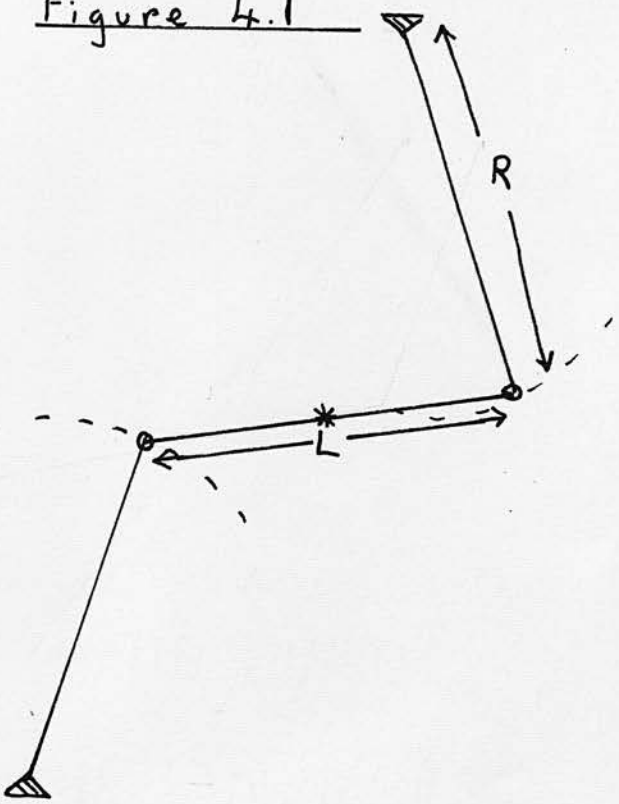

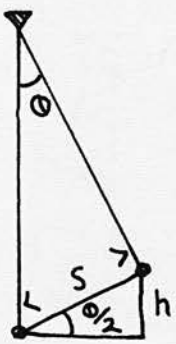

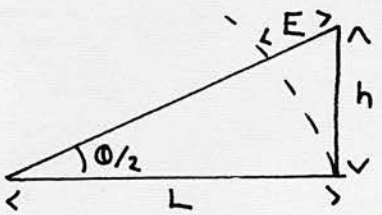

(i) $\Theta = S/R$

(ii) $h/S = \Theta/2 = S/2R$

$\therefore h = \frac{S^2}{2R} = H/2$

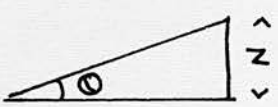

(iii) $E = \frac{H^2}{2L}$

(iv) $Z = E\Theta = \frac{S^5}{2LR^3}$

The Watt's Linkage

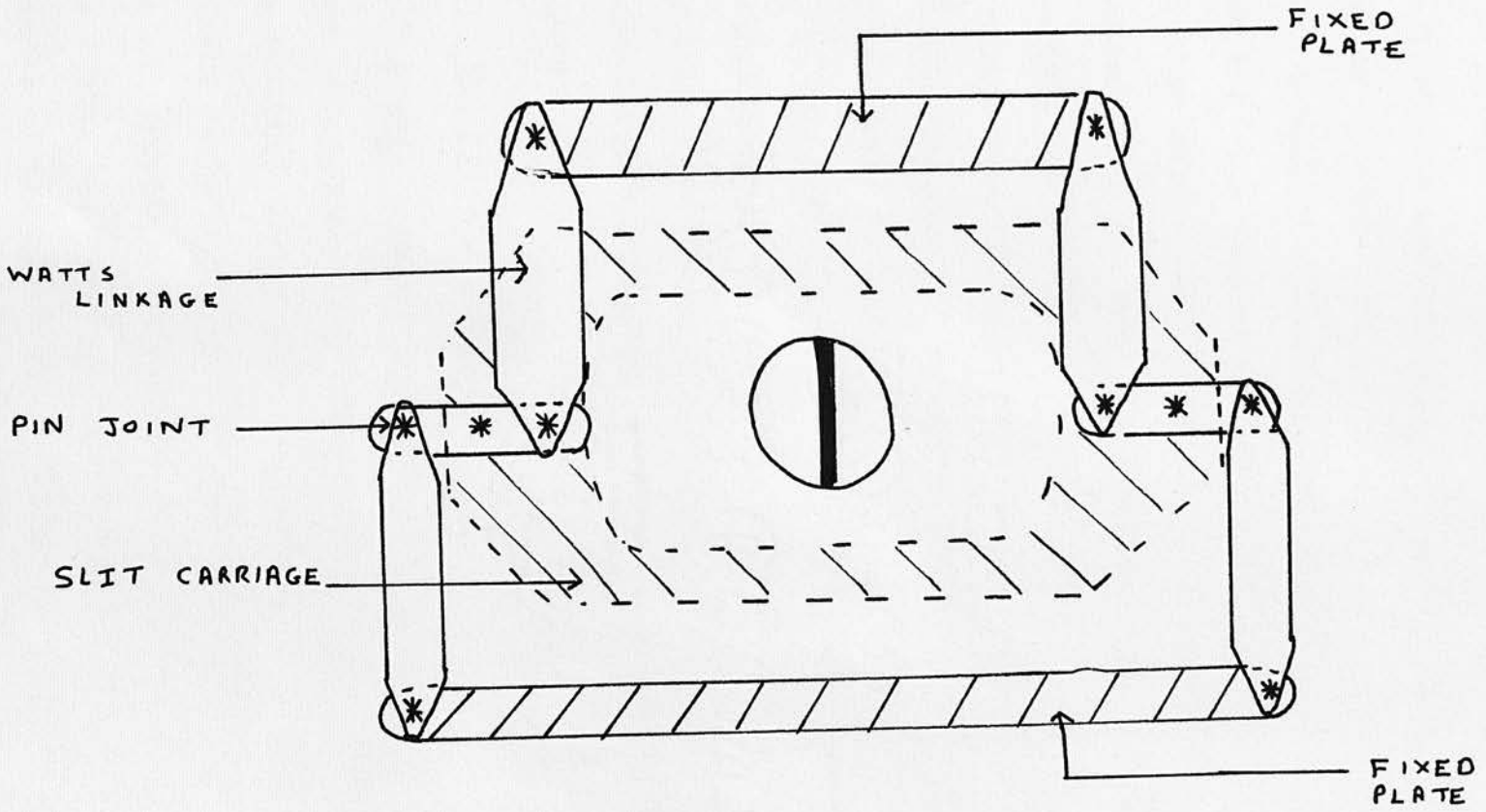

Figure 4.2

The Slit Assembly

where S is the scan length. For this design the values L = 4" ; R = 2" ; S = 1" were used and the error is at most 1/10 000". A computer programme was also used to solve the complex equations governing the motion by an iterative procedure and deviations of $5/10^5$" in a scan of 1" were found.

The actual slit suspension is in the form of a rigid hollow box with an oval hole cut in its rear face and a circular hole in the front face. The assembly is suspended at either end from the centre points of "Watts Linkages", the ends of which are attached to the base plate. The radius arms of the linkages are 4" long and the cross beam 2". The commercially produced slit unit is screwed onto the box's face.

The low friction hinges are of the sort using ball bearings clamped between phosphor-bronze cups, which are sunk into the arms of the hinge. Any wear can be accommodated by clamping up the top surface of the hinge (Figure 4.3).

(ii) The Drive System

The slit assembly is driven by an HS50 stepping motor through a system of six steel wires. These wires are attached to the slit carriage by tensioning devices. (Figure 4.4). Each wire is wound onto its capstan and its end trapped. Keeping it under tension it is led via a stop (d) around a roller bearing (c) to the drive spindle of the motor (b). It is then wrapped once round the spindle and returned via a second roller bearing (a) and

Figure 4.3

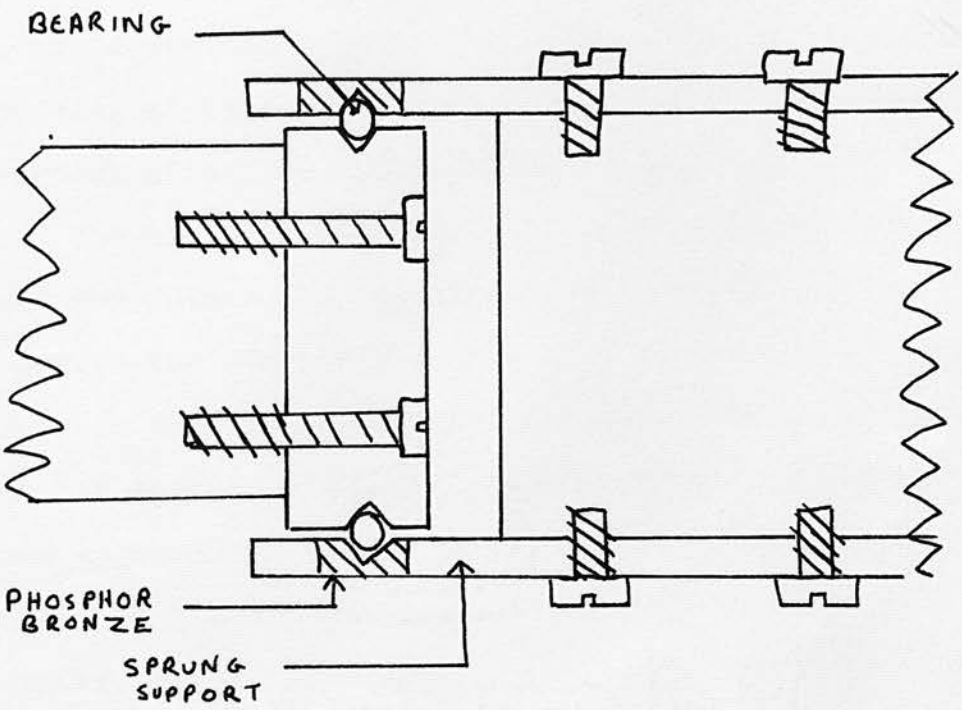

Low Friction Hinge

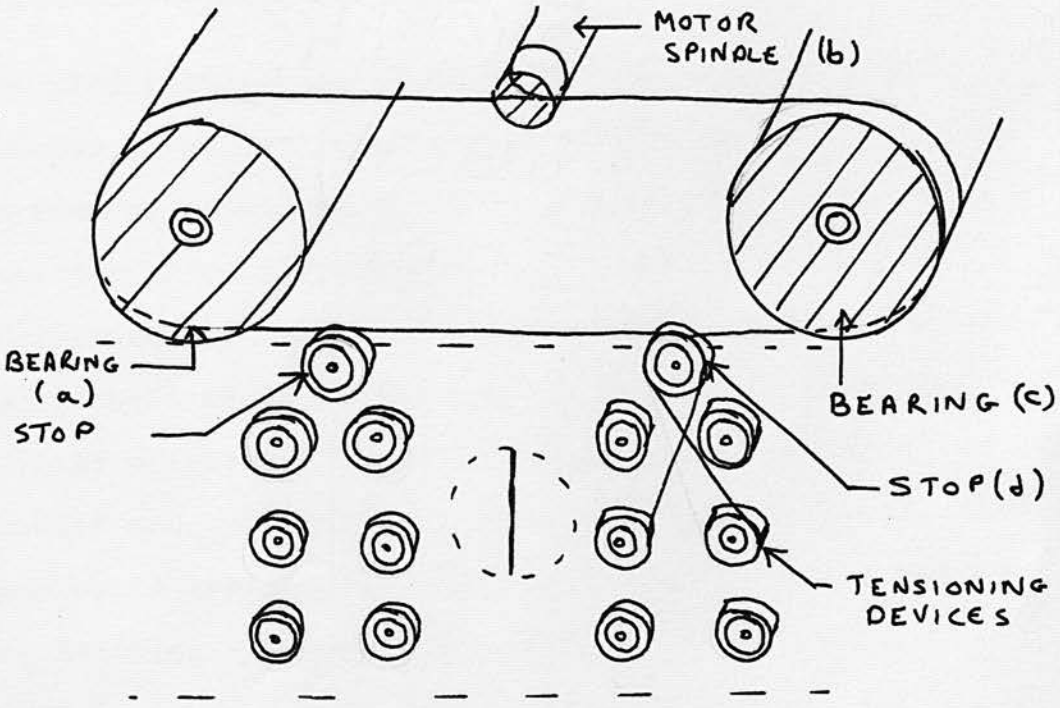

Figure 4.4
Drive System

stop (d) to a tensioning device opposite that to which the wire's other end is attached. The remaining wires are then strung and the final tensioning carried out by tuning to a predetermined pitch. The drive system is capable of running at full speed with only three of its wires intact, without affecting the accuracy of the scan.

The Slow Syn HS50 motor is capable of making 200 steps per revolution and 500 steps per second when driven through the STM 1800V supply card here used. The error in each step is $\pm 5\%$ and is nonaccumulative. One step of 1.8 degrees should move the slit carriage about six Angstroms. In actual operation a step length of 6.25A is found. The motor supply is from a 30 volt centre tapped D.C. supply with a maximum ripple of 5%.

(iii) Positional Read-out

The position on the scan is only known by the number of pulses input to the control system. A secondary system of transducers, one long-throw and one of a shorter throw (provides some positional information). The former can be used over the whole scan to operate the scan coils of an oscilloscope for real time displays of the spectrum. The second transducer operates over 0.025" and provides a moveable datum mark. Before use the whole system needs wavelength calibration achieved by scanning a comparison spectrum.

(iv) The Photomultiplier Head (Figure 4.5)

The space available at the rear of the spectrograph is severly limited, if the instrument is to pass through zenith without grounding. For this reason the whole scanner has been designed to be as short as possible. In such a compact design the photomultiplier lies close to the motor and the high level pulse carrying lines. For this reason the tube is shielded. This mu-metal shield extends t cover the dynode resistor chains at the base of the tube. The whole shield and photomultiplier tube fits within a second tube which carrier the Fabry imaging optics. The two element Fabry lens is simply held by four retaining rings which fit the screw threaded tube end. The whole assembly is clamped, by three screw clamps bearing on a circular collar brazed to the tube, to the back of the scanner. No cooling is provided for the tube and would be difficult to fit such into the restricted space

In order to image the camera lens onto the 1cm. photocathode a Fabry lens system that would not vignette the beam was required. The slit is mounted in the focal plane of the camera, 30cms. from its principal plane and close to the scanner's front plate. To achieve the necessary imaging a compound system with 4.5cm. aperture and 3cm. focal length was used. The component lenses of 10cm. and 5cm. focal lengths are separated by 5mm. and lose 16% of the light. Fitting such optics

Figure 4.5

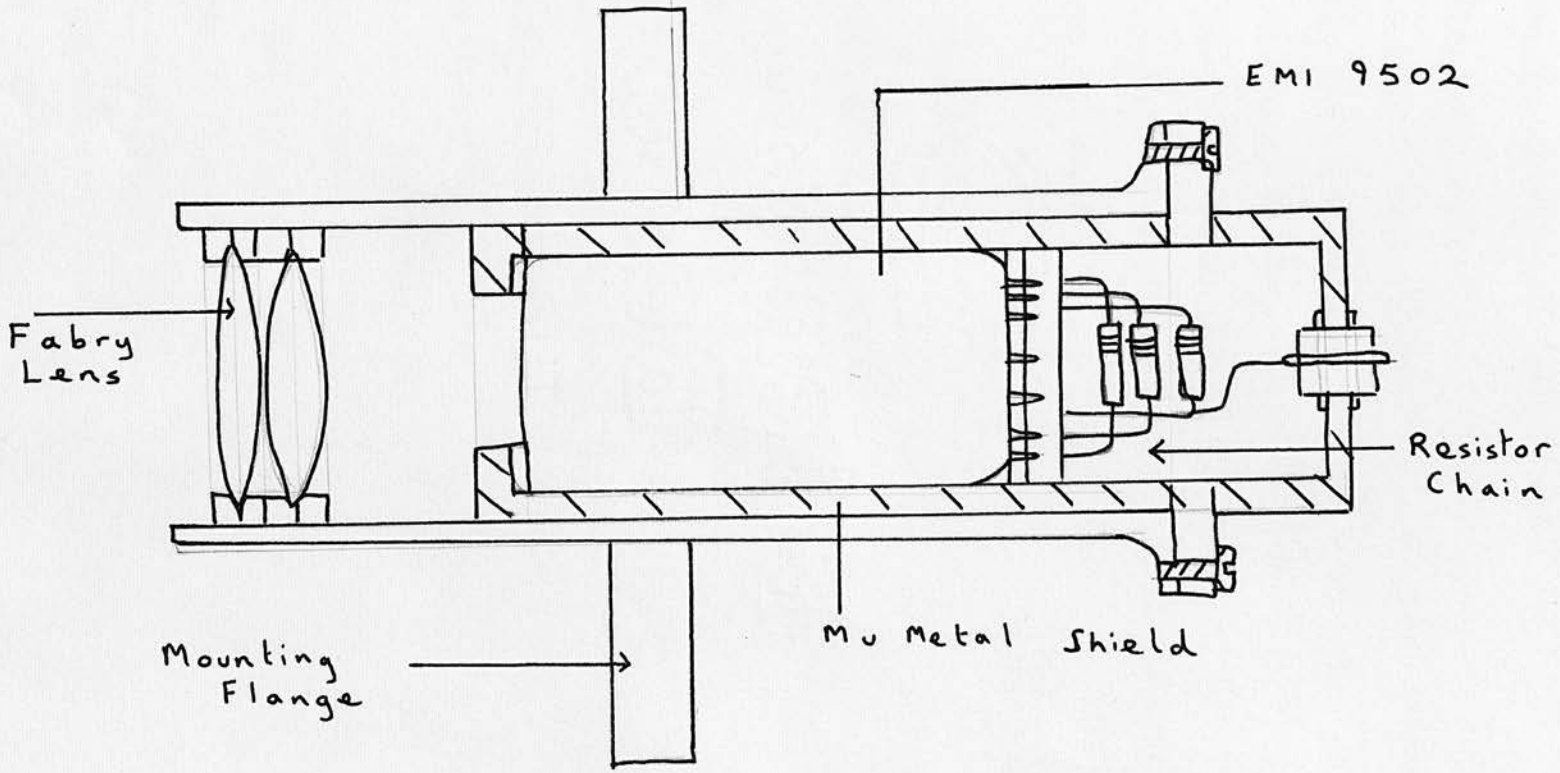

The Photomultiplier Head

required a large aperture at the rear of the slit carriage.

(v) Mounting on the 36-inch Reflector

The camera lens is removed from its usual mounting on the plate holder and relocated on the same mounting plate as used with the Spectracon. To this plate is attached a new mounting bed. Upon this the scanner is located by two large studs and is clamped by three screw clamps. This type of mounting allows rapid removal and alignment of the scanner.

4.5 Electronic Design

(i) The Photomultiplier Supply

The scanner was originally designed to use low noise, high gain EMI 9502 or 6256 tubes. These are venetian blind type photomultipliers with CsSbO photocathodes and CsSb bynodes. These S11 cathodes have quantum efficiencies close to 18% at 4000A and are 1cm. in diameter.

As mentioned the tube is mounted in a mu-metal can and is cushioned at the front by a sponge pad. A standard EMI 15 pin base plate is used and the recommended resistor chain is used with the cathode earthed and the anode at a positive potential. A maximum anode current of 1MA and a maximum operating voltage of 2500V dictate the use of 100KΩ resistors and the cathode to first dynode voltage is stabilised by use of a Zener Diode. The last dynode is decoupled to earth and the next two

decoupled to it. In this way large amplitude pulses can be measured by the system.

The output of the photomultiplier is passed to a Harwell Series Head Amplifier, Amplifier and Discriminator, all of which are well matched for use with the system. The head amplifier is mounted close to the scanner to avoid spurious pulses. All of the power supplies required are supplied by the Harwell supply. A full discussion of the operation of these units will be given later.

(ii) Control Unit

The sequence of operations is as follows:-

1. The motor is stepped
   The scalers are inhibited
   The scalers are output onto magnetic tape
2. The scalers are reset
3. Counting begins and is stopped after a set period

1. The motor is stepped.

The control unit utilises Texas Instruments Plastic Dual In Line integrated circuits. The heart of the system is a 16 channel data selector, which converts parallel data into series data. The simplest way to discuss the logic of the controller is in its various functions:-

1. Control of photon counting
2. Control of the motor drive
3. Control of data output

All sequencing of operations is carried out by a 12 bit

counter operating off positive going clock pulses. Logic operating off this counter provides data selection counter control and motor control.

1. Photon Counters

A second twelve bit counter (3 four bit binaries SN 7493N) receives signals, converted to the positive logic of the counters, from the Harwell discriminator. The input is gated by an 'AND' gate operated by the inverted pulse from the sixth bit of the sequencer (16th to 32nd clock pulses). The resulting waveform is again inverted and enters the counter. The counting circuits reset when the inputs R01 and R02 are both at logical '1'. This is achieved by taking the R01 signal from the fifth bit of the sequencer and the R02 signal from a cascade of three 'AND' gates operating off bits one to four of the sequencer. Each bit of the counter outputs to one contact of the sixteen bit data selector. (Figure 4.6).

2. Motor Control

The motor is driven from a Slow Syn card STM 1800V which has an inbuilt oscillator and facilities for single stepping and direction controls. During the rapid scanning the translator is triggered off the back of the signal from the fifth bit of the sequencer. This waveform is first amplified by a Hex Buffer Driver (SN7416N) so giving the 10 volt negative going pulse needed to drive the translator. The scan direction is

Figure 4.6
Reset Logic

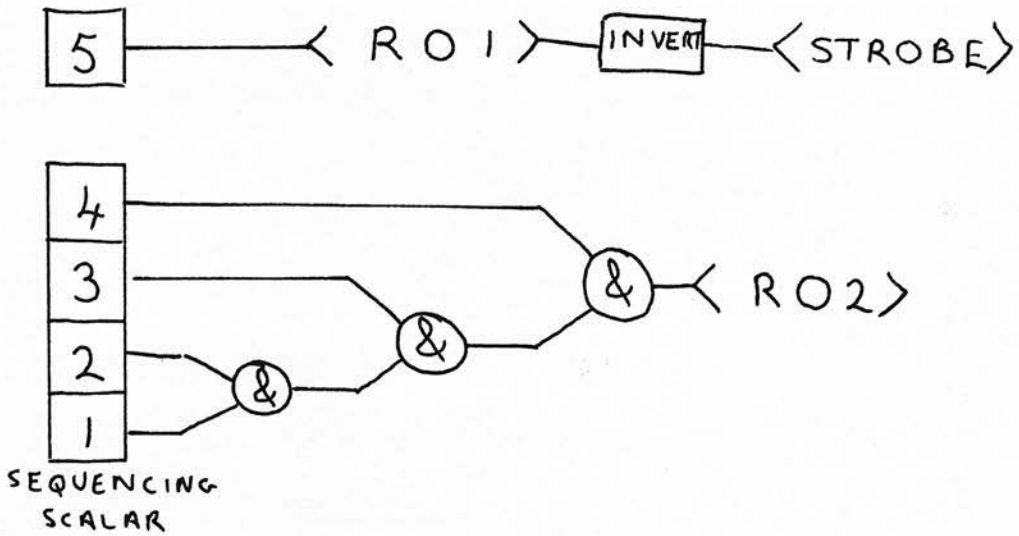

Figure 4.7
Motor Control Logic

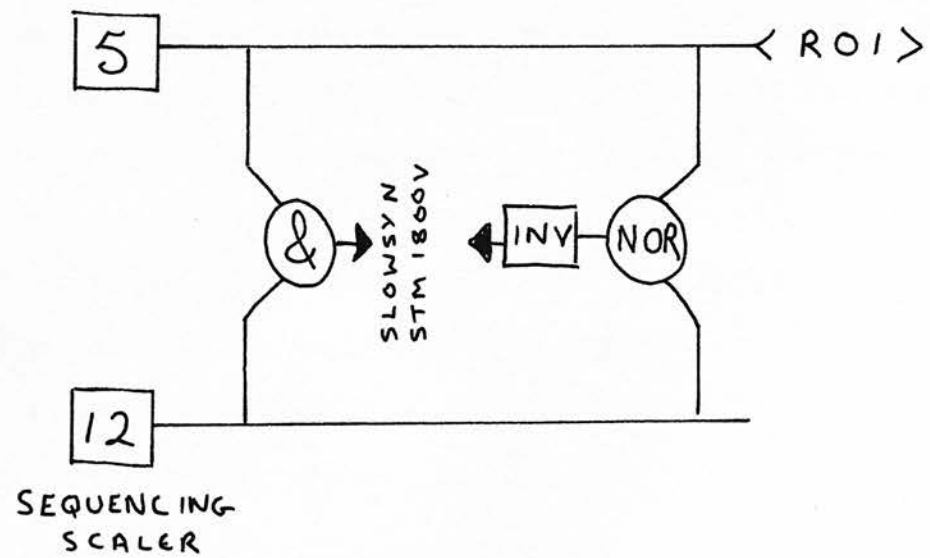

controlled by 'AND' gating the signals from pin 5 and pin 12 to provide the forward stepping, as well as 'NOR', gating these signals and inverting them to provide the reverse motion (Figure 4.7). A reversal in motion thus occurs every 2048 clock pulses or 128 motor steps. The length of scan may be altered by using pins other than pin 12 of the sequencer to gate the signals. At present the reversal is abrupt and a deceleration circuit is needed to smooth the motor's operation.

3. Control of Data Output

At the end of each counting period the input to the twelve bit photon counter is closed and the motor stepped. Each bit is read by a sixteen bit data selector (SN 74150N) operating from the first four bits of the sequencer (Figure 4.8). The selector is strobed by the inverted pulses from pin five of the sequencer. The first and last bits of data output are used as markers and the input pins of the selector maintained at +5 volts. The remaining input pins of the selector connect with the twelve pins of the photon counter. The output of the selector is inverted and fed to a Revox A77 recorder. A second channel of the recorder is fed clock pulses. These match the positive logic of the I.C.s and are square five volt waveforms derived from any suitable generator.

4. Computer Input

Originally the scanner was designed to operate in

Figure 4.8
Data Selection Logic

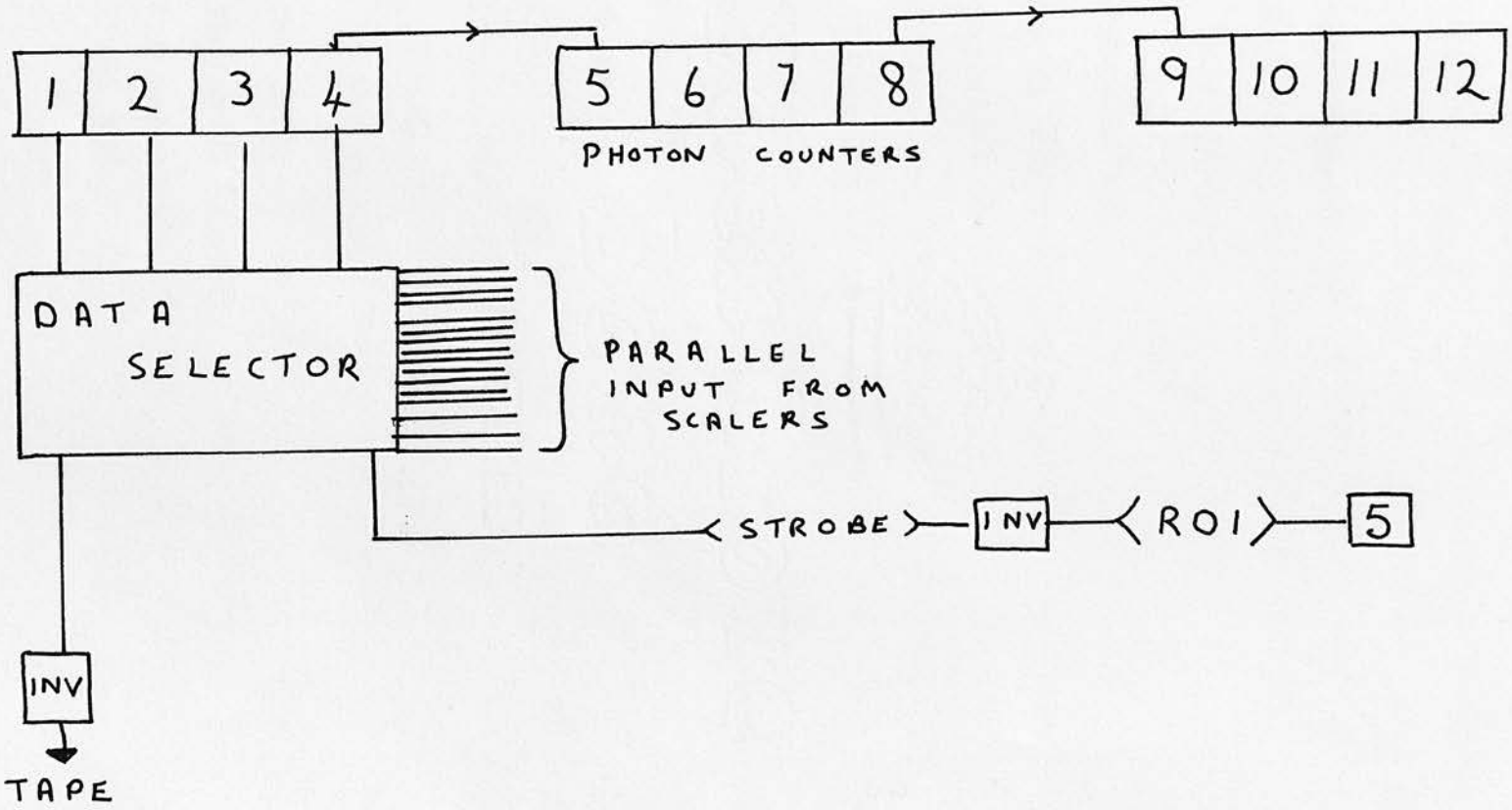

conjunction with the Elliot 4130 computer at the observatory. Since the design stages, the interface system has been dismantled and it was decided to operate and prove the mechanics of the scanner in a slow scanning mode and the electronics in the laboratory. At a later date it is hoped that the computer will be used to access data from the Revox tapes.

4.6 Slow Scanning Mode

Basically in this mode the control system as previously described is not used. Instead of rapid scanning and so reducing the effects of transparency variations the device is slow scanned and such variations monitored by a second photon counting channel. In the 36-inch spectrograph light is taken out of the beam after collimation and fed to a photomultiplier which operates the exposure meter. For these observations these signals were fed to an identical chain of Harwell pulse shaping equipment as was used for the main photon counting channel. The second channel was used to control the counting operations of the main channel. The operation is as follows:

(i) The motor is stepped.

(ii) The count is begun on both channels.

(iii) The comparison channel reaches a preset count limit and stops the main count.

Figure 4.9

Slow Scanning Control System

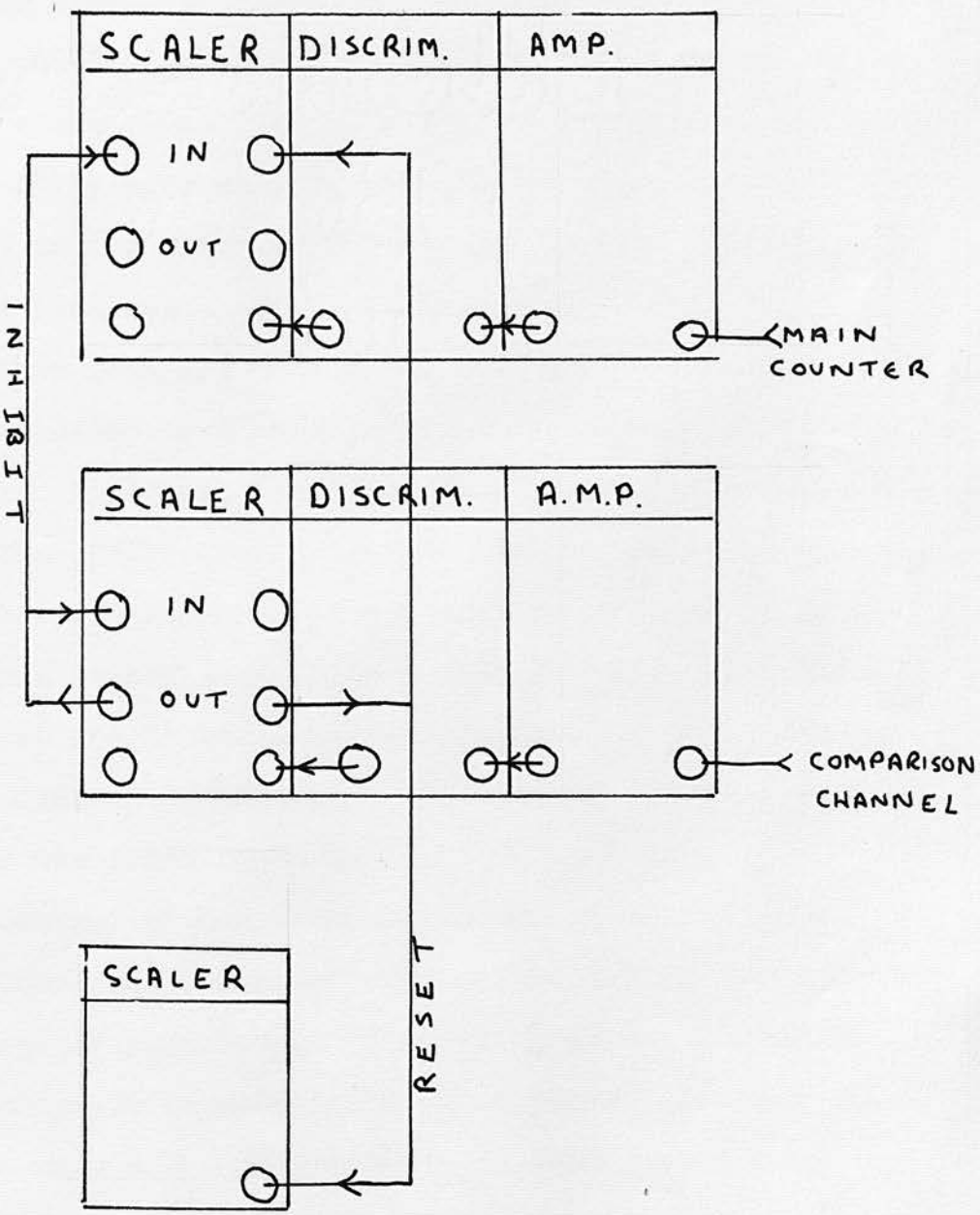

This slow scan method was used for all the observations so far made. The method of observation was as follows.

The main problems lay in the initial setting up and alignment of the scanner, so that the scan direction lay along the direction of dispersion. For this initial alignment the spectrograph was illuminated with a Helium discharge lamp. The spectrograph was adjusted so that the line at 4471A was nearly central in the field before the scanner assembly was mounted. With the scanner slit fully open and a microscope focussed on the slit jaws, in the place of the photomultiplier assembly, the 4471A line was located on the scanner slit. The spectrum was then focussed onto the slit jaws. The Helium spectrum was replaced by a white light spectrum and the scanner rotated until the direction of scan lay along the spectrum.

The spectrograph slit was then opened to give a projected width of 5A and the scanner slit adjusted so that it was just filled. A wavelength calibration scan of the Helium was then made and the step length and position of the 4471A line noted. For this a rate-meter was found to be sufficiently accurate.

Control of the stepping, counting etc. was from the count and reset switches on the Harwell comparison scaler. (Figure 4.9). On reaching a preset limit the scaler produced an inhibit signal which inhibited the main count and self-inhibited. Reset pulses from the comparison scaler also reset the main scaler and the

count was begun only when the inhibit signal on the comparison scaler was cancelled. The motor was stepped by a separate control and the number of steps made from the datum position counted on a Harwell timer. The scaler output was noted by hand.

In order to optimise the performance of the system normal methods were difficult to apply since these result in finite dark counts in both channels. These would be difficult to remove in subsequent processing. To simplify the initial trials the counting chains were adjusted to give the highest signal to noise ratio possible. The main channel photomultiplier was run at 1.9Kv with main amplifier gains of 73.5db and a discriminator level of 3 volts. The head amplifier and main amplifier had 0.1μ sec. differentiation and the latter 0.05μ sec. integration. The comparison channel's amplifier was set at 68db gain and 1μ sec. differentiation and 1μ sec. integration, while its head amplifier supplied 1μ sec. differentiation. The supply voltage was chosen from initial tests and was found to give the highest signal to noise ratio (James, 1967). The time constants were adjusted to give the best count rates. If the head amplifier has a greater time constant than the main amplifier then overload paralysis will occur. For high level signals the integration should be kept as low as possible. The levels here have been attenuated by a factor of about 3db by the choice of integration consta

4.7 Scanner Results

Initial calculations indicated that observations of an A0 star of fifth magnitude would take ten hours in order to reach a photon count of 10^4 or a one percent accuracy.

Observations began in the winter of 1972 but because of bad weather conditions the first scans of stars were made in February 1973. These trial scans were made in the slow scanning mode and were fifty steps in length (300A) centred on 4500A. The scans were set up on the 4471A line and extended 30 steps to the positive and 20 steps to the negative. Stars previously observed using the Spectracon were chosen, one reddened and one less so. The first star HD 36371 was scanned with 13A steps in a positive direction and then rescanned in a negative direction. Towards the end of the two hour observations it was noticed that a drift in the counts had occured. On subsequent tests it has been found that the drift occurs in the comparison channel, in spite of long periods being allowed for the equipment to stabilise before scanning commences. Later scans used a lower count limit and all observations were made at least twice at intervals separated by up to an hour.

Further scans were made of the star HD 91316, a fifty point scan with a count accuracy of $\pm 2\%$ being made in two hours. Bad weather terminated further work,

Figure 4.10.

and the final scans were complicated by lack of auto-guiding facilities and other telescope faults. Difficulty in calibrating the scan positions with wavelength also arose and a better system of calibration optics found to be necessary.

The scans obtained are shown in Figure 4.10 and comparison with the 'Spectracon's' observations shows well the effects of reduced resolving power. The 4430A absorption of 10% in HD 36371 is larger than that found in the spectra previously (7.5%). Comparison is hindered by the exclusion of the continuum to the blue of H γ. The main line absorptions have been resolved although the resolution is insufficient to separate the lines at 4471A and 4481A in HD 36371. The results encourage the use of the scanner to investigate the polarisation variations across the 4430A feature.

5. THE STARS, THEIR POSITIONS AND CHARACTERISTICS

The stars observed can be simply separated into those in the Sagittarius area and those towards the anticentre and local arm.

5.1 Sagittarius Direction

The stars observed from Pretoria lie in the region $355^{o} \leqslant l^{II} \leqslant 19^{o}$ and $-3.2^{o} \leqslant b^{II} \leqslant +1.7^{o}$. The area is dominated by the Sagittarius (-I) arm, extending from $274^{o} \leqslant l^{II} \leqslant 32^{o}$ at a distance of 1.5 Kpc. at $l^{II} = 338^{o}$. (Georgelin, 1970). Less obvious are the effects of the local arm, near the inner edge of which the Sun lies (Dickel, 1970). Extinction measurements made by Fitzgerald (1968) and Neckel (1967) and OB star distributions found by Klare and Neckel (1967) show large high density areas of absorption and stars delinating the -I arm and the local arm within 1 Kpc. Radio observations of Reigel and Krutcher (1972) indicate that an extensive cool, HI cloud lies closer than 1 Kpc. and obscures from $l^{II} = 355^{o}$ to $l^{II} = 25^{o}$, extending seven degrees on either side of the Galactic Plane.

The stars observed were all members of associations and are listed in Table VIII. Details of the associations are to be found in Table IX and were taken from Ruprecht, Morgan (1964) and Alter et al. (1965). To gain some insight into the Galactic structure in this region sky maps, a velocity longitude diagram and a distance longitude diagram are presented.

TABLE VIII

Stars Observed in the Southern Sky

HD	MK	Association	Distance	NGC
169034	B5I	Scutum OB3	1700pc	
-14° 5037	B1.5I	"		
169454	B1 Ia	"		
172488	B5V	Scutum OB2	730pc	
161061	B2III	Sag. OB5	2600pc	
161291	B1I	"		
164032	B1I	"		
160529	A2Ia	"		
168607	B9I	Serpens OB1	1600pc	6618
168626	B8I	"		6618
167838	B5I	"		
167451	BO.5I	"		6611
-12° 4970	B5I	Serpens OB2	2000pc	
167451	O8f	"		6604
167971	O8f	"		6604
168112	O6	"		6604
168076	O5			6611
168137	O8V			6611
168183	O8V			6611

TABLE IX

The Observed Associations and their Distances

Association	Distance	$\leqslant l^{II} \leqslant$		$\leqslant b^{II} \leqslant$	
Scutum OB3	1700pc	14°	19°	-1.5°	+1.5°
Scutum OB2	730pc	20°	26°	-2.8°	+1.5°
Serpens OB2	2000pc	18°	19.1°	+1.1°	+2.3°
Serpens OB1	1600pc	16.7°	18°	-1.6°	-0.1°
Sagittarius OB5	2600pc	358.8°	1.5°	-3.9°	+1.4°

==========

TABLE X

The Observed HII Regions and Distances

G.C.	NGC	Sharpless	Other	RCW	Distance
18.7+2.0	6604	S54	W35	167	2330pc
16.8+0.7	6611	S49	W37	165	2330pc
			M17		
15.0-0.7	6618	S45	W38	160	2810pc
			M17		

(i) Sky Maps

On a map of the Galactic Plane in the region $19^{\circ} \geqslant l^{II} \geqslant 14^{\circ}$ the majority of stars observed can be seen to lie near the HII regions of Rodgers, Campbell and Whiteoak (1960). The three main regions in which the stars are placed W35, W37 and W38 are all placed by Greeberg and Minn (1973), Georgelin Goss and Shaver (1970) and Reifenstein et al. (1970) in the Sagittarius arm and seem to share a less intense background emission nebulosity. According to Sharpless (1954) they may be physically connected. The regions designations and distances are given in Table X. The dark nebulae of Lynds are also shown, as are the reflection nebulae of Lynds (1962) and Racine (1968).

Of the stars lying at longitude less than $l^{II} = 14^{\circ}$, two lie in the Sagittarius arm at distances of 2.6 Kpc. and one HD160529 is difficult to position but is close to N.G.C. 6383. More detailed positioning of individual stars will be discussed later.

(ii) Distance - Longitude Map

The distance - longitude map shows the spiral arm tracers: HII regions, dust and open clusters. The HII distances are those from the H109α recombination observations of Reifenstein, and radio observations of Goss and Shaver. The optical absorption due to dust is taken from Fitzgerald and is only roughly positioned.

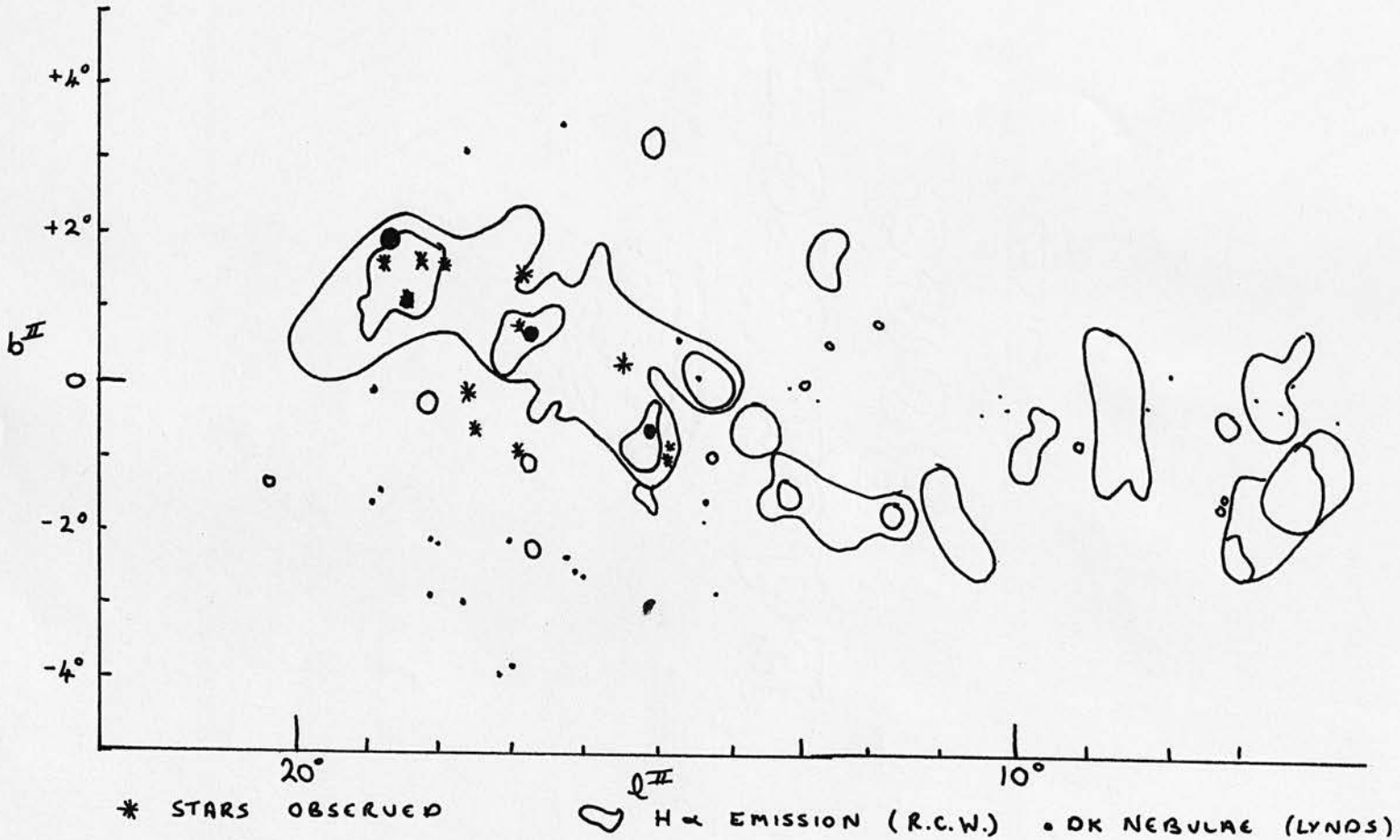

Positional Diagram For Stars Observed

Distance - longitude plot
20
l II 10
360
1
2
3 kpc
-14 5037
16745l
169034
169454
-12 4970
168607
168625
160529
161291
164032
161291
DUST (FITZGERALD)
N.G.C. CLUSTER
ASSOCIATIONS
OBSERVED STARS.
RADIO HII REGIONS

The positions of N.G.C. clusters (Hagen, 1970) and of associations (Ruprecht) are also shown.

The observed stars seem to lie in front of or on the outer edge of the Sagittarius arm. The three exceptions, HD160529, HD164032 and HD161291 lie behind this arm toward the Galactic Centre. Distances derived from kinematics are inaccurate towards the region $l^{II} = 0$ and the star distances taken from the spectrophotometric work of Humphreys (1970) depend on accurate luminosities being available for the stars. Conclusions drawn from the stellar distances can serve only as a rough indication of their relation to the spiral arms. All of the stars are reddened by absorption within 1 Kpc. of the sun as well as by interarm and Sagittarius arm absorptions. Only the star HD172488, at 800 pc and belonging to Scutum OB2 is affected by local arm absorption alone.

(iii) Velocity Longitude Diagram

A plot of the velocities of HII regions (Courtes, Georgelin), H109 (Reifenstein et al.), open clusters (Hagen) and the main HI ridge lines is presented along with the observed stars' radial velocities taken from Humphreys and Wilson (1953). It may be seen that the usual spiral tracers outline fairly well the -I arm. The majority of the stars observed appear to lie at the front of the Sagittarius arm, which begins to be viewed tangentially near $l^{II} = 25^{\circ}$. The later B type stars

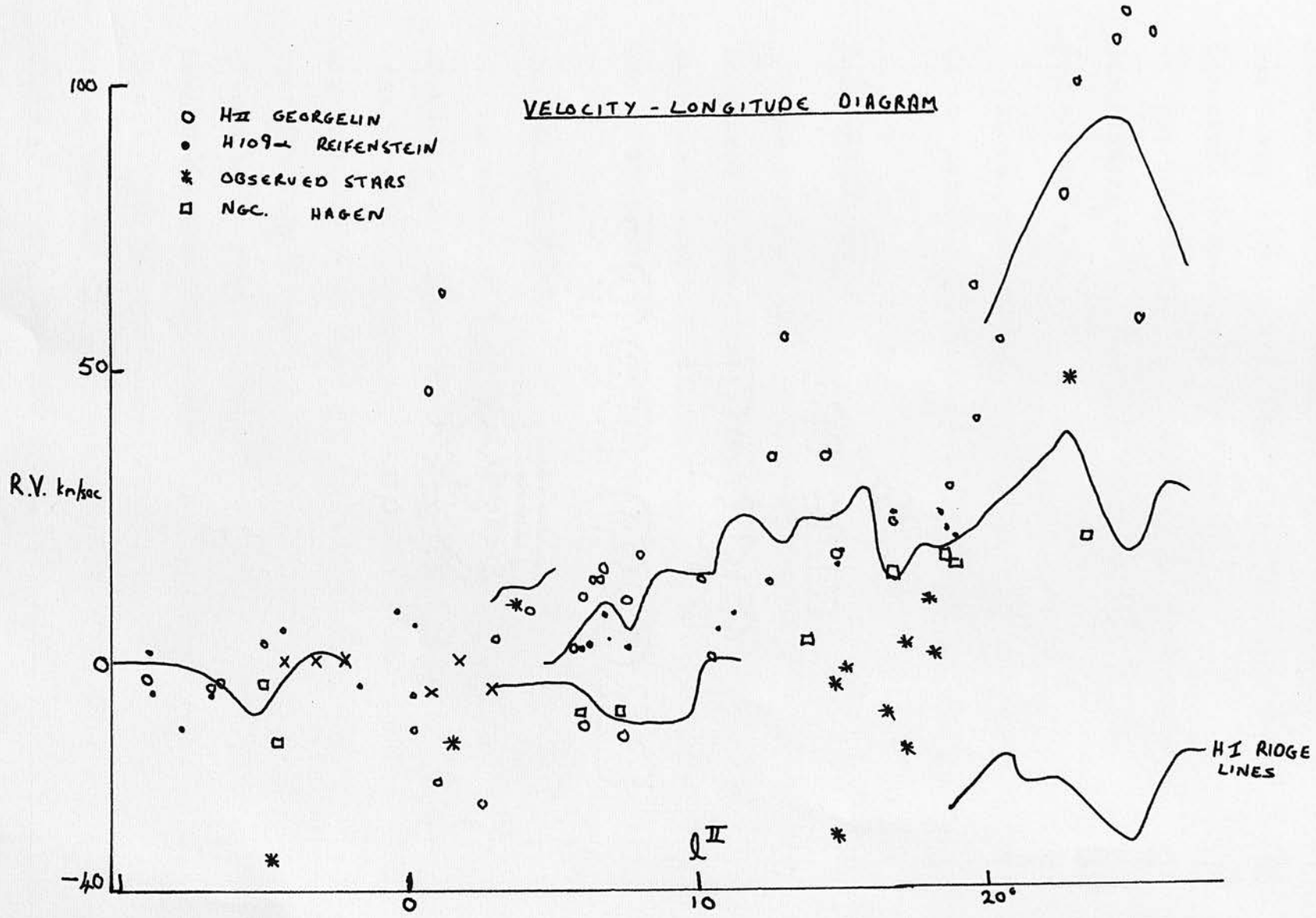
VELOCITY - LONGITUDE DIAGRAM
HII GEORGELIN
H109α REIFENSTEIN
OBSERVED STARS
NGC. HAGEN
100
50
0
−40
R.V. km/sec
HI RIDGE LINES
l II
0
10
20°

have possibly different kinematics from the gas and systematic differences between the stellar velocities and those of the associated HII regions have been discussed by Greenberg and Minn.

The diagram serves to confirm the approximate positioning of the stars at the near edge of the Sagittarius arm.

It is probably best to discuss each star in relation to the association to which it belongs.

5.2 Scutum OB3

The association lies at about 1700 pc. and seems to be placed to the front of the Sagittarius arm. Three stars were observed in this area, all at negative latitudes and to the south of the main HII regions.

(i) HD 169034

Classified as M.K. type B5I (Jaschek) this star shows the Balmer series in absorption and MgII 4481A less intense than HeI 4471A as would be expected. With a colour excess of 1.4^{m} and $M_V = 8.14$, the star lies away from any HII regions. Its distance of 1.65 Kpc. places it between the two other stars observed in Scutum OB3 although it possesses the largest colour excess. The interstellar absorption line intensities are normal for the reddening, when compared to the other stars observed. Only the 5780A, 5796A, 6200A and 6614A lines show low values.

TABLE XI 'A'

Observations of Stars in the Sagittarius Region

Star	Eb-v	A_c% 4430	5780	5796	Na D	6200	6270
169034	1.40	11.5	8.0	3.0	14.5	3.0	4.0
-14 5037	1.30	10.0	8.5	2.5	11.5	4.0	2.0
169454	1.10	7.0	10.5	3.0	13.0	5.0	2.0
172488	0.90	5.0	8.0	3.5	8.5	---	---
161061	1.01	10.0	6.5	---	8.0	5.5	4.0
164032	0.40	----	4.0	2.5	5.0	8.0	---
160529	1.22	----	10.0	3.5	18.5	4.0	---
168607	1.60	13.0	13.0	6.0	15.5	6.5	6.0
168625	1.46	12.0	15.0	6.0	13.0	5.0	4.0
167838	o.62	10.0	7.5	5.0	9.0	5.5	---
167451	1.07	11.0	12.0	7.0	13.0	6.5	3.5
167971	1.08	10.0	9.0	5.0	13.5	4.5	---
168112	1.01	9.0	10.5	7.0	15.0	9.0	---
168076	0.82	10.0	6.5	3.5	11.0	7.5	---
168137	0.75	9.0	11.0	4.0	12.0	5.0	5.0
168183	0.64	9.0	----	---	----	---	---
-12 4970	1.30	11.0	----	---	----	---	---

Errors ± 3 in Ac%

TABLE XI 'B'

Star	A_c			Equivalent Width				
HD	6284	6614	Ca	5780	5796	6200	6270	6284
169034	9.0	4.0	30.0	33	---	12	16	75
-14 5037	7.0	3.0	20.0	30	---	6	--	40
169454	10.5	---	19.0	49	---	6	--	57
172488	6.5	7.5	18.0	33	---	--	--	24
161061	8.0	---	17.0	34	---	--	--	38
164032	5.0	---	---	39	---	--	--	22
160529	7.5	4.5	41.0	39	---	12	--	36
168607	11.0	8.0	---	47	18	15	13	57
168625	10.5	7.0	17.0	50	17	11	--	48
167838	9.0	3.0	26.0	40	18	12	--	30
167451	8.5	3.0	---	40	24	12	11	53
167971	9.0	---	---	90	15	16	--	33
168112	8.0	5.5	---	44	17	35	--	29
168076	9.0	5.5	28.0	38	11	29	--	79
168137	9.5	9.0	18.0	44	23	18	14	75
168183	---	---	15.0					
-12 4970	---	---	13.0					
Errors	± 3% in A_c			±9	±10	±10	±9	±13

EWs are in Picometres (PM) 100PM = 1A

TABLE XI 'C'

Star	P/Av	θ_g	r(kpc)	RV km/sec	l^{II}	b^{II}
169034	.010	128	1.65	3.0	17.6	-0.1
-14 5037	.013	58	1.08	----	16.9	-0.9
169454	.013	74	1.85	-15.2	17.5	-0.7
172488	.005	100	0.73	----	23.9	
161061	.043	52	----	----	0.5	0.6
161291	.048	58	2.73	----	1.5	0.8
164032	.011	90	2.63	-3.2	0.9	-3.2
160529	.041	78	1.98	-34.4	355.7	-1.7
168607	.009	81	2.36	-30.0	15.0	-0.9
168625	.020	75	2.81	-40.0	15.0	-1.0
168738	.001	--	2.57	0.3	15.4	0.3
167451	.007	98	1.45	-9.3	16.8	1.5
167971	.009	31	----	----	18.2	1.7
168112	.008	8	----	----	18.4	1.6
168076	----	--	----	----	17.0	0.9
168137	----	--	----	----	17.0	0.9
168183	----	--	----	----	17.0	0.9
-12 4970	.014	150	1.88	----	18.0	1.6

Polarisation data from Hiltner

r = distance from Humphreys

RV = radial velocity from Humphreys and Wilson

(ii) -14 5037

Although classified by Mendoza (1958) as B1 Ia^+ the accepted type is B1.5Ia for this star. The Balmer lines from Hγ to Hα show in emission, Hγ as a central emission on the absorption, Hβ as emission with central absorption and Hα an emission with absorption to the blue. The star has a colour excess of Eb-v = 1.3^m, and is placed at a distance of 1.08 Kpc. by Humphreys. The HII region S46 seems associated with the star and this region is believed to be related to NGC 6611. Like HD 169034 the absorptions 5780A, 5796A, 6200A and 6614A are lower than expected as are the Sodium D lines.

(iii) HD 169454

The Balmer lines of this B1 Ia star again show emission effects. Unlike the previous star Hβ is an emission with absorption to the blue and the Hα is almost wholly in emission. Merrill and Burwell (1949) and Wallerstein (1970) both found P Cygni profiles in Hα and Hβ as well in some Helium I lines. Humphreys places the star at a distance of 1.85 Kpc. and classes it B1 Ia^+ although Andrews (1968) finds a distance of 2.78 Kpc. The star lies clear of any HII regions or nebulosity and has the lowest colour excess, Eb-v = 1.1^m, of the three stars in this association.

It is of note that while the Sodium D lines show reasonable intensities, the radial velocities of the Calcium and Sodium interstellar lines are some of the highest known. Adams (1949), Routly and Spitzer

(1952) and Wallerstein found velocities of nearly 100km/sec while the radial velocity of the star is -7km/sec (Wilson) to -15km/sec (Humphreys). Using similar observations Wallerstein places HD 169454 more distant than 1.8 Kpc. Hutchings (1967) finds evidence for mass loss in the rapidly expanding envelope. The reddening law calculated from Johnson and Borgman's (1960) photometry and found by Whittet, Van Breda and Nandy (1973) is similar to that found in Cepheus by Nandy (1967).

Unlike the other two stars of this association only the 4430A and 5796A lines are weak, the others being of expected strength.

5.3 Scutum OB2

This association is placed at a distance of 730 pc. by Ruprecht and is thus in the Local Arm. One star only was observed in this area.

(ii) HD 172488

Classed BO.5V in the MK system the Balmer lines in this star appear in absorption. The Balmer series is very much sharper than expected for the stated luminosity and it seems to be wrongly classed. Whittet et al. also found this. It has a colour excess of 0.9^{m} indicating that for most of the stars observed in the Sagittarius arm the reddening occurs in the local arm.
The reddening law derived for this star shows a Cygnus

type curve. There seems to be no near emission regions or dust clouds on the Palomar Charts although there is a close planetary nebula at

R.A. 18hr. 37' 40.3" Dec. $-8^{\circ}46.6'$

The 1950 co-ordinates for the star are

R.A. 18hr. 37.8' Dec. $-8^{\circ}46.6'$

The close coincidence may affect the interstellar absorptions.

For its reddening the star shows low values of 4430A and Sodium D lines. The absorption 6618A seems unexpectedly high.

5.4 Serpens OB2

Complete observations of two stars were made in this association. Situated at 2000 pc. the association includes the open cluster NGC 6604. Of the stars observed HD 167971 is the brightest of a compact group of 'O' stars in this HII region.

NGC 6604 is the largest of HII regions observed by Reifenstein et al. and is between 26.5 pc. (Goss and Shaver) and 54.8 pc. (Reifenstein et al.) at a distance of 1.9 Kpc. (Miller, 1968) up to 3.2 Kpc. (Reifenstein). Lying two degrees above the Galactic Plane, the region has been resolved into four sources at 5000 MGHZ. (Goss and Shaver). Gum classifies this region as type II, being of irregular shape and less concentrated towards the centre than NGC 6611 and NGC 6618. At least two

multiple systems exist within the nebulae, surrounding the stars HD 167971 and HD 167834 and within sixty seconds of arc lie twenty early type stars (Sharpless). Sharpless also associates this nebula with NGC 6611 and NGC 6618 as well as that surrounding the star -14^{o} 5037. Two stars were observed from this association.

(i) HD 167971

Generally classed as O8f only Hα appears solely in emission. This star is in the centre of the HII region S54 and is part of the multiple system of O stars previously mentioned. Strong Calcium lines are present for the colour excess of Eb-v = 1.08. Although the lines 4430A and 5796A also appear strong those for the Sodium D lines are normal. The reddening relation calculated from observations made by Johnson and Borgman and Walker et al. is similar to that found by Nandy for stars in the Perseus region.

(ii) HD 168112

Classified as O6 the Balmer absorptions all have absorption profiles. The star lies away from the centre of NGC 6604 near the edge of an absorption lane. For a colour excess of Eb-v = 1.01^{m} the absorptions at 6200A and of the Sodium D lines are large. Like HD 167971 the star's reddening curve is similar to that of the Perseus region.

5.5 Serpens OB1

This association is placed at 1600 pc. from the Sun by Ruprecht and is in the Sagittarius (-I) arm. Included in the association are the two HII regions M17 and M16 (NGC 6611, NGC 6618) placed at distances of 2.4 Kpc and 2.2 Kpc. (Goss and Shaver). The association thus seems to be linked to Serpens OB2 by the connection between these HII regions and NGC 6604. The character of these two HII regions will be discussed first.

NGC 6618

Also called M17 or the Omega Nebula, NGC 6618 has been extensively observed and has been compared to the Orion Nebula. Optical observations in H α (Ishida, 1967) indicate dust obscuration greater than seven magnitudes. Kleinman was able to observe a double source in the infra-red. Radio observations also indicate that there are two sources at 15.1 + 0.7 and 15.0 + 0.7 (Schramel and Mezger, 1969; Goss and Shaver). As well as a generally symmetric structure Hobbs (1961) found emission features extending in the direction of HD 168607 and HD 168625. At a distance of between 2.1 and 2.4 Kpc. (Reifenstein et al.; Goss and Shaver; Georgelin) the HII region has a diameter of between 3.7 and 5.4 pc. The main exciting stars are thought to be obscured but HD 168607 and HD 168625 excite a small part of the gas.

(i) HD 168607

Classified by Popper (1940) as CB8e γ , this star is now classed B9I. Duke also found H γ to be in emission, although this series of observations find it now to be in absorption. The Balmer lines H α and H β show P Cygni profiles, the H α being almost solely emission. The 4481A line of Magnesium is stronger than the Helium 4471A line and the Helium lines are weak in both the red and blue. Within 0.1' of arc of HD 168625 this star has a colour excess of Eb-v = 1.6^m the largest of the observed stars. Placed at a distance of 2.36 Kpc. (Humphreys), HD 168607 is associated with NGC 6618. Hiltner found a polarisation value P/Av = .009, a very much lower value from that of its neighbour. Both stars lie in what appears to be an absorption bay to the south of M17, and on Palomar plates there appears to be an arc of nebulosity surrounding them, although distant from them.

The interstellar absorptions are of the predicted strength, while the reddening curve (Divan, 1954) lies between those observed for Cygnus and Cassiopeia.

(ii) HD 168625

Classed CB2 with suspected H α emission (Popper and Seyfert, 1946), HD 168625 is now classified B8I. H γ shows as a pure absorption, H β appears weak and H α is in emission with absorption to the blue. The Magnesium line 4481A is weaker than the Helium line at 4471A and all the Helium I lines are prominent. With a colour excess Eb-v = 1.46^m the star is placed at 2.81 Kpc. (Humphreys) and lies near HD 168607. The

observed polarisation P/Av = .020 is very much greater than its neighbour.

Of the interstellar lines only that at 6200A is different from the expected strength.

(iii) HD 167838

Classed B5I the Balmer lines are in absorption. The colour excess Eb-v = 0.62 seems low for the distance of 2.81 kpc. given by Humphreys or even of 2.32 kpc. given by Andrews (1968). The star lies one degree from M17 and is clear of nebulosity and absorption lanes. With the exception of the line at 6614A all of the interstellar lines are stronger than expected. Whittet et al find a reddening law similar to that of the Cepheus region.

NGC 6611

Also called M16 and W37 this young cluster is associated with an HII region between 7.6 pc and 12.8 pc in diameter at a distance of between 2.2 kpc. and 2.7 kpc. (Goss and Shaver; Reifenstein). Heavy obscuration is evidenced by absorption lanes and globules (Sim.1968) while within the nebulosity is a group of OB stars(Hubble, 1922). Walker (1961) has carried out good photometry on this cluster. Spectral types are available (Morgan et al., 1953) and polarimetry (Hiltner) and reddening laws(Johnson, 1968) are available for the brightest stars. Reddish (1967) found a lack of stars with magnitudes between V = 11.5^{m}

and V = 12.5^{m} while investigating the correlation between colour excess and absolute magnitude of the stars in this and other clusters. Reddening laws similar to those in Perseus are found for stars in this cluster.

(i) HD 168076

Classified O5 to O6f this star shows Hγ and Hβ in absorption and Hα in emission. The MagnesiumII line at 4481A is stronger than the 4471A Helium I line indicating that there exists an extended atmosphere (Underhill, 1966). The brightest star in the cluster HD 168076 has a colour excess of Eb-v = 0.82^{m} and lies in a relatively unobscured part of the emission nebula. All of the interstellar lines are stronger than expected.

(ii) HD 168137

Classified O8V the Balmer lines Hγ and Hβ are seen in absorption while Hα is in emission. Again the 4481A line is stronger than the 4471A line and the Helium I lines are weak. Positioned near the centre of the nebulosity the star has a colour excess Eb-v = 0.75^{m} All interstellar lines are stronger than expected.

(iii) HD 168183

Classified O8V to BOIII the star shows Hγ and Hβ in absorption. No observations were made in the red but Wackerling (1970) makes no mention of any emission characteristics. Although it is inside the emission

nebulosity the star lies 90" from the main radio sources. The colour excess agrees well with the Calcium II strength but the value Eb-v = 0.64^m is too low to explain the strong 4430A absorption if the mean relationship is used. The 4430A strength however agrees with this reddening if a relation derived from the other members of the cluster is used. This star is also a binary (Walker).

(iv) HD 167451

Classified BO.5I HD 167451 shows absorption in all the Balmer lines. A reddening of Eb-v = 1.07^m and a distance of 1.45 Kpc. (Humphreys) do not seem to agree unless most of the absorption seen in all these stars is caused by the local arm obscuration. Although Greenberg and Minn associate the star with M16, the observed radial velocities make the relation unlikely. Situated almost a degree from this HII region, HD 167451 lies clear of emission nebulosity although in the general obscuration around the nebula.

The strengths of the interstellar lines agree well with the reddening except for the 4430A line which shows a high value.

5.6 Sagittarius OB5

Situated at a distance of 2.6 Kpc. towards the Galactic Centre, this association is placed beyond the Sagittarius (-I) arm. Three stars were observed from this area.

(i) HD 164032

The Balmer series appear in absorption in this B1I star. Although the colour excess is only Eb-v = 0.4^{m} and the Sodium D lines weak Humphreys gives a distance of 2.63 Kpc. and Beer (1961, 1964) 2.9 Kpc. The star is in an area of emission nebulosity on the Palomar charts, but no one nebula seems to be responsible.

The interstellar lines are all strong for the reddening.

(ii) HD 161061

Again all the Balmer lines are in absorption in this B2III star except H α which is filled. There seems to be no nearby nebulosity on the Palomar plates. The colour excess Eb-v = 1.01 is the second highest of the stars observed in this area and is in keeping with the interstellar line strengths. The polarisation is however P/Av = 0.43 the highest observed in this investigation.

(iii) HD 160529

Classified A2 Ia only H γ is in absorption. The lines H α and H β are totally in emission. Wallerstein on the basis of Sodium D velocities of -61km/sec. places the star beyond the 3 Kpc. arm. Although an A type star is not likely to provide enough radiation pressure, Wallerstein suggests that an alternative explanation of mass loss is possible. Distances of 1.98Kpc(Humphreys) and 1.47Kpc(Andrews) place the star in the Sagittarius arm.

The reddening law for this star is similar to that observed in Cygnus. With the exception of very high Sodium and Calcium II strengths the interstellar lines were normal. The 4430A line was weak for the reddening.

5.7 Northern Hemisphere Observations

Apart from the observations in the red and blue made in Pretoria many observations of the interstellar line at 4430A were made using the I.N.T. and the 36-inch telescopes previously mentioned. Discussion of these observations and the stars involved will be more brief than that of the southern stars because less information was obtained from the spectra.

(i) Thirty-six Inch Observations

The main reason for these observations were to obtain profiles of the 4430A line. We will discuss the stars' relations to reflection and emission nebulae, their binary nature, the nature of their reddening laws and their Balmer profiles.

HD 199478, HD 21291 and HD 21389 all lie in reflection nebulae (Racine). HD 13267, HD 42087, HD 21389, HD 183143, HD 208501, HD 199478 and HD 21291 all show variability in the higher Balmer lines to some extent. In particular HD 21389 and HD 21291 have shown inverse P Cygni profiles in H α (Rosendahl, 1973).

The Bright Star Catalogue gives HD 13267, HD 42087, HD 199478, HD 21291 and HD 40589 as binary stars, and

HD 91316, HD 208501 and HD 21291 as possible variables. The reddening laws derived for the stars HD 36371 and HD 13267 are of the Cygnus type, those of HD 21291, and HD 208501 like Perseus and that of HD 21389 like Cepheus. It is interesting to note that of the stars in which Bromage found large emission wings to the 4430A feature, HD 12301, HD 20041, HD 21389, HD 39970 and HD 199478, two are double and at least three lie in reflection nebulae.

(ii) I.N.T. Observations

The stars observed between Winter 1971 and 1972 are confined to the associations Cepheus OB1 and OB3. The latter is at a distance of 700 Kpc. and is young. There is no central cluster but an HII region S155, with exciting stars HD 217035, HD 217061 and HD 217086, exists (Garrison, 1970). Again these are probably not the main exciting stars. The association is considerably dusty and a ring of dust is said to lie around the region. Distances of less than 1 Kpc. (Georgelin) make this the youngest group within that distance. The 21cm. maps of the region show high HI densities in the area (Burton, 1972). Lambrecht and Schmidt find a low Hydrogen to dust ratio for the association. (Lambrecht and Schmidt, 1958) The stars observed were:-

HD 217035

A double star (Doremus, 1970; Garmany, 1972) the brighter component of which is B0.5V this star has a reddening of $E_{b-v} = 0.74^{m}$. The reddening law is similar

to that of the Cassiopeia region. The observed intensity for the 4430A feature of 8.0% is high for the colour excess.

HD 217061

A B1Vn star (Wackerling), HD 217061 is also a binary with a period of 2.66 days. The observed central intensity of the 4430A feature of 6.0% is low for a colour excess Eb-v = 0.96^{m}.

HD 217086

Classified O5 or O7 (Garrison) this star is possibly composite. Crawford and Barnes(1970) give a class of O9 for this star. The 4430A diffuse line is strong 10.0% for the colour excess of 0.97^{m}

HD 216711

A B1V star with a colour excess of 0.88^{m} this star is also a binary with a period of 5.66 days. Unlike the previous three stars, HD 216711 is not associated with the HII region S155. The central depth of the 4430A line, 8.0% is higher than might be expected for a colour excess Eb-v = 0.88^{m}.

The remaining stars belong to Cepheus OB1, an association placed at a distance of 3.6 kpc (Morgan). A high gas to dust ratio was found for this region by Lambrecht and Schmidt. The stars thus lie in the Perseus arm as defined by Georgelin (1971). Radio maps show a ridge extending from 90^{o} l^{II} 120^{o} at distances of between 6 kpc and 2.5 kpc (Burton). In the same region

Fitzgerald finds dust out to 1 kpc but little absorption beyond this, while Klare and Neckel find slight density increases at 3 kpc.

The stars observed were:-

HD 210809

Classed as an O9Ib this star shows a low colour excess of 0.36^m and a high polarisation P/Av = .030. High interstellar velocities 20 km/sec more negative than the stellar velocities have been observed. $H\alpha$ is believed to be in emission (Johnson, 1968). The 4430A intensity of 6.0% is high for the reddening.

HD 216927

A B9Ia type star with a large colour excess of $Eb-v = 0.92^m$ and a loww polarisation of P/Av = .o14,this star has a central depth for the 4430A feature of 9.0%.

HD 212455

Classified B5Iab HD 212455 has a colour excess of $Eb-v = 0.54^m$ and shows high values for the Sodium D lines, (Munch,1957), the diffuse lines (Merril et al.) and for the 4430A feature. The reddening law derived from work by Fernie (1968) is similar to that of the Perseus region.

HD 235781

Classed as a B6Ib with a reddening of $Eb-v = 0.57^m$ HD 235781 shows a normal intensity for the 4430A feature.

HD 209678

Classed B2I, with a reddening of Eb-v = 0.63, HD 209678 shows a high 4430A intensity of 11.0%.

From the preceding details of the stars observed it may be seen that many of them lie in or near HII regions, that over half have emission characteristics, many were binary and several were in reflection nebulae. To discuss the relations between the diffuse lines and other parameters is difficult in such a small sample of stars. However the more obvious relations may be detected.

6. CORRELATIONS BETWEEN THE INTERSTELLAR LINES AND GALACTIC PARAMETERS

In all previous investigations various correlations have been attempted, mainly between the strength of the 4430A feature's strength and parameters associated with galactic structure. The first part of this chapter is concerned with extending these correlations to include lines observed in southern association members in the red and blue. The second section compares some of the correlations with those found in northern associations and for collated 4430A data.

The galactic parameters may best be discussed in the following groups.

(i) Positional

(ii) Spectral Type

(iii) Grain related parameters

(iv) Interstellar atomic absorptions

(v) Inter-relations between diffuse lines

In the presentation which follows correlation coefficients calculated from least squares fit (Table XII) are defined by

$$r = \frac{COV(x,y)}{sigx\ sigy}$$

where COV(x,y) is the covariance of x and y, sigx and

TABLE XII

Correlation coefficients referred to in Chapter 6

	Eb-v	MK	O_g	R	4430	5780	5796	Na	6283	6614	W5780	W5796	W6284	Ca	b^{II}
Eb-v	10^2	47	00	00	64	67	25	71	54	00	00	00	29	10	00
mk		10^2	00	12	00	34	00	31	13	00	00	27	00	41	00
Og			10^2	57	27	00	00	00	28	00	00	21	82	33	00
R				10^2	00	00	24	00	11	00	00	35	11	43	00
4430					10^2	53	54	42	70	00	16	00	49	00	46
5780						10^2	65	66	70	40	25	48	26	00	17
5796							10^2	35	42	00	31	40	00	00	54
Na								10^2	51	00	24	00	32	70	19
6283									10^2	39	35	00	61	19	35
6614										10^2	52	00	22	00	00
W5780											10^2	00	00	00	00
W5796												10^2	26	70	00
W6284													10^2	00	25
Ca														10^2	00
b^{II}															10^2

The correlation coefficients are here multiplied by 100

Fig 6.1

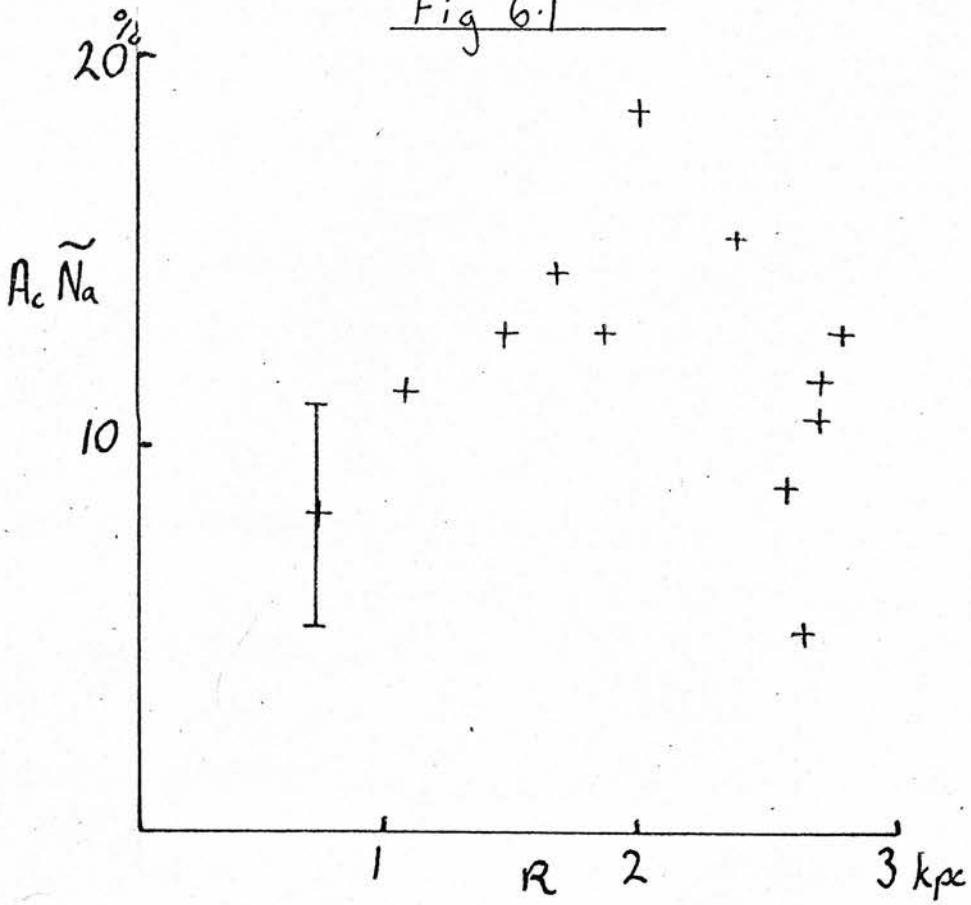

Fig 6.2

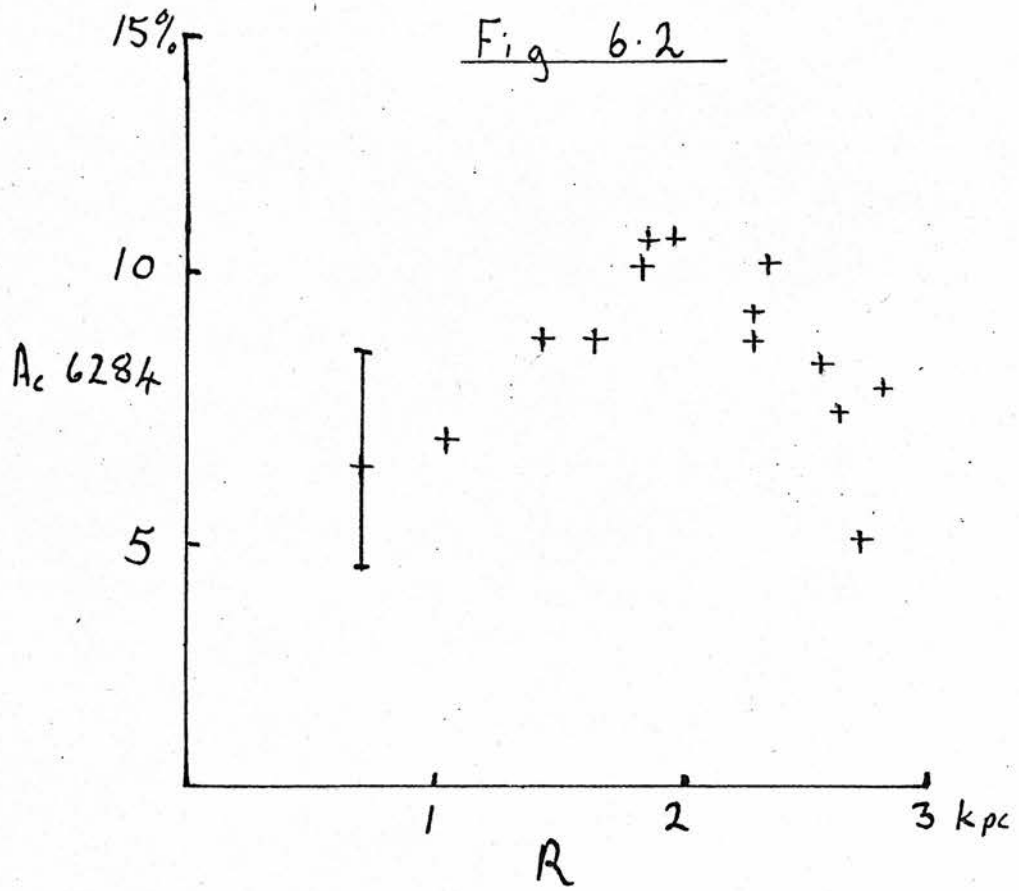

sigy the standard deviations of x and y. The slopes of the relations are defined by

$$M = sigy/sigx$$

with extremes defined by the regression of x on y

$$Mx = r\ sigx/sigy$$

and by the regression of y on x

$$My = r\ sigy/sigx$$

The intercepts are defined by

$$C = M\ \bar{X} - \bar{Y}$$

The diffuse lines 6270A and 6200A were found to have low intensities and within the defined errors the correlations had little meaning. For this reason they are not included in table XII.

6.1 Positional Relationships

(i) Distance

As previously discussed most of the stars observed lie in the Sagittarius arm, the main absorption occuring in the Local arm (Fitzgerald,1968). Correlations of distance with all of the diffuse lines is poor.(fig. 6.1,6.2)

The poor correlations seen can be explained by reference to the reddening - distance relation.(fig. 6.3) The expected form of the relation is indicated by the solid curve. Nine stars follow this relation, the remainder have lower reddening than expected. Similar relations for the diffuse lines would be expected by virtue of the strong

Fig 6.3

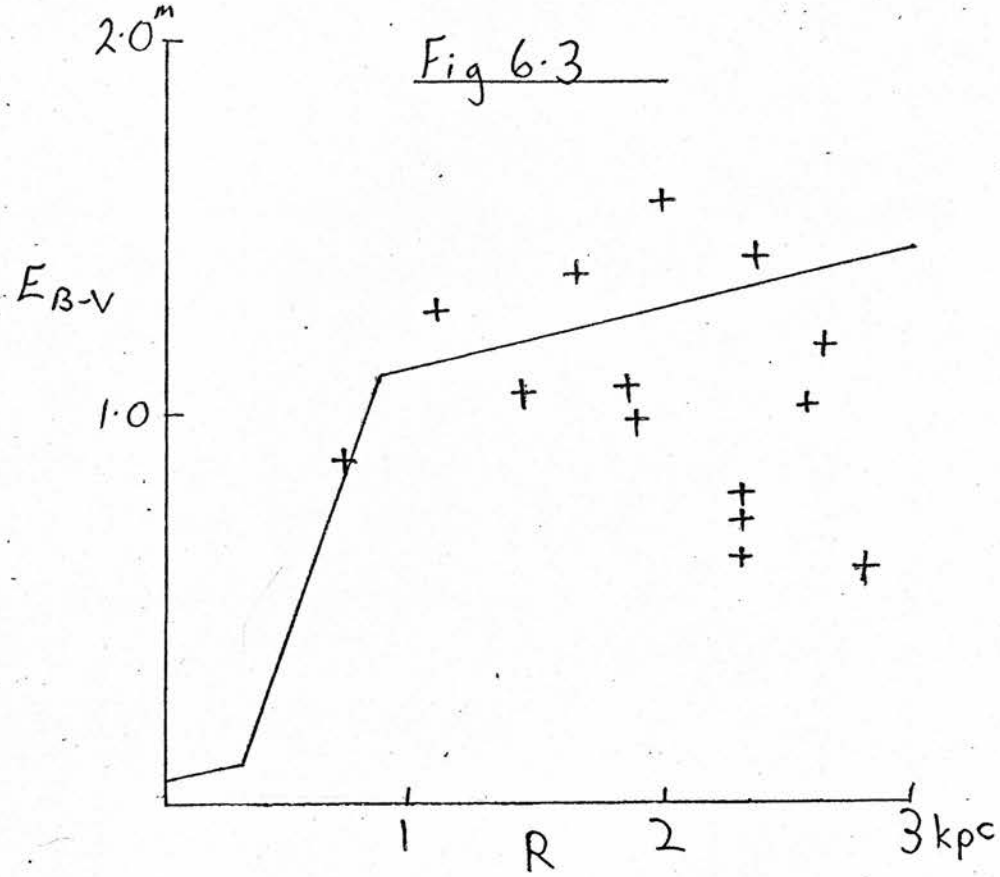

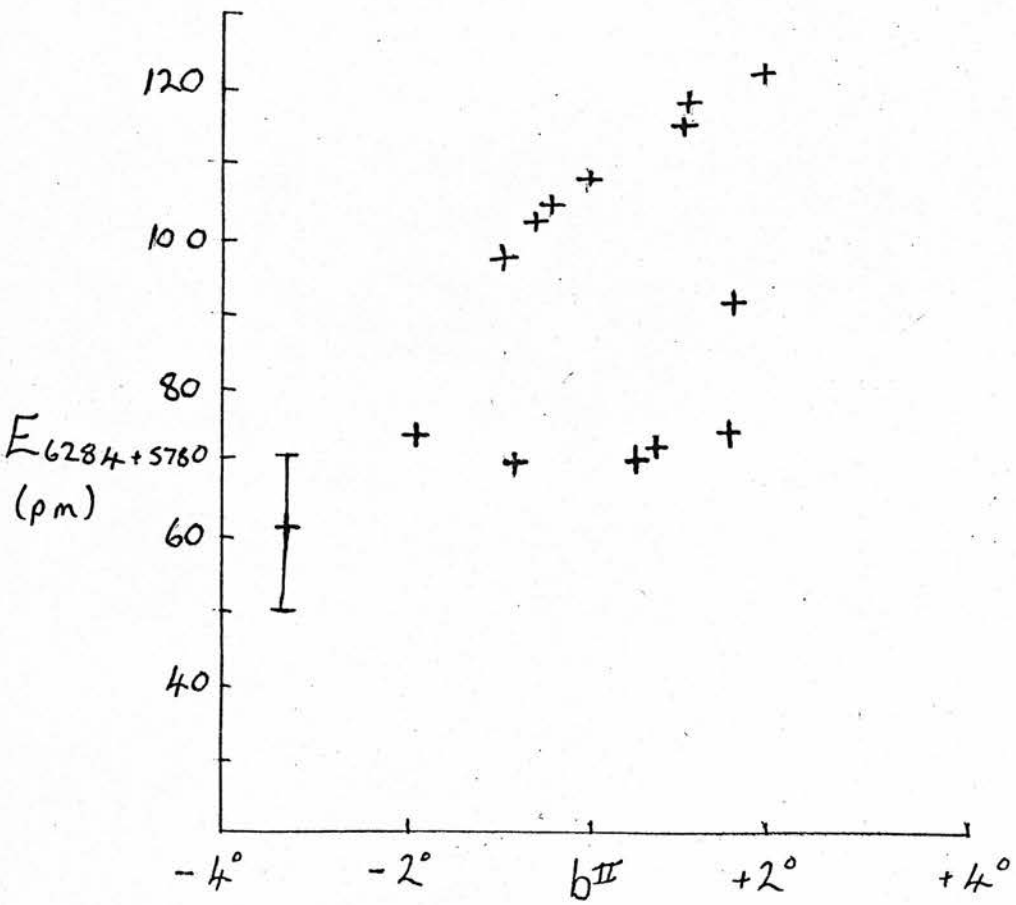

Fig 6.4

reddening - line strength relations.

The poor distance- reddening relation seems to indicate that the distribution of the reddening is patchy and inhomogenous (Schmidt Kaler, 1973). Wether these inhomogeneities are local to us (1kpc.) or not is problematical. Of the stars showing low Eb-v for distance the members of NGC 6611 are prominent. These like the other stars with anomalously low reddening are at distances of greater than 2 kpc. Most of the reddening occurs in the first kiloparsec however and it therefore seems reasonable to assume that to give the observed variations this local material is inhomogenous.

(ii) Galactic Longitude and Latitude

The distribution of stars is too clumped in longitude for discussion of the longitude- line intensity relation. Later discussion will relate these observations with the variation observed with longitude for collated values of the 4430A feature.

The relations between latitude and line strengths are poor. The strongest between latitude and the 4430A and 5796A lines yield correlation coefficients of 0.46 and 0.54. The observed trends are towards higher line strengths at more positive latitudes. This might be expected since the local absorption appears to be due to a cool cloud (Riegel and Crutcher, 1972) lying to the

north of the galactic plane.

6.2 Spectral Type

Low correlations are found for the relation between MK type and the strength of all the diffuse lines. Similarly low correlations exist between MK type and the ratios of line strength to reddening. Thus stellar blending has played little part in the absorptions measured.

Only Eb-v shows any correlation with spectral type with a correlation coefficient of $r = 0.46$, the later types showing higher reddening.

6.3 Grain Related Parameters

(i) Colour Excess

As mentioned the colour excess increases only slowly with distance between one and three kiloparsecs. Most of the absorption occurs in the Local arm. Several stars show low reddening for their distance, in particular those in NGC 6611.

All of the lines show high correlation with reddening with the exception of 5796A and 6614A. The strongest relations are for the Eb-v versus Sodium, 4430A, 5780A and 6284A central depths. These are represented by the straight line fits

$$A(Na(D_1+D_2)/2) = 10.5Eb\text{-}v + 1.0 \quad \text{fig. 6.5}$$

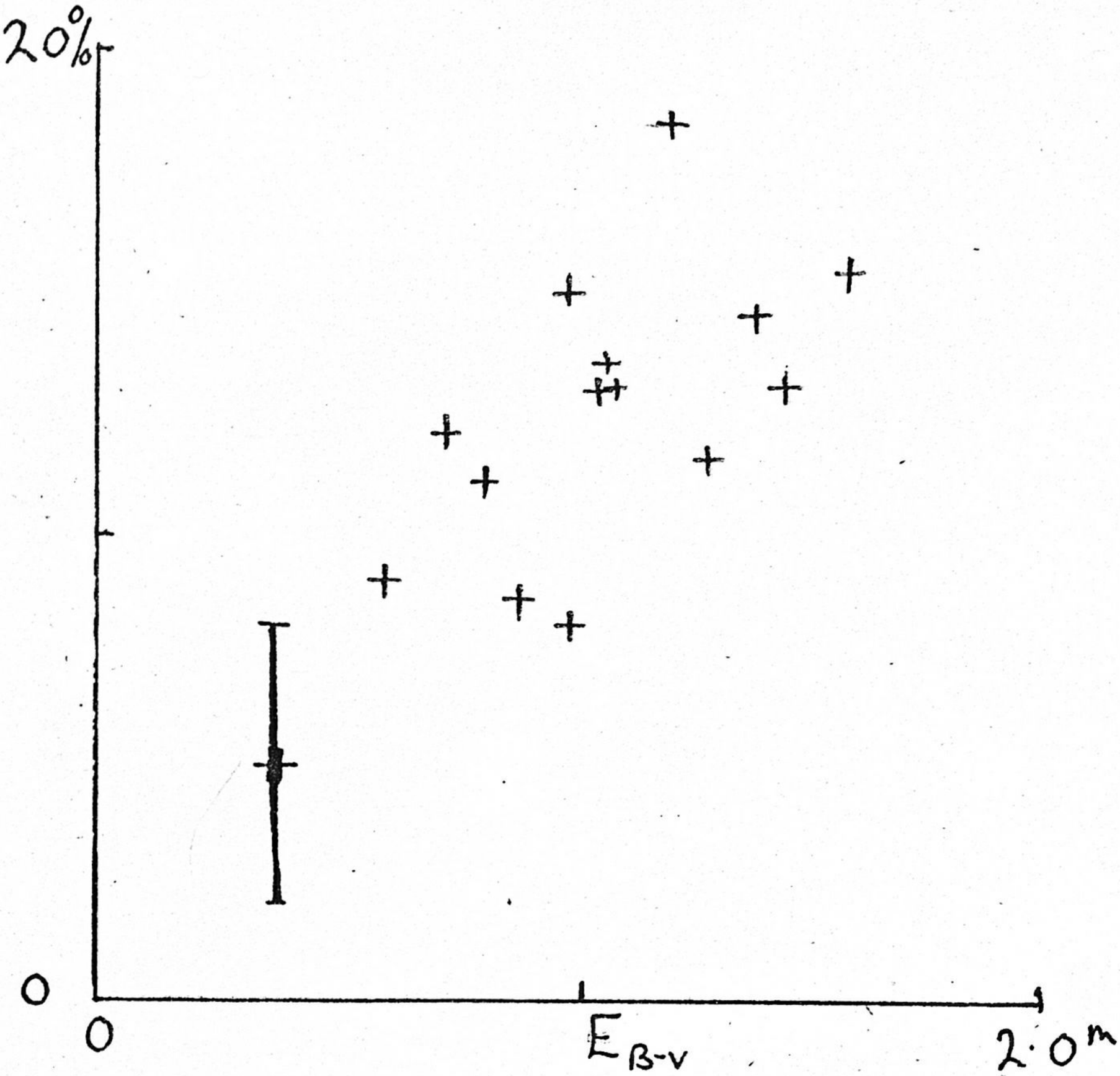

Fig 6·5

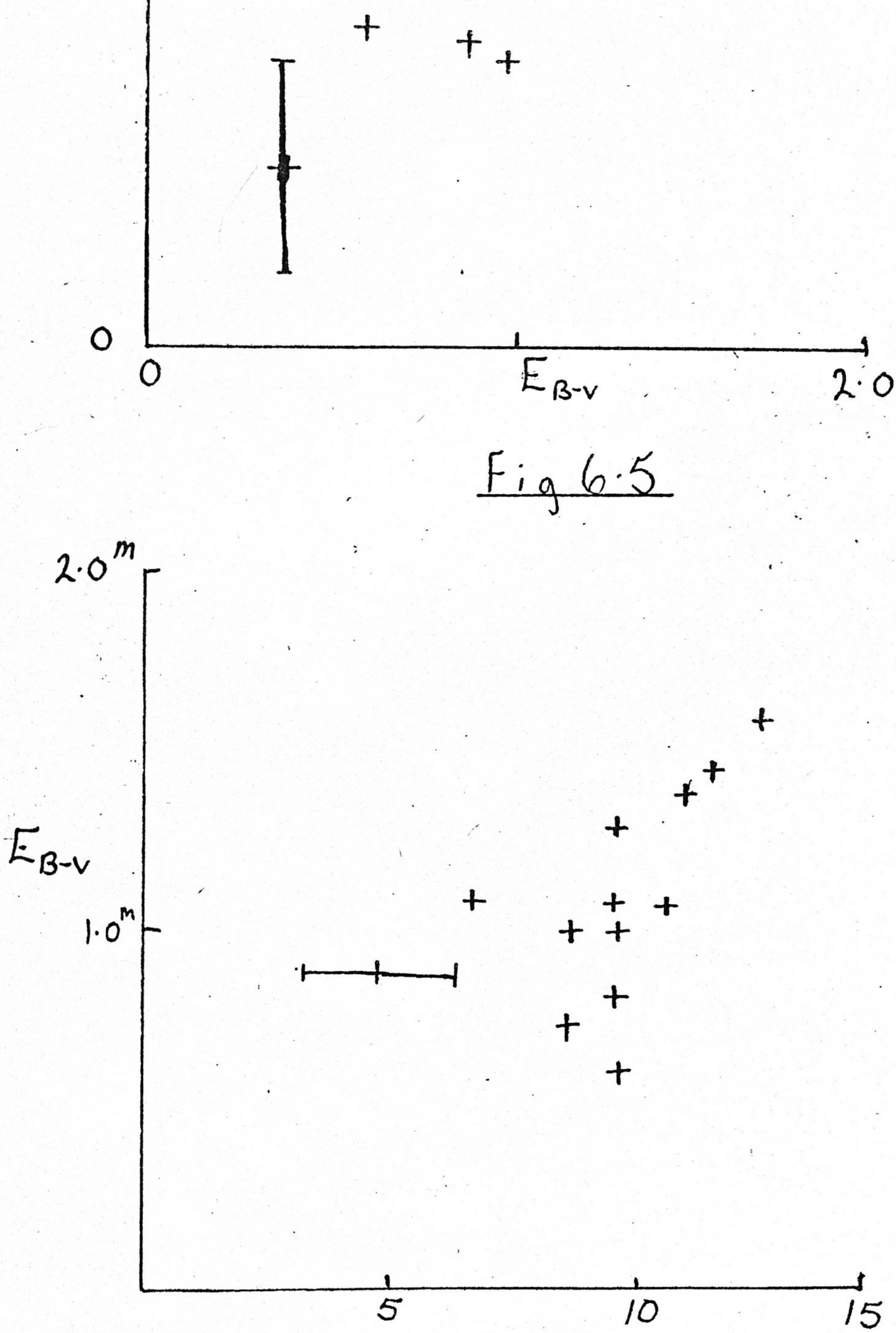

Ac4430

Fig 6·6

Fig 6.7

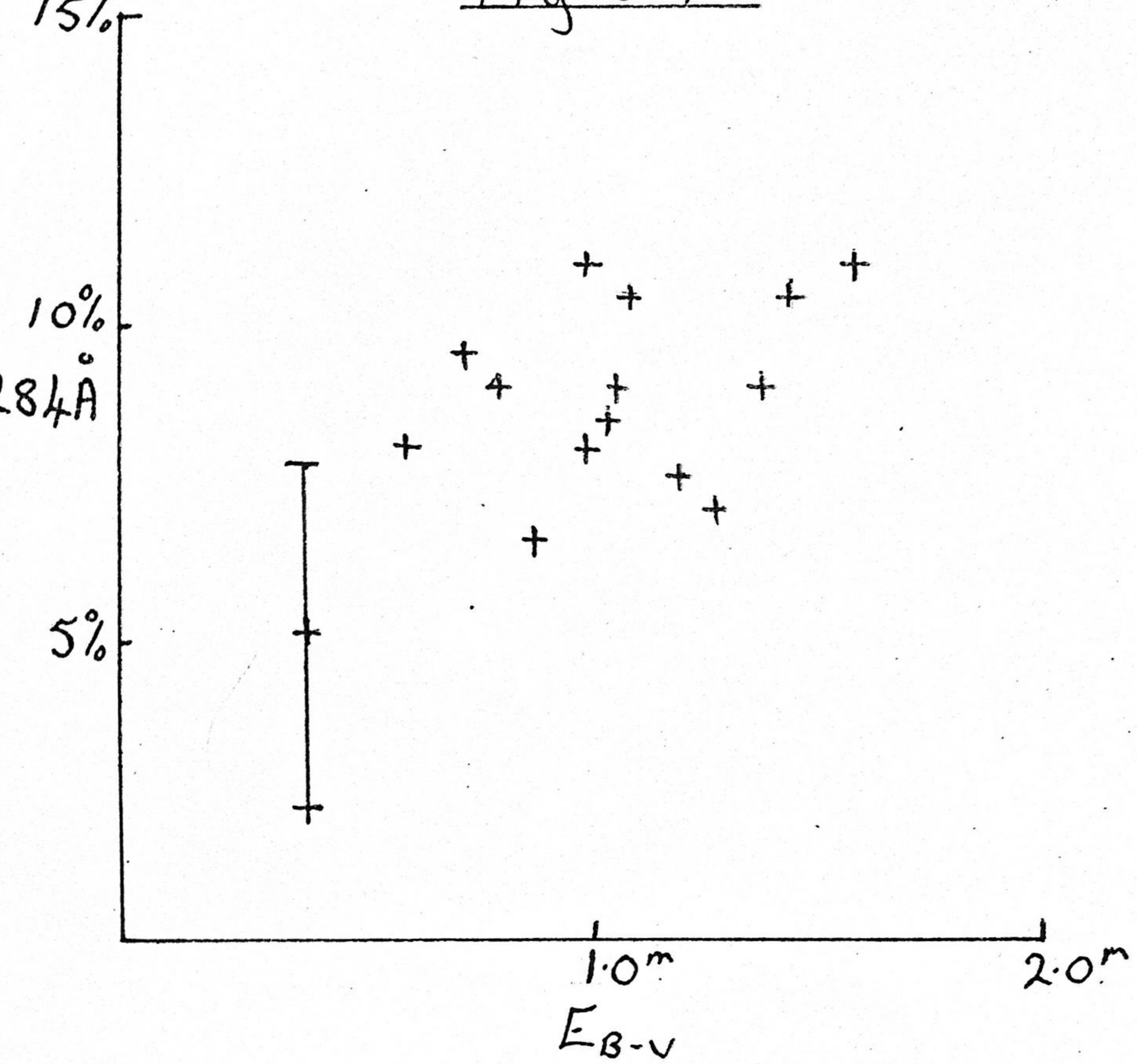

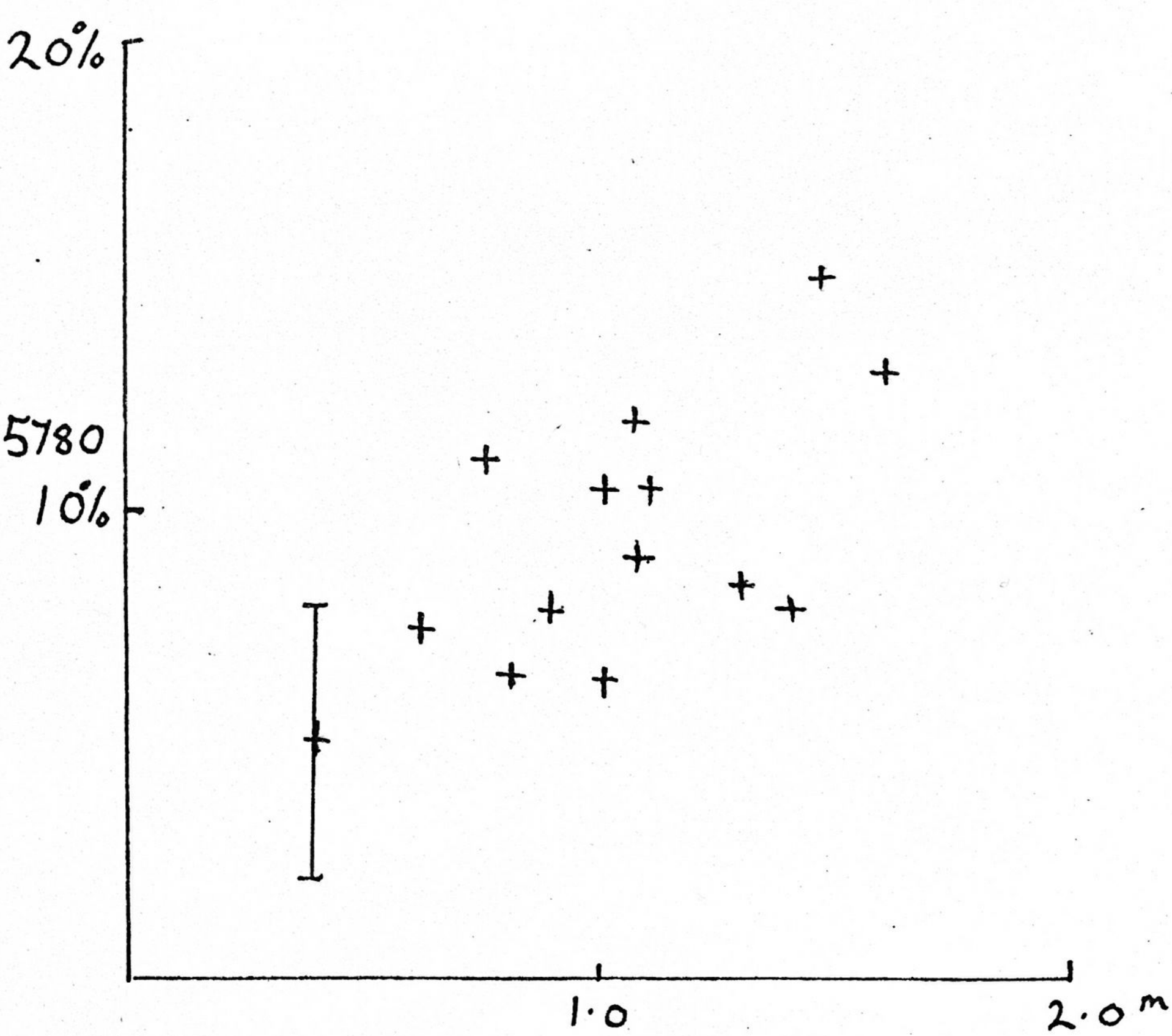

Fig 6.8

Fig 6.8

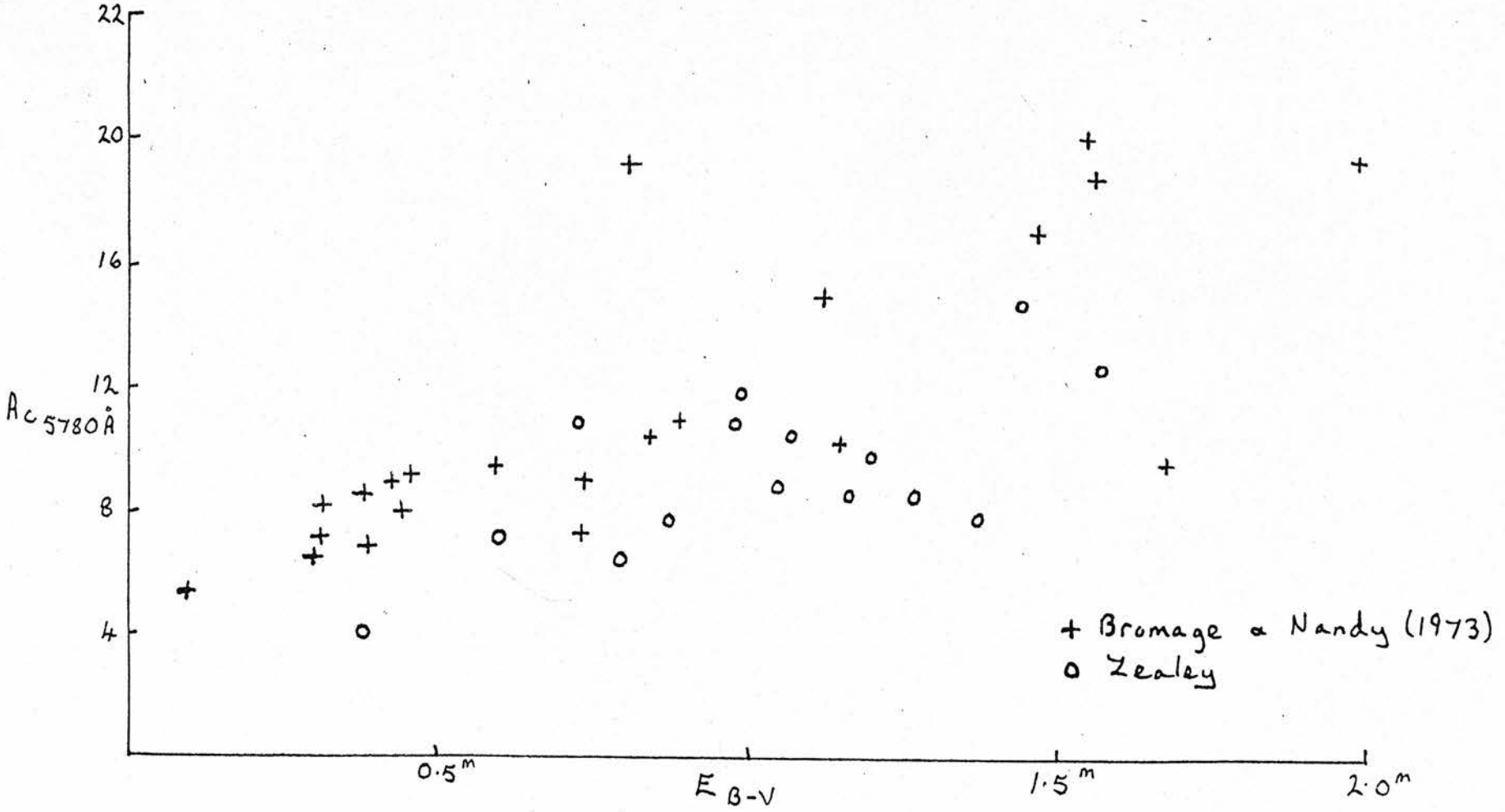

The Intensity v E_{B-V} Relation for the 5780Å Feature

$$A(4430A) = 7.6E_{b-v} + 1.3 \qquad \text{fig. 6.6}$$

$$A(6284A) = 5.0E_{b-v} + 3.3 \qquad \text{fig 6.7}$$

$$A(5780) = 8.7E_{b-v} + 2.0 \qquad \text{fig. 6.8}$$

The relation for the 4430A band agrees well with those found by Wampler(1966), Kellman(1970) and Kristenson (1965). For a colour excess of unity these relations predict central depths of 4430A band of

$A(4430A) = 7.7\%$ Wampler

$A(4430A) = 9.0\%$ Kellman

$A(4430A) = 9.6\%$ Kristenson

The relation here predicts a value of 8.9%.

The 5780A strength versus Eb-v is in close agreement with that found by Bromage and Nandy(1973)(fig. 6.9)

Although the correlation coefficient for the relation between the sterength of 6614A feature is low the values fit the lower part of the relation found by Bromage and Nandy(1973) with similar scatter to their observations.

Comparison with the relations found by Butler and Seddon (1958, 1966) are similarly good. For colour excesses of unity they predict

$A(5780A) = 9.4\%$

$A(\ 6284A) = 8.3\%$

$A(\ Na(D_1+D_2)/2) = 11.5\%$

The stars of NGC6611, and HD 167838 which have low values of Eb-v for their distance also show anomalously high absorption strengths for their reddening.

Fig. 6.10

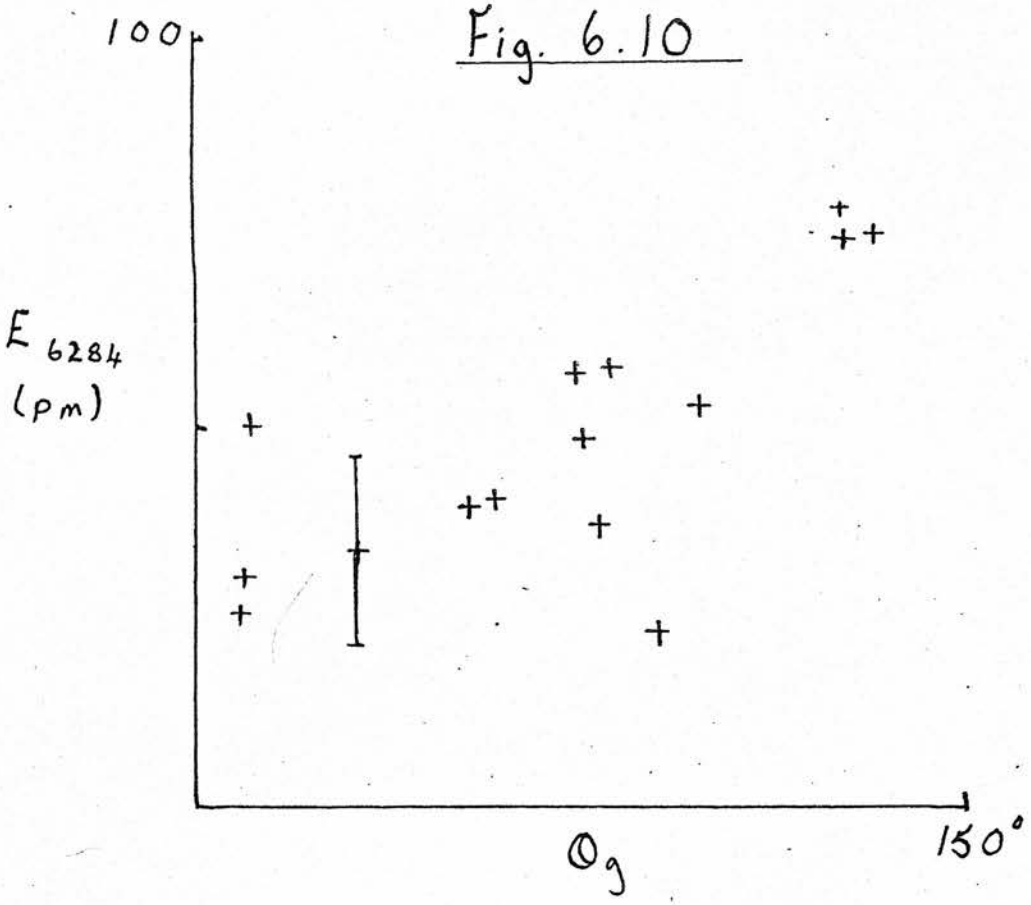

Fig 6.11

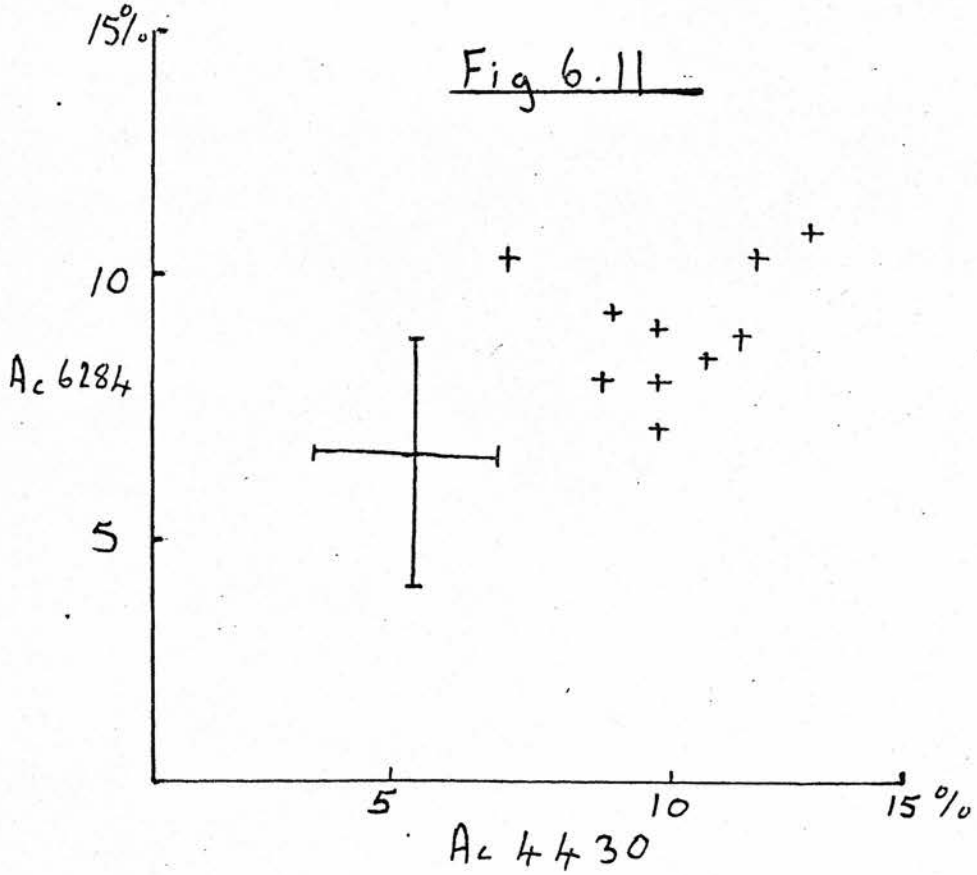

In order to fit the reddening versus line strength relation derived for the remaining stars the reddening of these would need to be about 0.4^m greater in Eb-v. Such an increase in reddening would also correct the distance versus reddening relation. Therefore there seems to be some abnormality affecting these stars. Full discussion follows in the second part of this chapter.

(ii) Polarisation

The angle made by the polarisation vector to the perpendicular to the galactic plane (Θ_g) as measured by Hiltner(1956) and Matthewson and Ford(1970) was plotted against the diffuse line strengths. In the case of the 6284A feature a strong correlation was found, the features intensity increasing with increasing Θ_g. None of the other lines show so strong a correlation.The relation between Θ_g and distance is strong but of a similar form to the reddening versus distance relation.

The relationship between line strengths and P/A_v is poor in all cases, in part due to the small range of values of P/A_v.

6.4 Interrelations between the Interstellar Lines

The relation between the strength of the Sodium

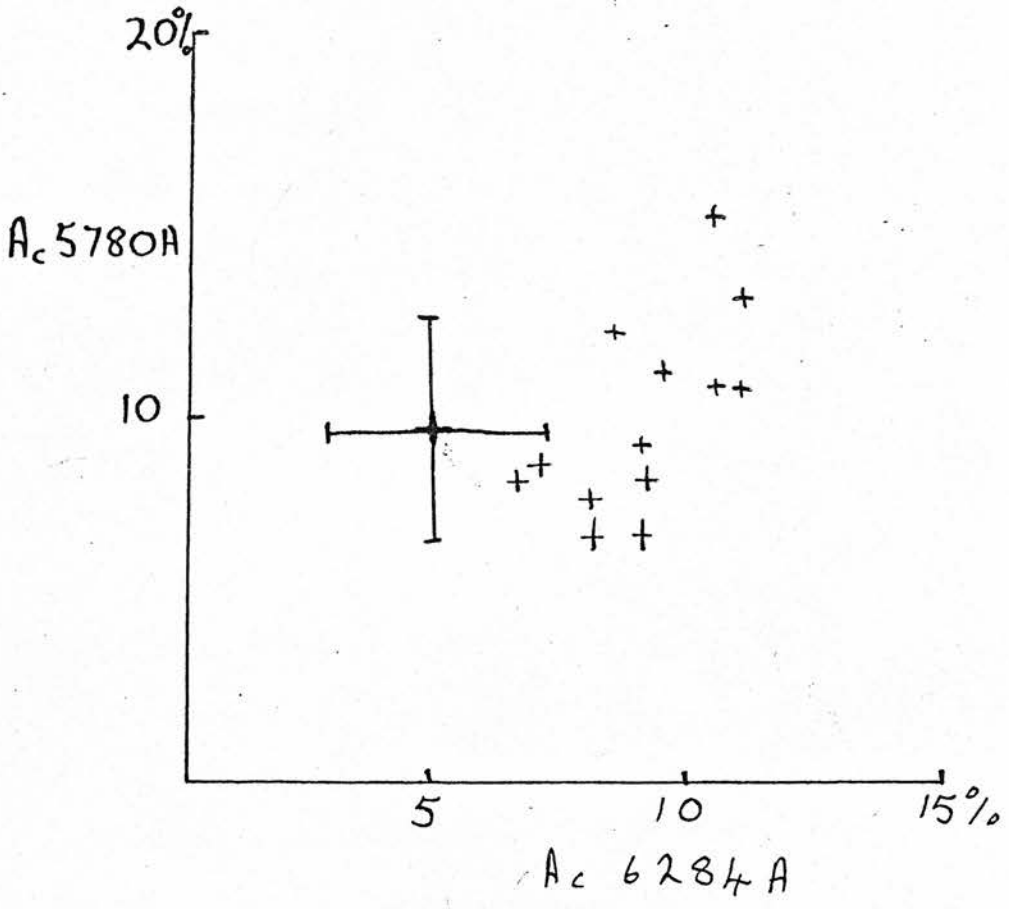

Fig 6.12

D lines and reddening is strong. A similarly strong correlation is found between this strength and that of the Calcium lines.However the Sodium strengths correlate well with the diffuse lines while those of Calcium do not. The relation between Sodium intensities and those at 4430A,5780A and 6284A are particularly strong and the relation is

$$\frac{EW(Na(D_1+D_2)/2)}{EW(6284A+5780A)} = 0.32$$

This value is very much lower than the value found by earlier lower resolution observations of Merril et al (1938).

The diffuse lines interrelate well. Those at 4430A 5780A,5796A and 6284A (figs. 6.11, 6.12) show high intercorrelations. The strength of the 6614 line relates well with that at 5780A but shows only low correlations with the other lines.This line is however of low intensity.

Thus strong relations are found between the four strongest line intensities. Work by Butler and Seddon (1958,1960) and Bromage and Nandy(1973) show that the interrelation between all diffuse lines except possibly that at 4890A is strong.

6.6 A Discussion

In order to discuss the relation these observations bear to previous investigations made at all galactic longitudes, use has been made of a tabulation by Bromage of all observations of the 4430A feature. The values are reduced to Wampler's system using the workers own relations or those of Deeming and Walker(1967). The reduction to Wampler's system was chosen because of the close agreement between Wampler's observations and those presented in previous sections.

In this discussion the I.N.T. and 36-inch observations are discussed more fully.

In the analysis of the southern association members we found

(i) Anomalies in the distance- reddening relation

(ii) Anomalies in the line strength- reddening relation.

(iii) A possible line strength - polarisation angle relation.

The first two anomalies are possibly linked, correction of the reddening values of the four stars restoring both relations to normal. They will therefore be discussed to together.

(i and ii) Distance, Line Strength and Reddening Anomalies

For the observed stars the distances are by no means

Fig 6.13

The 4430Å v E_{B-V} Relation

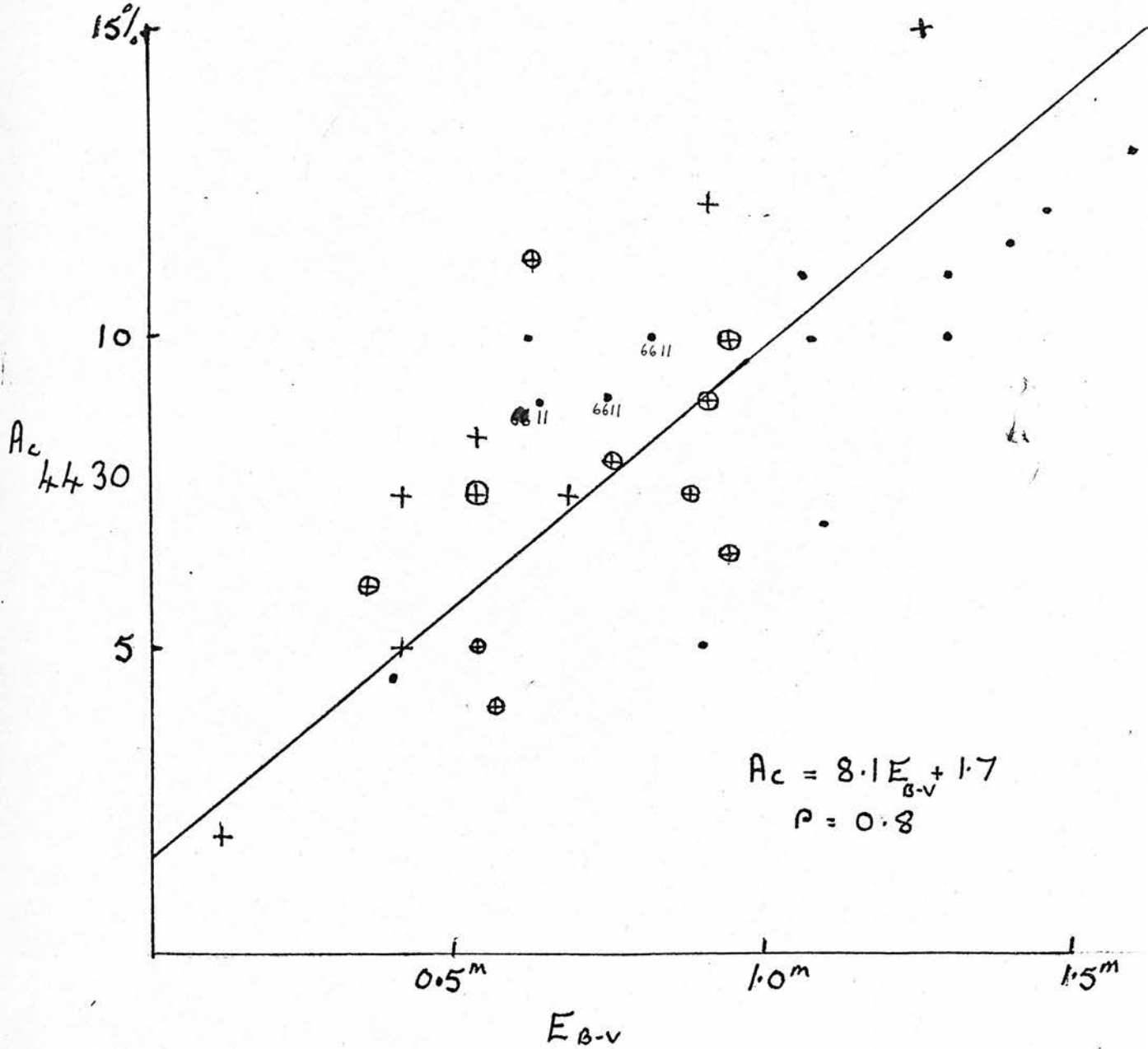

\+ 36-inch observations ± 1% in A_c

⊕ 98-inch observations ± 2% in A_c

• 74-inch observations ± 2% in A_c

certain, those used being dependent on spectral type, reddening corrections and luminosities, often for stars in emission nebulae. Kinematically derived distances as quoted for the HII regions are less reliable. However the reddening-distance relation cannot be improved merely by decreasing the distances for these stars. Patchiness may account for this anomaly in the distance - reddening relation if the second anomaly in the reddening- line intensity relation did not also occur.

This latter effect indicates that the ratio of line strengths to colour excess is not constant. Evidence for this has been provided by Stoekly and Dressler(1964) who found a decrease in the ratio for the feature at 4430A with increasing latitude. Wampler(1966), Kellman(1970) and Walker have all investigated the variation of the ratio A_c/E_{b-v} for the 4430A feature with galactic longitude. Wampler found evidence for the reddening relation in different associations to have different slopes.
In figure 6.13 results of the 4430A intensity derived from the 36-inch, 74-inch and 98-inch observations are plotted against colour excess. A mean relation was found

$$A_{4430} = 8.1\ E_{b-v} + 1.7$$

and a correlation coefficient of

$$r = 0.8$$

found. Indicated also are the members of NGC 6611 and the

association Serpens OB1.

The variation of the ratio $A_{4430}/Eb-v$ with longitude was investigated using the collated values already mentioned. The relation is presented in figure 6.14 along with similar relations derived by Wampler, Kellman and Walker as well as the galactic distribution of open clusters. An analysis by Deeming and Walker of Walker's data concludes that the variation of the ratio with l^{II} is real. The collated material shows similar variations in $A_{4430}/Eb-v$ to those found by the other investigators. Each point is the mean of up to forty stars within twenty degree intervals in l^{II}. From these relations it is clear that minima are found in the regions

$$80^{o} \leqslant l^{II} \leqslant 100^{o}$$
$$140^{o} \leqslant l^{II} \leqslant 180^{o}$$
$$240^{o} \leqslant l^{II} \leqslant 360^{o}$$

Similar minima are to be seen in the distribution of open clusters.

In the regions where these minima occur we are looking toward interarm regions (Becker and Fenkart, 1970; Bok et al, 1970). Near $l^{II}=30^{o}$, $l^{II}= 60^{o}$, $l^{II}=240^{o}$ and $l^{II}= 280^{o}$ we view the Sagittarius, Local and Carina arms tangentially, confirming the fact that low ratios are seen away from the arms.

The present observations give values of $A_{4430}/Eb-v$ of 10 ± 3 in the region $0^{o} \leqslant l^{II} \leqslant 20^{o}$ and 11 ± 3 in the

Cepheus region, $\overset{II}{l} = 110^{o}$. These ratios would represent peaks in the ratio-longitude relation.

The existence of the variation of $A_{4430}/Eb\text{-}v$ is strengthened by observations of bands and lines in the red. These also show local variations in the ratio. It therefore seems possible that the reddening and diffuse absorptions are not caused by the same mechanism. It has already been suggested that the grains invoked to explain reddening act as carriers for the cause of the diffuse lines. High values of $A_{4430}/Eb\text{-}v$ could thus be explained by the grains operating at maximum efficiency as carriers. Lower values for the ratio may then be caused by preferential destruction of the line producing material , by conditions in the interarm medium.

A second possibility exists to explain this variation. If the diffuse line strength is directly related to the total and not the selective absorption and if the ratio of total to selective absorption is not constant then the ratio $A_{4430}/Eb\text{-}v$ would also vary. A variation in R of fifty percent would explain the $A_{4430}/Eb\text{-}v$ versus longitude relation. Although early work suggesting values of 'R' of between two and six have been discredited, high values of 'R' are still being considered (Whittet, 1974).

Figure 6.14

The Variation of A_{c4430}/E_{B-V} With l^{II}

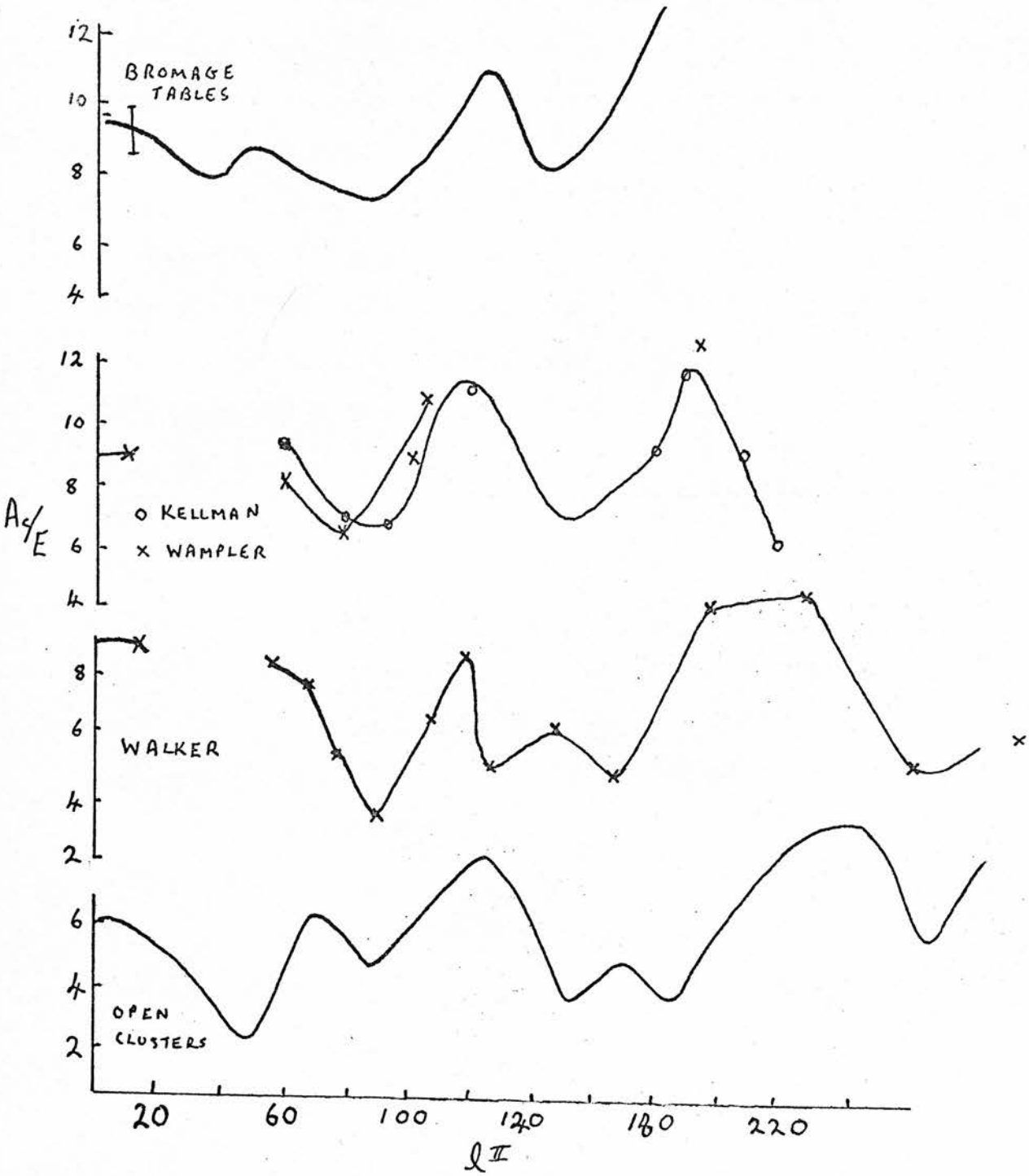

(iii) The Polarisation- Intensity Relation

It has been suggested by several workers that there sshould be a relation between the intensity of the diffuse lines and polarisation(Wilson,1966). Such a relationship is suggested by the possible carrier for both being grains of graphite, silicateor other material(Kelly, 1972; Greenstein and Aller,1950). Wilson in particular predicted a linear relation between the ratios ofabsorption to colour excess and of polarisation to colour excess. Using data from the observed stars and from the tabulated 4430A values no such relation was found.

The correlation between the equivalent width of the 6284A feature and Θ_g is strong and difficult to explain. Similar trends could be observed for the central depth of 6284A although the correlation coefficient was of low significance. Investigation of the collated 4430A values showed no correlations better than r= 0.46. However the coefficients obtained for different regions each from the same number of stars,differed greatly. A maximum was found in the Casseopeia, Cameleopardus area.

Work by Gammelguard and Rudkjobing on the 6180A band assuming it to be caused by predissociation of H^- predicts line strengths related to the angle between the line of sight and the magnetic field direction.It is however unlikely that the cause of the diffuse lines is this mechanism.

One interesting observation is that both areas in which better than usual correlations are found are near where we observe galactic loops or spurs. These are believed to be local structures possibly caused by old supernova explosions. Such events will have affected the local interstellar medium causing inhomogeneities in the obscuration and realigning polarisation vectors. These loops can be seen on the plots of polarisation versus longitude of Mathewson and Ford (1970) and on radio polarisation maps.

6.7 Conclusions

The profiles of the 4430A feature derived from 36-inch observations do not all show evidence for a blue emission wing. Only HD 21389 shows such a wing, while HD 183143 shows shallow emission wings to the red and blue of the feature. In general assymetric profiles are found.

The relations between the diffuse bands in the red and blue and the Sodium lines are as found previously.

The relation between distance, reddening and line strengths is confused in the Sagittarius region. The distance- reddening relation is indicative of inhomogeneities in the absorbing medium.

The reddening- line intensity relation is good except for members of NGC6611 and HD 167838 where high

ratios of intensity to colour excess occur. Analysis of collated 4430A data confirms the variation of this ratio with galactic longitude and leads to the conclusion that colour excess and the diffuse line causes are not directly related. High values of A_{4430}/E_{b-v} occur toward the arm regions of the galaxy.

A new correlation between Θ_g and the intensity of the 6284A band. No explanation has been found, but it is noted that the correlation is found in an area close to galactic spurs.

For the future further accurate observations of lines in the red are needed and the detailed structure of the regions in which they are found should be related to their intensities. Selected regions in which there are well determined distances available should be studied in depth , for example Ara OB1. Work has already been done by Bromage and Nandy (1973) in the Cygnus OB2 region.

DECLARATION OF AUTHENTICITY

With the exception of the mechanical design of the 'Spectrum Scanner' (Chapter 4), the work in this thesis is my own, except where otherwise stated eg. in references.

W.J.Zealey

APPENDIX I

Error Evaluation in Photographic Spectrophotometry

Baker et al.(1955,1949) derive standard errors for the equivalent widths of spectral lines. These are of the form

$$S.E^2 = (.92*(L_1-L_2)*d)^2 * \left[\frac{1}{N_c} + \frac{1}{N_L}\right] + \frac{a^2 * W^2}{M}$$

Where

W is the equivalent width

F is the contrast factor = $-\Delta/m$

L_1-L_2 is the extent of the spectrum measured in Angstroms

N_c is the number of points in the continuum

N_1 is the number of points in the line

d is the standard error of each point

a is the standard error of the contrast factor

The equation simplifies to

$$S.E. = \sqrt{N*d}$$

if the second term is small, one spectrum is considered, the contrast factor is nearly one and $N_c > N_L$. These are so for this investigation.

APPENDIX II

The Significance of the Correlation Coefficient 'r'

The significance of 'r' depends only on its own magnitude and on 'n', the number of points used in its determination. The standard error in 'r' is represented by

$$s.e._r = \sqrt{\frac{1 - r^2}{n-2}}$$

In the analysis of chapter 6 the number of points range from eight to fifteen. The values of 'r' for which $r - s.e._r = 0.0$ are then between $r = 0.4$ and $r = 0.3$. For a five percent level of significance using fifteen data points we need a correlation coefficient of $r = 0.5$. Less data points require a higher 'r' for such a level of significance. For a ten percent level of significance $r = 0.4$ for fifteen points ; $r = 0.6$ for eight points, are required.

Flow Diagram WZ202

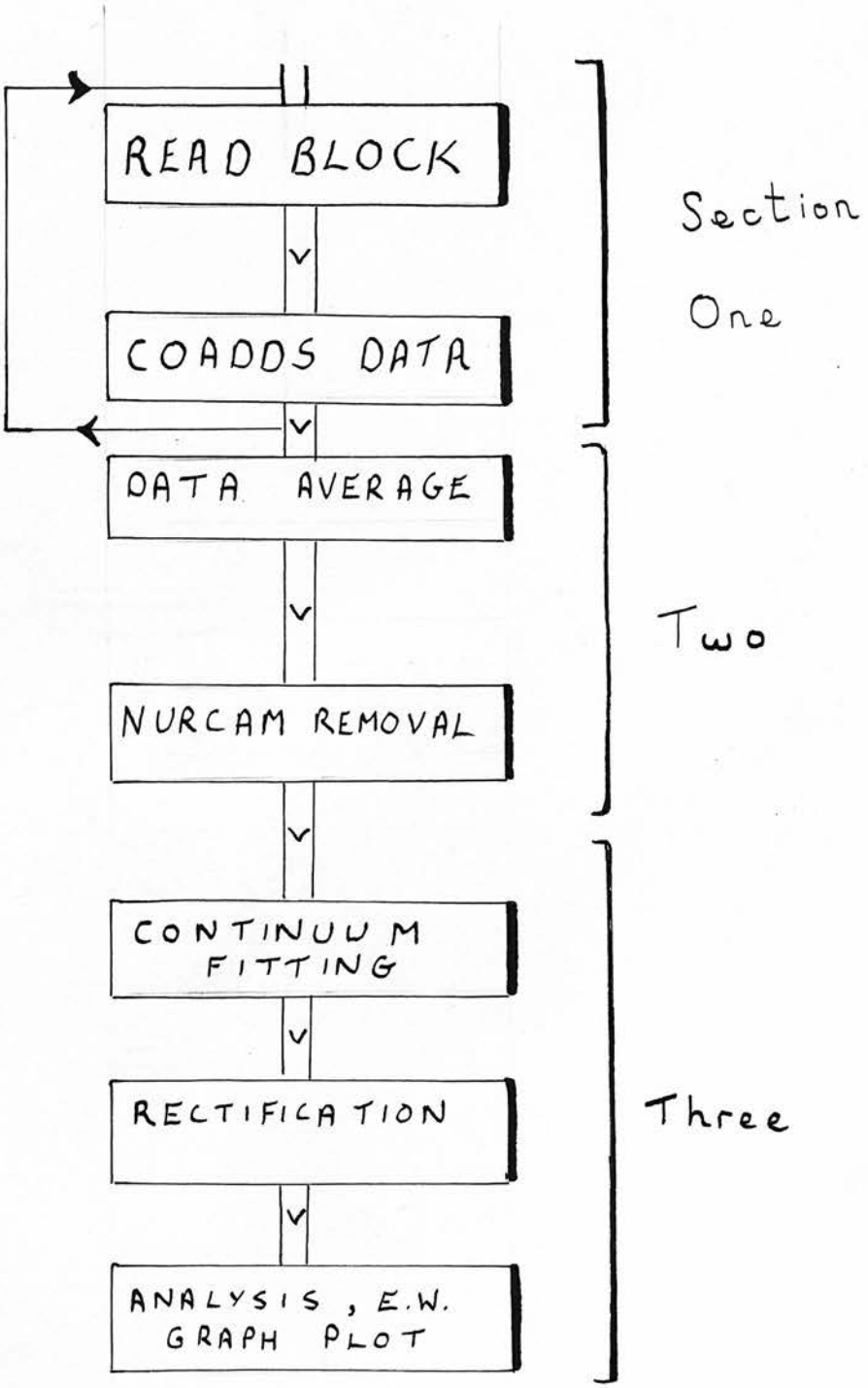

WZ 202 Section One

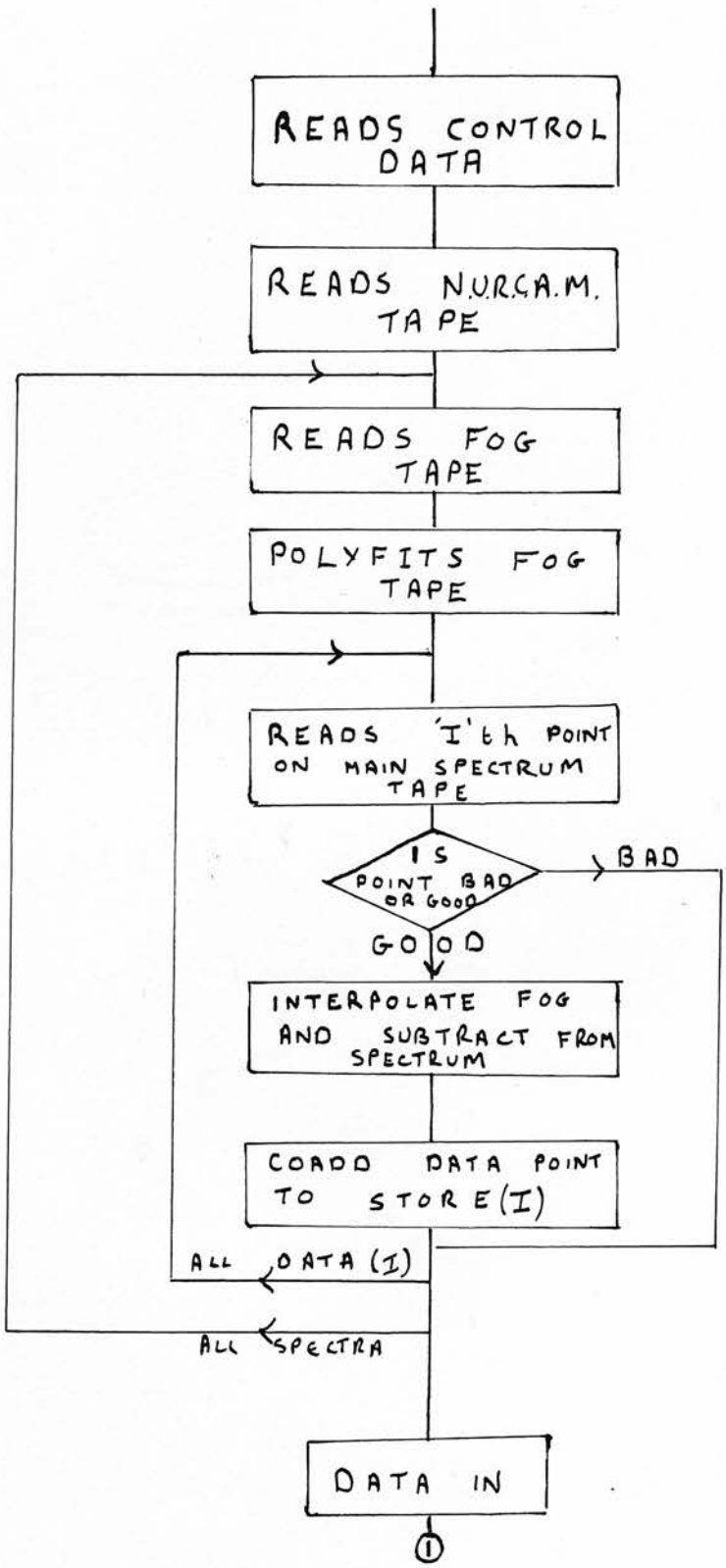

WZ 202 Section Two

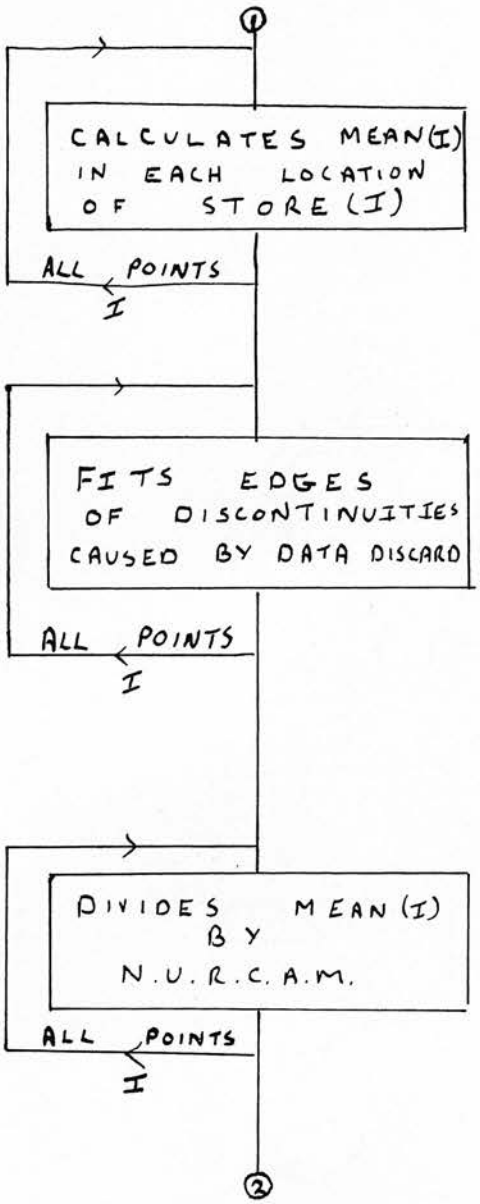

WZ 202 Section Three

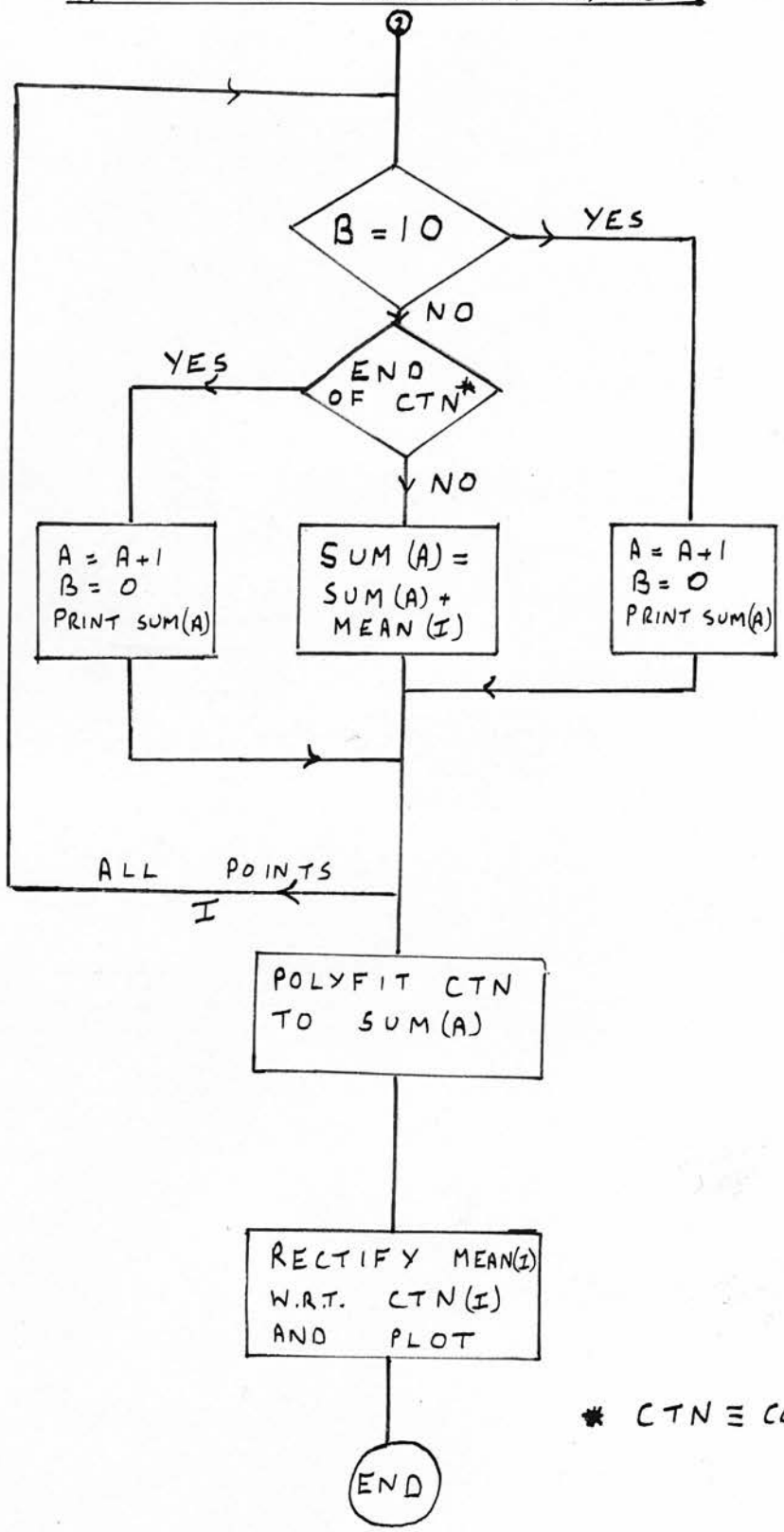

* CTN ≡ CONTINUUM

REFERENCES

Adams, D.J. : 1949, Astrophys. J. 109, 354.

A'Hearn, M.F. : 1971, Astron. J. 76, 264.

A'Hearn, M.F. : 1972, Astron. J. 77, 302.

Airey et.al. : 1970, Private Communication.

Alter, G. and Ruprecht, B. : 1965, Bull. Astron. Inst. Czech. 16, 1.

Alter, G. and Ruprecht, B. : 1967, Bull. Astron. Inst. Czech. 18, 1.

Anderson C.M. : 1970, Astrophys. J. 160, 507.

Andrews, P.J. : 1968, Mem. Roy. Astron. Soc. 72, 35.

Aydin, C. : 1972, Astron. Astrophys. Supp. 7, 331.

Babcock, H.W. and Herzberg, G. : 1948, Astrophys. J. 108, 167.

Bacik, H. : 1972, Adv. Electronics and Electron Physics 33B, 747.

Baerentzen, J. and Gammelgaard, P. : 1967, J. Obs. 50, 83.

Baker, E.A. : 1949, Publ. R.O.E. 1, 15.

Baum, W.A. : 1962, Stars and Stellar Systems II, Astronomical Techniques, Chicago Press, p1.

Beals, C.S. : 1942, Monthly Notices Roy. Astron. Soc. 102, 96.

Beals, C.S. and Blanchet, G.H. : 1938, Monthly Notices Roy. Astron. Soc. 98, 398.

Becker, W. and Fenkart, R. : 1970, I.A.U. Symp. No. 38 'The Spiral Structure of Our Galaxy', 205.

Beer, A. : 1961, Monthly Notices Roy. Astron. Soc. 123,

Beer, A. : 1964, Monthly Notices Roy. Astron. Soc. 128, 261.

Binnedjic, L. : 1952, Astrophys. J. 115, 432.

Bok, B.J. et al. : 1970, I.A.U. Symposium No 38, 'The Spiral Structure of Our Galaxy', 246.

Bonsack, W.K. : 1971, Publ. Astron. Soc. Pacific 83, 602.

Boksenberg, A. : 1972, E.S.O./C.E.R.N. Conference on 'Auxiliary Instrumentation for Large Telescopes', edited by S. Lausten and A. Reiz, 295.

Borgman, J. : 1960, Bull. Ast. Inst. Netherlands, 15, 25.

Borgman, J. and Blauw, A. : 1964, Bull. Ast. Inst. Netherlands, 17, 36.

Borgman, J. and Johnson, H.L. : 1963, Bull. Ast. Inst. Netherlands, 17, 115.

Brand, P.W.J.L.B. : 1967, Ph.D. University of Edinburgh.

Brand, P.W.J.L.B. and Smyth, M.J. : 1966, Adv. Electron & Electron. Physics, 22B, 741.

Bromage, G.E. : 1971, Ph.D. University of Edinburgh.

Bromage, G.E. : 1971, Nature, 230, 172.

Bromage, G.E. : 1972, Astrophys. Space Sci. 15, 426.

Bromage, G.E. and Nandy, K. : 1973, Astron. Astrophys. 26, 17.

Bruck, M., Nandy, K. and Seddon, H. : 1969, Physica, 41, 128.

Burton, W.B. : 1966, Bull. Ast. Inst. Netherlands, 18, 247.

Burton, W.B. : 1972, Astron. Astrophys. 19, 51.

Butler, H.E. : 1950, Observatory, 70, 235.

Butler, H.E. and Seddon, H. : 1958, Pub. R.O.E. II No 4.

Butler, H.E. and Seddon, H. : 1960, Pub. R.O.E. II No 5.

Butler, H.E. and Thompson, G.J. : 1961, Pub. R.O.E. II No 6.

Buscombe, W. and Kennedy, P.M. : 1969, Mem. Roy. Astron. Soc. 139, 417.

Cannon, A.J. : 1919, Harvard Ann. 94, 288.

Churchwell, E. and Mezger, P. : 1970, Astrophys. Letters 5, 227.

Cohen, M. and Kahan, E. : 1971, Adv. Electron. and Electron Physics 33A .

Courtes, G. : 1966, J. Obs. 49, 329.

Crampton, D. 1971, Astron. J. 76, 270.

Crawford, D.L. and Barnes, J.V. : 1970, Astron. J. 75, 952.

Deeming T.J. and Walker, G.A.H. : 1967, Z. Astrophys. 66, 175.

De Vaucouleurs, G. : 1968, Applied Optics 7, 1513.

Dickel, H.R. : 1970, I.A.U. Symposium No 38 'The Spiral Structure of Our Galaxy', 216.

Divan, L. : 1954, Ann. D'Astrophys. XVII, 456.

Dixon, M.E. : 1970, Monthly Notices Roy. Astron. Soc. 151, 89.

D'Odorico, S.D. and Felli, M. : 19 , Oss. Astrophys. Arcetri Contributions, 226.

Doremus, C. : 1970, cf. Garrison, P.C.

Dorschner, J. and Gurtler, J. : 1963, Astron. Nachr. 287, 257.

Dorschner, J. : 1965, Astron. Nachr. 289, 57.

Duke, D. : 1951, Astrophys. J. 113, 100.

Ellison, M.A. and Seddon, H. : 1952, Monthly Notices Roy. Astron. Soc. 112, 73.

Felli, M. and Churchwell, E. : 1972, Astron. Astrophys. Supp. 5

Fernie, D.J. : 1968, Astrophys. J. 771, 150.

Fitzgerald, M.P. : 1968, Astron. J. 73, 983.

Foord, R. and Jones, R. : 1969, Applied Optics 8, 1975.

Gammelgaard, P. : 1968, J. Obs. 51, 297.

Gammelgaard, P. and Rudkjobing, M. : 1973, Astron. Astrophys.

Garmany, C.D. : 1972, Astron. J. 77, 38.

Garrison, R.F. : 1967, Astron. J. 72, 797.

Garrison, R.F. : 1970, Astron. J. 75, 1001.

Georgelin, Y.M. and Georgelin, Y.P. : 1970, Astron. Astrophys. 6, 349.

Georgelin, Y.M. and Georgelin, Y.P. : 1970, Astron. Astrophys. 8, 117.

Georgelin, Y.M. and Georgelin, Y.P. : 1970, Astron. Astrophys. Supp. 3.

Goss, W.M. and Shaver, P.A. : 1970, Australian J. of Phys. Supp. 14.

Greenberg, J.M. and Minn, Y.K. : 1973, Astron. Astrophys. 22, 13

Greenberg, J.M. and Stoekly, R. : 1971, Nature Phys. Sci. 230, 15.

Green stein, J.M. and Aller, L.H. : 1947, Pub. Astron. Soc. Pacific 59, 139.

Greenstein, J.L. and Aller, L.H. : 1950, Astrophys. J. 111, 328.

Griboval, P. and Griboval, D. : 1972, Advances in Electron. Electron Physics 33A.

Griffin, R.F. : 1968, A Photometric Atlas of the Spectrum of Arcturus, Camb. Phil. Soc.

Gum, C. : 1955, Memoirs Roy. Astron. Soc. 67, 155.

Hagen, G.L. : 1970, Pub. David Dunlap Obs. V4 'An Atlas of Open Cluster Diagrams '

Hall, J.S. and Mikesell, A.H. : 1950, U.S. Naval Pub. 17.

Harris, J. : 1969, Nature 223, 1046.

Harris, J. : 1969, Ph.D. Thesis, University of Edinburgh.

Hartmann, J. : 1904, Ap. J. 19, 268.

Heger, M.L. : 1921, Lick Obs. Bull. 10, 146.

Herbig, G. : 1966, Z. Astrophys. 64, 512.

Herbig, G. : 1967, I.A.U. Symposium 31, 85.

Herbig, G. : 1970, I.A.U. Symposium 36, 315.

Herz, M. : 1952, J. Sci. Inst. 29, pps. 15 and 60.

Hiltner, W.A. : 1956, Astrophys. J. Supp. 2, 389.

Hiltner, W.A. : 1954, Astrophys. J. 120, 41.

Hiltner, W.A. and Johnson, H.L. : 1956, Astrophys. J. 124, 367.

Hoag, A.A. and Applequist : 1965, Astrophys. J. Supp. 12, 107.

Hoag, A.A. and Iriate, B. : 1961, Publ. U.S. Naval Obs. 17, 366.

Hoag, A.A. et al. : 1951, J.O.S.A. 41, 689.

Hobbs, R.W. : 1961, Astron. J. 66, 517.

Honeycutt, A. : 1970, Astron. J. 75, 600.

Honeycutt, A. : 1971, Applied Optics 10, 1125.

Honeycutt, A. : 1972, Astron. J. 77, 24.

Hosfield, R. : 1954, J.O.S.A. 44, 284.

Hubble, E. : 1922, Astrophys. J. 56, 162.

Humphreys, R.M. : 1970, Astron. J. 75, 602.

Hutchison, R.B. : 1971, Astron. J. 76, 711.

Hutchings, J.B. : 1967, Observatory 87, 273.

Hutchings, J.B. : 1967, Dominion Astrophys. Obs. Contr. 128.

Ishida, K. : 1967, Tokyo Astron. Bull. 2nd. series, No. 178, 2147.

James, J.F. : 1967, Monthly Notices Roy. Astron. Soc. 15, 137.

Jaschek, C. et al. : 1964, Publ. Astron. Univ. Nac La Plata.

Johnson, F.M. : 1970, N.A.S.A. CR 1667.

Johnson, F.M. : 1963, Bull. Astron. Inst. Neth. 17, 115.

Johnson, F.M. : 1968, 'Stars and Stellar Systems' VII 'Nebulae and Interstellar Matter' Chicago.

Johnson, F.M. and Borgman : 1965, Astrophys. J. 141, 923.

Kahan, E. and Cohen, M. : 1969, Advances in Electron. and Electron Physics 28B, 725.

Kahan, C. and Cohen, M. : 1972, Advances in Electron. and Electron Physics 33A.

Kellman, S.A. : 1970, Publ. Astron. Soc. Pacific 82, 1368.

Kelly, A. : 1972, M.Sc., University of Edinburgh.

Kerr, F.J. : 1971, I.A.U. Symposium No 36 'Structure and Evolution of the Galaxy'.

Klare, G. : 1967, Z. Astrophys. 67, 131.

Klare, G. and Neckel, T. : 1967, Z. Astrophys. 66, 45.

Klare, G. and Neckel, T. : 1967, Z. Astrophys. 67, 249

Kleinman, D.E. : 1973, Astrophys. Letters 13, 49.

Kristenson, H. et al. : 1965, J. Obs. 48, 107.

Lambrecht, H. and Schmidt, K.H. : 1958, Astron. Nach. 284, 71.

Lynds, B.T. 1962, Astrophys. J. Supp. 7, 1.

Lynds, B.T. : 1965, Astrophys. J. Supp. 12, 163.

Lynds, B.T. and Aikens, R.I. : 1967, Publ. Astron. Soc. Pacific 77, 347.

Lynga, G. : 1972, Astron. Astrophys. Supp. 6.

Mathewson, P.S. and Ford, V.L. : 1970, Mem. Roy. Astron. Soc. 74, 5.

McGee, J.D. and Wheeler, B.E. : 1962, Advances in Electron. Electron Physics 16, 47.

McGee, J.D. and Khogali, A. : 1966, " " " " 22A, 11.

McGee, J.D. et al. : 1969, " " " " 28A, 61.

McGee, J.D. et al. : 1972a, " " " " 33A

McGee, J.D. et al. : 1972b, " " " " 33A

Mees, H.A. : 1959, 'Theory of Photographic Processes' MacMillan.

Mendoza, E.F. : 1956, Astrophys. J. 128, 207.

Merril, P.W. : 1930, Astrophys. J. 72, 98.

Merril, P.W. : 1936, Astrophys. J. 83, 126.

Merril, P.W. and Burwell, C.G. : 1933, Astrophys. J. 78, 87.

Merril, P.W. and Burwell, C.G. : 1943, Astrophys. J. 98, 153.

Merril, P.W. and Burwell, C.G. : 1949, Astrophys. J. 110, 387.

Merril, P.W. and Burwell, C.G. : 1950, Astrophys. J. 112, 72.

Merril, P.W. and Humason, M.L. : 1922, Publ. Astron. Soc. Pacific 34, 180.

Merril, P.W. and Wilson, H.A.: 1938, Astrophys. J. 87, 9.

Merril, P.W. et al. : 1937, Astrophys. J. 86, 274.

Mezger, P.G. : 1970, I.A.U. Symp. 38 'The Spiral Structure of Our Galaxy'.

Mikesell, A.H. : 1952, Publ. U.S. Naval Obs. 17, 64.

Miller, S. : 1968, Astrophys. J. 151, 473.

Millikan, A.G. : 1971, A.A.S. Photobul 1, 13.

Minn, Y.K. and Greenberg, J.M. : 1973, Astron. Astrophys. 22, 13.

Minnaert, M. et al. 1940, 'Photometric Atlas of the Solar Spectrum' Utrecht.

Moore, C. : 1945, 'Table of Multiplets', Princetown.

Morgan, W.W. : 1939, Astrophys. J. 10, 632.

Morgan W.W. : 1944, Astron. J. 90, 634.

Morgan, W.W. : 1953, Astrophys. J. 118, 318.

Morton, G.A. : 1968, Applied Optics 7, 1.

Munch, G. : 1957, Astrophys. J. 125, 42.

Murdin, P. : 1972, Monthly Notices Roy. Astron. Soc, 157, 461.

Nandy, K. : 1967, Publ. R.O.E. 5, No 2.

Nandy, K. : 1967, Publ. R.O.E. 5, No 11.

Nandy, K. : 1968, Publ. R.O.E. 6, No 3

Nandy, K. : 1968, Publ. R.O.E. 6, No 7

Nandy, K. : 1964, Ph.D. Thesis University of Edinburgh.

Neckel, T. : 1967, Landessternwarte Heidlberg - Konigsstuhl Veroffentl 19, 105.

Oliver, M. : 1972, Advances in Electron. Electron Physics 33A.

Palmer, D.R. and Milson, A.S. : 1972, Advances Electron. Electron Physics. 33B, 769.

Panofskie, K.H. : 1941, Astrophys. J. 53, 239.

Panofskie, K.H. : 1943, Astrophys. J. 97, 180.

Pearse, R.W.B. and Gaydon, A.G. : 1950, 'Identification of Molecular Spectra' Chapman Hall.

Popper, D.M. : 1940, Publ. Astron. Soc. Pacific. 52, 401.

Popper, D.M. and Seyfert, C.K: 1946, Publ. Astron. Soc. Pacific 52, 407

Racine, R. : 1968, Astron. J. 73, 233.

Reddish, V.C. : 1967, Monthly Notices Roy. Astron. Soc. 135, 251

Reifenstein, E.C. et al. : 1970, Astron. Astrophys. 4, 357.

Riegel, K.W. et al. : 1972, Astron. Astrophys. 18, 55.

Rodgers, A.W., Campbell, C.T., Whiteoak, J.B. : 1960, Mt. Stromlo Publ.

Rohlfs, K. : 1971, Astron. Astrophys. 13, 46.

Rosendhal, J.D. : 1973, Astrophys. J. 182, 523.

Roslund, C. : 1968, Ark. Astr. 4, 441.

Routly, P.M. and Spitzer, L. : 1952, Astrophys. J. 115, 227

Rowlands, H. : 1928, 'Revised Tables of Rowlands Wavelengths' (Revised by S John, Moore et al.) Carnegie Publ. No. 396.

Rudkjobing, M. : 1970, Astrophys. Space Sci. 6, 157.

Rudkjobing, M. and Kristenson, W. : 1965, J. Obs. 48, 107.

Rudnick, P. : 1936, Astrophys. J. 83, 468.

Ruprecht, J. : 1964, Trans. I.A.U. 12B, p. 336.

Rusconi, L. and Sedmak, G. : 1971, Applied Optics, 10, 473.

Sanford, R. : 1949, Astrophys. J. 110, 117.

Schraml, J. and Mezger, P. : 1969, Astrophys. J. 56, 269.

Seddon, H. : 1967, Nature, 214, 257

Seddon, H. : 1967, Nature, 215, 495.

Seddon, H. : 1968, Nature, 217, 232

Sedmak, G. : 1972, Astron. Astrophys. 18, 232.

Serkowski, K. : 1965, 'Interstellar Grains' N.A.S.A. S.P.140.

Sharpless, S. : 1953, Astrophys. J. 118, 362.

Sharpless, S. : 1954, Astrophys. J. 119, 340.

Sharpless, S. : 1959, Astrophys. J. Supp. 4, 257.

Schmdt Kaler T, : 1973, Astron. Astrophys. 25, 191.

Sherman, F. : 1939, Astrophys. J. 90, 630.

Sim, M.E. : 1968, Publ. R.O.E. 6, No 8.

Simonson III S.C. : 1968, Astrophys. J. 154, 923.

Sinnerstad, U. : 1961, Ann. Stockholm Obs. 21, No 6.

Sinnerstad, U. : 1961, Ann. Stockholm Obs. 22, No 2.

Smyth, M.J. and Brand, P.W.J.L. : 1969, Advances Electron. Electron Physics 28B, 737

Spitzer, L. Jr. : 1948, Astrophys. J. 113, 283

Steavenson, W.H. and Knox-Shaw, H. : 1935, Monthly Notices Roy. Astron. Soc. 95, 447.

Stoekly, R. and Dressler, K. : 1964, Astrophys. J. 139, 240.

Svolopoulos, S.N. : 1961, Publ. Astron. Soc. Pacific 75, 73

Treanor, P.J. : 1964, Publ. R.O.E. 4, 81.

Tull, R.G. : 1968, Applied Optics 7, 2019.

Underhill, A.B. : 1956, Dominion Astrophys. Obs. 10, No 8.

Underhill, A.B. : 1966, 'Early Type Stars' Reidel.

Van den Berg, S. : 1966, Astron. J. 71, 990.

Van de Hulst, H.C. : 1945, Ann D'ap. 8, 1.

Wackerling, L.C. : 1970, Mem. Roy. Astron. Soc. 73, 3.

Walker, G.A.H. : 1963, Monthly Notices Roy. Astron. Soc. 125, 141.

Walker, G.A.H. and Hodge, S.M. : 1966, Publ. Dominion Astrophys. Obs. 12, 40.

Walker, G.A.H. and Hodge, S.M. : 1968, Publ. Astron. Soc. Pacific 80, 290.

Walker, G.A.H., Hutchings, J.B. and Younger, P.F. : 1967, Astron. J. 74, 1061.

Walker, M.F. : 1961, Astrophys. J. 133, 438.

Walker, M.F. : 1969, Advances Electron. Electron Phys. 28B, 773

Walker, M.F. : 1972, Advances Electron. Electron Phys. 33B, 667

Wallerstein, G. : 1970, Publ. Astron. Soc. Pacific 82, 9.

Wampler, E.J. : 1963, Astrophys. J. 137, 1071.

Wampler, E.J. : 1966, Astrophys. J. 144, 921.

Warren, P. : 1972, Private Comm.

Whiteoak, J.B. : 1966, Astrophys. J. 144, 305.

Whitted, D.C.B. et al. : 1973, Nature Phys. Sci. 243, 21.

Williams, E.G. : 1936, Astrophys. J. 83, 288.

Wilson, R.E. : 1953, 'General Catalogue of Radial Velocities'.

Wilson, R. : 1956, Publ. R.O.E. II, No 1.

Wilson, R. : 1958, Publ. R.O.E. II, No 3.

Wilson, R. : 1958, Astrophys. J. 128, 57.

Wilson, R. : 1966, Monthly Notices Roy. Astron. Soc. 120, 51.

Wimbush, M.H. : 1961, Cambridge Labs. A.F.C.R.L. 697 Airforce Cont. No 19(604), 2292 'Optical Astronomical Seeing'.

Wright, W.H. : 1921, Lick Obs. Bull. 10, 109.

Wu, C.C. : 1972, Astrophys. J. 178, 681.

York, D.G. : 1971, Astrophys. J. 166, 65.

Zacharov, B. and Dowden, : 1960, Advances Electron. Electron Phys. 11, 31.

==========

ACKNOWLEDGEMENTS

I wish to thank Professor H.A. Brück and Dr. M.J. Smyth for the provision of wide ranging facilities and for providing guidance when needed.

Dr. P.W.J.L. Brand for provoking thought when observations became too engrossing.

The workshop and electronics workshop staff for allowing me the freedom of their kingdoms.

Mr. S. Salter for engineering the mechanics of the scanner in spite of the almost impossible specifications.

All at Radcliffe and Herstmonceux Observatories for training an astronomer in the use of large telescopes.

All at Imperial College for making available their expertise in the use of 'Spectracon' intensifiers.

And all who provided encouragement and support.